universität wien

MASTERARBEIT / MASTER'S THESIS

Titel der Masterarbeit / Title of the Master's Thesis

Synthesis of stable heavy isotope containing small molecules

^{15}N-containing substitued pyridines and fluorinated ^{13}C-compounds for selective protein labeling

verfasst von / submitted by

Cherilyn Cikan, BSc

angestrebter akademischer Grad / in partial fulfilment of the requirements for the degree of

Master of Science (MSc)

Wien, 2022 / Vienna, 2022

Studienkennzahl lt. Studienblatt / degree programme code as it appears on the student record sheet:	UA 066 863
Studienrichtung lt. Studienblatt / degree programme as it appears on the student record sheet:	Masterstudium Biologische Chemie
Betreut von / Supervisor:	Mag. Dr. Roman J. Lichtenecker, Privatdoz

Acknowledgements

I would like to extend great thanks to my supervisor, Dr. Roman Lichtenecker, for giving me the opportunity to be part of his working group. I want to thank him for his trust to let me work independently while always being ready to give support and advise or just drink a cup of coffee. His understanding and humorous manner ensured a pleasant working atmosphere together with patient and friendly advise.
I would also like to thank my other colleagues, especially Giorgia, for her constant help and care.

Many thanks to Univ.-Prof. Dipl.-Chem. Dr. Lothar Brecker for his helpful and patient guidance throughout my master's study.

Finally, I want to express my gratefulness towards my friends and family for helping me each in their own way. Immense gratitude goes to my spouse for having my back and many hours of listening and unconditional support. I would also like to pass on sincere thanks to my little daughter for allowing me to work and being incredibly patient for her young age.

Contents

Abstract I

This project derives from an industry cooperation, which involves the synthesis of [4-^{15}N]amino-[3-^{15}N]nitropyridine. A synthetic route was optimized starting from commercially available isonicotinic acid. A ^{15}N-labeled amino group was introduced via amidation using $^{15}NH_4Cl$ as an isotope source. For the next step three variations of Hofmann degradation were evaluated to obtain the aminopyridine. In the final step a ^{15}N-labeled nitro group was implemented via aromatic nitration utilizing $K^{15}NO_3$. Overall 1.63 g of ^{15}N-labeled ANP could be produced with an overall yield of 17 % via three steps.

Abstract II

High-resolution NMR spectroscopy allows three-dimensional structure investigation at atomic resolution under near native conditions. The analysis and interpretation of large proteins relies on the incorporation of unnatural and/or isotope-labeled amino acids into proteins. This master project focused on the synthesis of fluorinated phenylalanine and its late metabolic precursor, phenylpyruvate. Starting from [1-^{13}C]glycine a synthetic route of three steps was conducted to yield para-fluorophenyl-[1-^{13}C]pyruvate; 3,5-difluoro-4-hydroxyphenyl-[1-^{13}C]pyruvate and 2,6-difluoro-4-hydroxyphenyl-[1-^{13}C]pyruvate; respectively. To obtain para-fluorophenylalanine four steps were performed starting from unlabeled glycine. The compounds were synthesized to assess the bacterial uptake of fluorinated phenylalanine species via the shikimic acid pathway to achieve highly-selective ^{13}C and ^{15}N backbone labeling combined with fluorinated aromatic ring systems. The knowledge gained will be used to design further labeling patterns of phenylalanine, with high regard to ^{12}C – ^{2}H and ^{13}C – ^{19}F spin systems for the investigation of aromatic ring system dynamics via transverse relaxation-optimized spectroscopy (TROSY).

Zusammenfassung I

Dieses Projekt ist eine Industriekooperation, welche die Synthese von 4-^{15}N-Amino-3-^{15}N-Nitropyridin beinhaltet. Ausgehend von kommerziell erhältlicher Isonicotinsäure wurde ein Syntheseweg optimiert. Die ^{15}N markierte Aminogruppe wurde über Amidierung mittels $^{15}NH_4Cl$ eingführt. Im nächsten Schritt wurden drei Syntheseprotokolle für den Hofmann Abbau evaluiert um Aminopyridin zu erhalten. Im letzten Schritt wurde die ^{15}N markierte Nitrogruppe über aromatische Nitrierung mit $K^{15}NO_3$ eingeführt. Gesamt konnten 1,63 g markiertes 4-^{15}N-Amino-3-^{15}N-Nitropyridin erzeugt werden, mit einer Gesamtausbeute von 17 % über drei Schritte.

Zusammenfassung II

NMR-Spektroskopie ermöglicht die dreidimensionale Strukturaufklärung von Proteinen in wässriger Lösung. Für die Analyse und Interpretation ist der Einbau unnatürlicher und/oder isotopenmarkierter Aminosäuren entscheidend. Dieses Masterprojekt beschäftigt sich mit der Synthese von fluoriertem Phenylalanin und der direkten Vorstufe im Metabolismus des exprimierenden Organismus (*E. coli*), Phenylpyruvat. Ausgehend von [1-^{13}C]Glycin wurde eine Synthese in drei Schritten durchgeführt um jeweils para-Fluorphenyl-[1-^{13}C]Pyruvat; 3,5-Difluor-4-Hydroxyphenyl-[1-^{13}C]Pyruvat und 2,6-Difluor-4-Hydroxyphenyl-[1-^{13}C]Pyruvat zu erhalten. Um para-Fluor Phenylalanin zu gewinnen wurde eine vierstufige Synthese ausgehend von unmarkiertem Glycin durchgeführt. Diese Verbindungen wurden synthetisiert um ihre Metabolisierung über den Shikimisäureweg von *E. coli* zu untersuchen, durch dessen Aufnahme eine selektive ^{13}C und ^{15}N Rückgratmarkierung, zusammen mit fluorierten aromatischen Ringsystemen erzielt werden kann. Mit den erlangten Kenntnissen können weitere Markierungsmuster von Phenylalanin entwickelt werden, mit besonderem Fokus auf ^{12}C – ^{2}H und ^{13}C – ^{19}F Spinsysteme für die Untersuchung von Proteindynamiken aromatischer Ringsysteme mittels TROSY.

List of Tables

List of Schemes

Part I

Synthesis of 4-^{15}N-Amino-3-^{15}N-Nitropyridine

Chapter 1

Summary

The first part of this master's thesis results from an industry cooperation with LOBA Feinchemie GmbH[1]. This funded project covers the synthesis of a double ^{15}N-labeled aromatic compound, [4-^{15}N]amino-[3-^{15}N]nitropyridine **6**. The synthetic route comprises three steps as outlined in Scheme 1. Starting from a commercially available pyridine-4-carboxylic acid (isonicotinamide) **1** an amidation via the activated carbon acid anhydride is performed to gain the respective ^{15}N-labeled amide **3**. Then a Hofmann degradation is enforced to obtain the amine **5** and in the final step an electrophile aromatic substitution is carried out to insert a ^{15}N-labeled nitro-group in ortho position to the amino group to yield the target compound **6**.

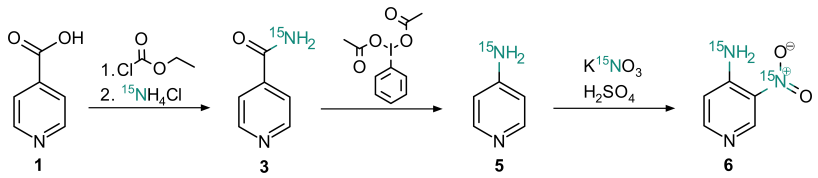

Scheme 1: synthesis path of [4-^{15}N]amino-[3-^{15}N]nitropyridine

In the first chapter an outline of the theoretical aspects of key synthetic steps is given (chapter 2), which involves carboxylic acid reactions, Hofmann degradation and aromatic nitration. In chapter 3 practical results are discussed, including tables of detailed optimization efforts for the first and second synthetic step. The last chapter contains the experimental protocols used to carry out the labeled synthesis, as well as two alternative protocols for Hofmann degradation. This is concluded by the NMR and MS spectra analysed for the ^{15}N-labeled compounds of each synthetic step and for the two alternative protocols.

[1] https://www.loba.co.at

Chapter 2

Theoretical aspects of synthetic key steps

2.1 Nucleophile substitutions on the sp^2 carbonyl carbon

The reactivity of carbonyl compounds results from the electronegativity of the carbonyl oxygen. This oxygen induces a positive partial charge on the carbonyl carbon, making it prone to nucleophilic attacks. The level of reactivity is determined by the atom or group which is bound to the acyl group (Z). In carboxylic acid derivates (carbonyl compounds class I), a weak base is a good leaving group and therefore may be easily replaced by a nucleophile (Nu^-). Further inductive effects of Z increase the electrophilic properties of the carbonyl carbon and resonance stabilizations decrease the electrophile's reactivity as outlined in Scheme 2.

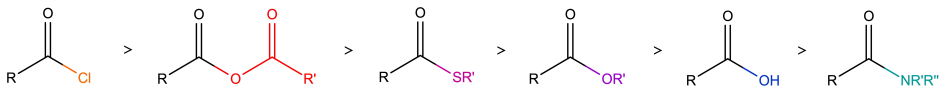

Scheme 2: relative reactivity of carboxylic acid derivates

Nucleophilic attacks at the electrophilic carbonyl carbon lead to a break of the π-bond between carbonyl carbon and oxygen, subsequently forming an unstable sp^3-hybridized tetrahedral intermediate. Due to the electronegativity of Z and Nu^-, an oxygen electron pair rebuilds the π-bond to the carbonyl carbon which leads to a depart of the better leaving group and back to sp^2 hybridization of the carbon atom. If the previously attacking Nu^- is the better leaving group, the reaction is called nucleophile acyl substitution because Z is substitued by Nu^-.

2.1.1 Carboxylic acid reactions

Carboxylic acids don't react in acyl substitutions with halide or carboxylate ions. Because these nucleophiles are weaker bases than the leaving group of the carboxylic acid, the hydroxy ion (OH^-), they would be discharged from the tetrahedral intermediate, leading to a back reaction to the educt.
In presence of an acid catalyst, carboxylic acids may react with alcohols by forming esters under dissociation of water (esterification). Acid reaction conditions are necessary to keep the carboxylic acid protonated, hence the deprotonated carboxylate ion is unreactive due to its good resonance stabilization. Because of the similar basicity of the hydroxide and alcoholate ion they are both possible leaving groups of the tetrahedral intermediate, causing

the reaction to be reversible. Therefore, an excess of alcohol and/or the utilization of a water separator (Dean-Stark apparatus) is needed to force the equilibrium to the ester production (Le Chatelier's principle). (Scheme 3a)
Carboxylic acids react with amines in acid-base reactions and not in acyl substitutions. Amines act as Brønsted bases and immediately deprotonate the carboxylic acid leading to the formation of the unreactive carboxylate ion and the aminium ion, which is no longer nucleophilic. (Scheme 3b)

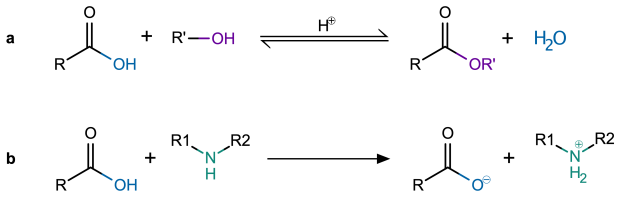

Scheme 3: reactions of carboxylic acids

2.1.2 Activation of carboxylic acids

Carboxylic acids are not very prone to nucleophilic substitutions because of the relatively strong basicity of the OH^- leaving group. Therefore, carboxylic acids are commonly activated i.e. by replacing the hydroxy group with a good leaving group, resulting in a conversion to acetic halides or anhydrides.
Carbon acid halides may be obtained by reaction of carboxylic acids with thionyl chloride ($SOCl_2$), phosgene ($COCl_2$), oxalyl chloride ($(COCl)_2$)[1], phosphor(III)-chloride or phosphor(V)-chloride (Scheme 4a).
Carbon acid anhydrides may be obtained by eliminating one molecule of water from two molecules of carboxylic acid (dehydration). This may be accomplished by heat[2] or dehydrating agents i.e. phosphor(V)-oxide (P_2O_5) or phosphorpentoxide (anhydride of phosphoric acid) (Scheme 4b). Mixed anhydrides, anhydrides with two different acyl groups (R1/R2), may be built by reaction of acetic chlorides[3,4] with carboxylic acids (Scheme 4c).

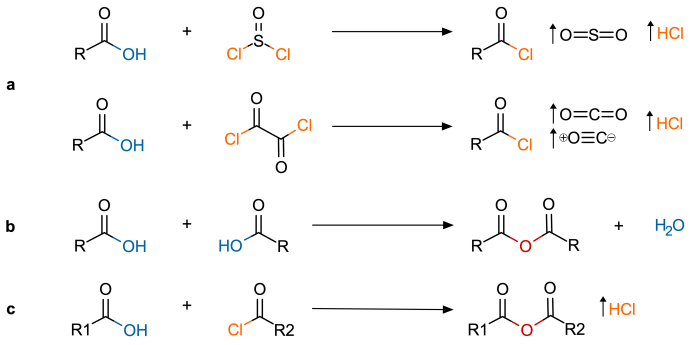

Scheme 4: overview activation of carboxylic acids

Acetic anhydrides don't react in acyl substitutions with sodium chloride or sodium bromide. Because these halide ions are weaker bases than the leaving group of the acetic anhydride, the carboxylate ion, they would be discharged from the tetrahedral intermediate, leading to a back reaction to the educt.
Acetic anhydrides react with alcohols by forming one molecule of ester and one molecule of carboxylic acid, with water by forming two molecules of carboxylic acid (hydrolysis) and with two molecules of amine (or one amine and one tertiary amine) by forming an amide and a carboxylate ion with its corresponding ammonium counterion (Scheme 5). Because the deprotonated state of each entering nucleophile is a stronger base than the carboxylate

ion of the acetic anhydride, the carboxylate ion will be the leaving group of the tetrahedral intermediate, leading to the formation of the respective products.

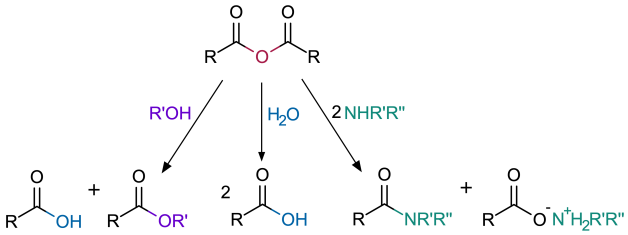

Scheme 5: reactions of carboxylic anhydrides

Also activation agents have been used, not utilizing the conversion to acetic halides or anhydrides (Scheme 6), i.e. benzotriazols[5] **a**, dicyclohexylcarbodiimide (DCC)[6] **b**, diphenylphosphoryl azide (DPPA)[7] **c**, 4-(4,6-dimethoxy-1,3,5-triazin-2-yl)-4-methylmorpholinium chloride (DMT-MM)[8,9] **d**

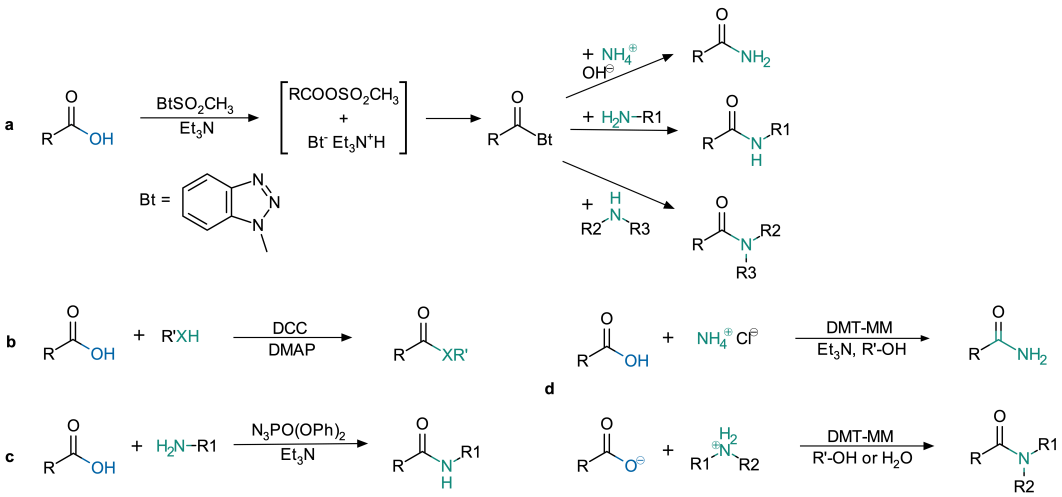

Scheme 6: methods for carboxylic acid activation

Futher, primary amides may be acquired by the hydration of nitriles[10–12] or the rearrangement of oximes (Beckmann rearrangement)[13–15] (Scheme 7).

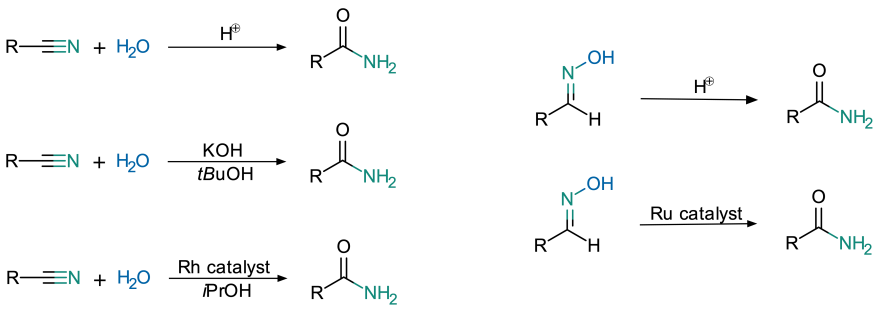

Scheme 7: alternative routes to amides

2.2 Hofmann rearrangement

Amides are relatively inert, since resonance stabilization via their lone pair at the nitrogen hinders nucleophilic attacks at the carbonyl carbon. Amides of the Hofmann rearrangement (Scheme 8) may form amines by degradation reactions as found by Curtius[16], Hofmann[17], Schmidt[18] and Lossen[19,20].

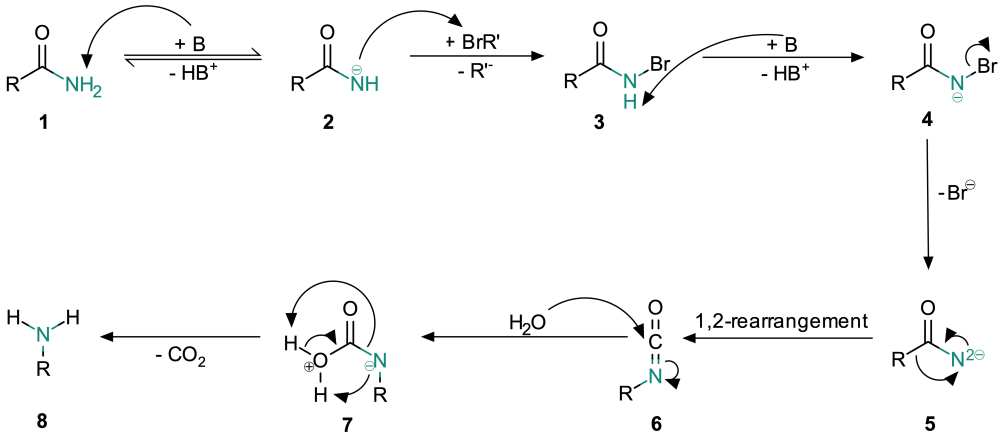

Scheme 8: general mechanism of Hofmann rearrangement

At the Hofmann degradation, shown in Scheme 8, an acidic N-H (pK_a ~22) of the carboxyl acid amide (**1**) is deprotonated by a base, creating a negatively-charged ion (**2**). The anion reacts with iodine or bromine catalysts in nucleophile substitutions by the transfer of the partial positively-charged iodine or bromine atom to get iodo or bromo amides (**3**). The base deprotonates the remaining N-H (**4**) which discharges the iodide/bromide ion, forming an acylnitrene (**5**). In a 1,2-rearrangement the acyl rest migrates to the (negatively-charged) nitrogen assembling the isocyanate intermediate (**6**). In a nucleophilic addition the isocyanate adds water to form the unstable carbamide acid (**7**), which spontaneously decarboxylates to yield the desired amine (**8**).

Hofmann rearrangement has been successfully conducted in literature reported protocols employing the following reagents, shown in Scheme 9: potassium hypobromide (KOBr), sodium hypobromide (NaOBr), sodium hypochloride (NaOCl)[21,22], calcium hypochloride (CaOCl), iodobenzene with potassium peroxymonosulfate (Oxone®)[23], pentamethyliodobenzene[24], iodosylbenzene (PhIO)[25], phenyliodo diacetate (PIDA)[26,27], bis-[(trifluoroacetoxy)iodo]benzene[28], 3-[hydroxy(tosyloxy)iodo]benzoic acid[29], N,N-dibromo-p-toluensulfonamide ($TsNBr_2$)[30], N-bromosuccinimide (NBS)[31,32], 1,3-dibromo-5,5-dimethylimidazolidine-2,4-dione[33], N-bromoacetamide[34], tribromoisocynuric acid[35], trichloroisocyanuric acid[36] and lead(IV) acetate[37]

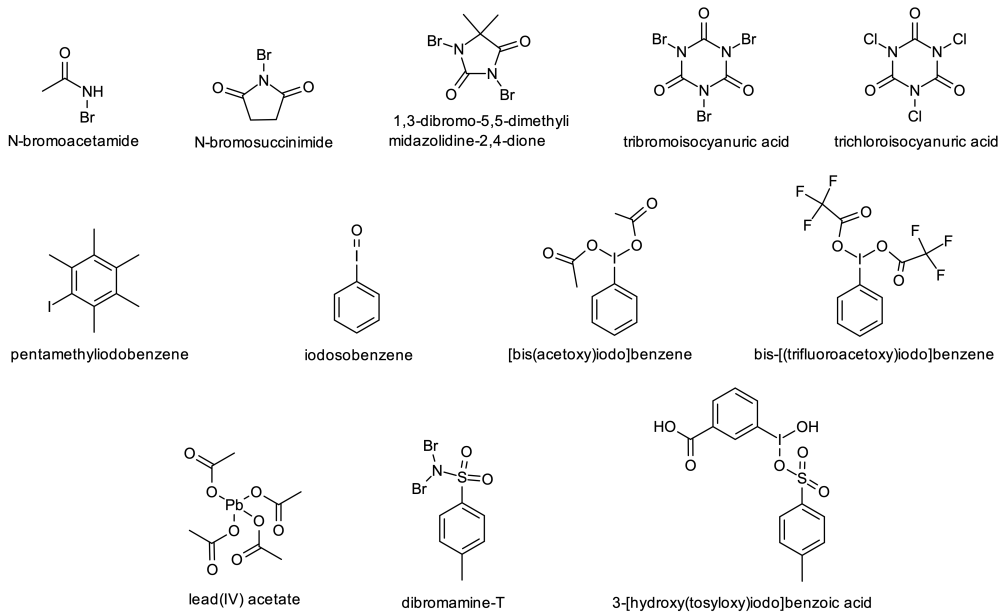

Scheme 9: reagents previously used for Hofmann rearrangement

2.3 Electrophilic aromatic substitution: nitration

Nitration of aromatics is essential in chemical and pharmaceutical industries and is therefore very well studied[38–40]. Traditionally, a nitronium ion (NO_2^+) reacts in electrophilic substitution with an aromatic carbon by forming a less-stable, not-aromatic carbocation (σ-complex, 'Wheland intermediate'). A base then abstracts the proton to re-establish the stable aromatic state (Scheme 10).

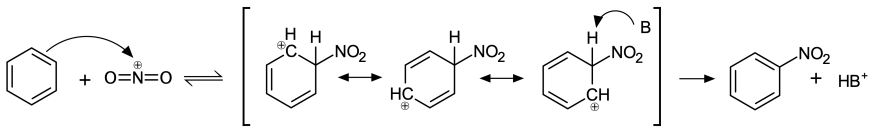

Scheme 10: aromatic nitration

In the majority of cases a mixture of concentrated nitric acid (HNO_3) and sulfuric acid (H_2SO_4) is employed, whereas H_2SO_4 protonates HNO_3 to form the NO_2^+[41]. The choice of solvents is crucial[38,39] concerning not only the formation of the NO_2^+ and the deprotonation of the σ-complex but also regarding solvation effects on electronic structure and state[42]. Also substituents on the arene nucleophile influence the electronic environment, consequently affecting activation and direction. Due to issues of isomeric mixtures, over-nitration and poor selectivity there is ongoing research on alternative reagents and methods[43] including possible reaction pathways without σ-complex formation[44–46].

	activating substituents	deactivating substituents
cationic σ-complex	stabilizing	less stable
electron	donating	withdrawing
effects	+ inductive	- inductive effects
	+ resonance	unfavorable charge-charge repulsive interactions
direction	para/ortho	meta
groups	amino, hydroxy, alkyl, alkoxy, amido, aryl	nitro, ammonium, sulfonium, aldehydes, ketones, acids, exters, carboxamides
exception		halogens (ortho/para directing)

Table 1: substituents in S_EAr

2.3.1 Nitration of pyridines

Electrophile aromatic substitutions of pyridine and its derivates has been challenging owing to the reduced reactivity due to nitrogen protonation (formation of pyridinium salts)[47]. Compared to benzene, pyridine undergoes nitration more than 1000 times slower[48], resulting in low yields[49]. In early studies, nitration of pyridines resulted in 3 % of 3-nitropyridine using HNO_3 in H_2SO_4[50] and 1 % using KNO_3 in H_2SO_4 at 330°C[51]. In 1994 Bakke et al. reported a new method employing dinitrogen pentoxide (N_2O_5) in sulfur dioxide (SO_2) solution, to give N-nitropyridinium ion intermediates which resulted in 3-nitropyridines in good yield upon treatment with H_2O[52]. In 2005 Katritzky et al. developed a procedure for the nitration of pyridines utilizing HNO_3 (Scheme 11) with high yields by optimizing conditions and the relative amounts of reactants[47].

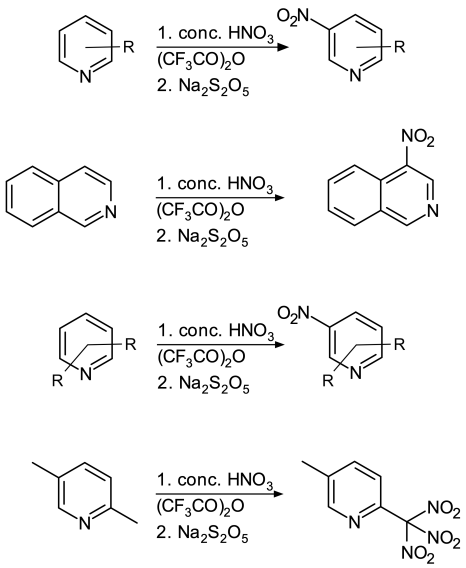

Scheme 11: direct nitration of substitued pyridines by Katritzky et al.[47]

Chapter 3

Results

To obtain the double [4-^{15}N]amino-[3-^{15}N]nitropyridine (^{15}N-labeled ANP) **6**, a three-step synthesis was pursued as outlined in Scheme 12. The synthetic protocols were optimized using unlabeled ammonium chloride (NH_4Cl) and unlabeled potassium nitrate (KNO_3) as will be described within this chapter.

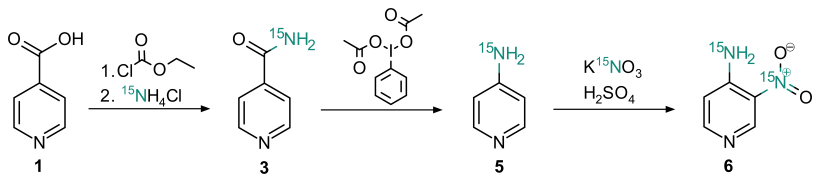

Scheme 12: synthetic route to yield the target compound [4-^{15}N]amino-[3-^{15}N]nitropyridine **6**

Starting from isonicotinic acid **1** by Sigma-Aldrich®, amidation of the carboxylic acid was performed as proposed by Ezawa et al.[4] and illustrated in Scheme 13. In the first step the activation of isonicotinic acid was conducted by adding ethyl chloroformate ($ClCO_2Et$) in presence of triethylamine (Et_3N) to obtain the mixed anhydride **2**. Subsequently NH_4Cl was added in-situ in the second step to yield isonicotinamide (INA) **3** and carbonic acid ethyl ester as side product.

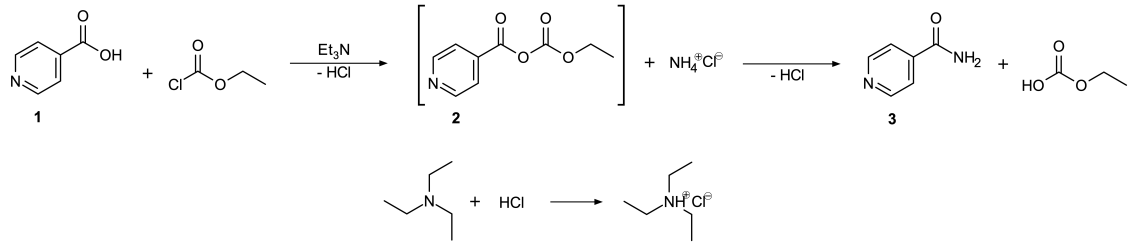

Scheme 13: synthesis of isonicotinamide

An excerpt of optimization efforts for the synthesis of INA is displayed in Table 2. Based on the protocol for INA from Ezawa et al.[4] changes of reactants and reagents did not reveal improvements regarding yield or purity. Changes in reaction times, particularly the final stirring duration to form INA **3** from the anhydride intermediate **2** after in-situ addition of NH_4Cl did not show any correlation to the amount of formed product **3**. Unsuccessful work-ups and purifications were carried out in alkaline pH through 1 M NaOH, by extraction with Et_2O, by water evaporation, recrystallization (EtOH, toluol) and column chromatography (EE/heptane, ratios from 1:1 to 95:5) respectively. Increased

yields were mastered by targeting INA's polarity through deliberate selection of solvent volumes, especially for the extraction with EtOAc. Summarizing, Ezawa et al. stated yields of 95 %, but only a maximum of 76 % was accomplished after optimization efforts (Table 2). The labeled synthesis was performed as described in section 5.2 resulting in 51 % yield of isonicotin-[^{15}N] amide **3**.

Table 2: overview of optimization efforts of isonicotinamide synthesis

Isonicotinamide 3	literature[4]	08-24	10-08	11-05	11-11	11-22
Isonicotinic acid [mg]	3080 mg	1000	1000	2000	1000	3080
THF_{dry} [ml]	400 ml	130	100	200	100	400
Et_3N [equ]	3 equ	3	3	3	3	3
$ClCO_2Et$ [equ]	1.4 equ	1.4	1.4	1.4	1.4	1.4
NH_4Cl [equ]	1.5 equ	1.5	1.5	1.5	1.5	1.5
stirring duration	30 min	0-2 days	5-7 days	0-2 days	1. 30 min	1. overnight
					2. overnight	2. + 3. 45 min
extraction	3x EtOAc	3x EtOAc	EtOAc	5x EtOAc	5x DCM	DCM
			cont. liqu-liqu			cont. liqu-liqu
wash	brine	brine	-	-	-	-
column chromatography	silica	silica	-	-	-	silica
	EtOAc	EE/MeOH/NH_4				EE/MeOH/NH_4
yield	**95 %**	**26-37 %***	**53-57 %**	**38-76 %**	**1. 51 %**	**1. 46 %**
		56 %			**2. 71 %**	**2. 76 %***
						3. side product*

*no purification via column chromatography

To gain the amine, 4-aminopyridine (4AP) **5**, Hofman degradation was initially performed as suggested by the Chinese patent CN106554306A[27], embodiment 5 (Scheme 14). Due to very low yields down to complete absence of product, various optimization efforts were conducted as summarized in Table 3.

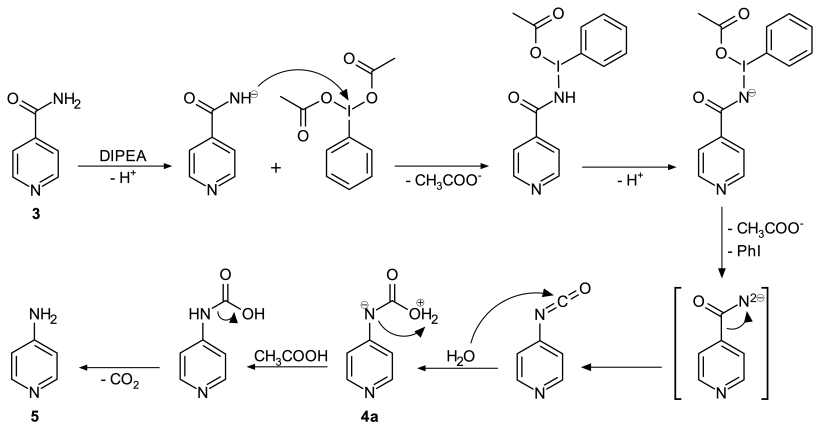

Scheme 14: mechanism of 4-aminopyridine synthesis

Table 3: overview of optimization efforts of 4-aminopyridine synthesis

Aminopyridine 5	literature[27]	09-06	09-16	09-20	09-23
INA	2500	367	334	210.5	300
ACN/H_2O 1:1 [ml]	30 ml	5	4	4.5	4
DIPEA [equ]	1.1 equ	1.1	1.1	1.1	*1.1 Et3N*
PIDA [equ]	1.1 equ	1.1	1.2	1.2	1.2
stirring T [°C]	30 °C	30	30	*45*	30
stirring duration	4 h	4 h	1. + 2. 4 h 3. *overnight*	4 h	*overnight*
acid	acetic	acetic	*hydrochloric*	*hydrochloric*	*hydrchloric*
stirring duration	30 min	30 min	1. + 3. 30 min 2. *overnight*	*overnight*	30
wash	-	-	*3x DCM*	-	*3x DCM*
alkalisation	-	-	*1 M NaOH*	*1 M NaOH*	*1 M NaOH*
extraction	3x DCM	3x DCM	3x DCM	3x DCM	3x DCM
wash	brine, water	brine, water	brine, water	brine, water	brine, water
recrystallisation	toluol	toluol (reflux)	MeOH/DCM (US)	DCM/heptane (US)	EE/heptane (US)
product	grey-beige solid	yellow-brown oil	red solid/brown oil	yellow oil	red oil
yield	**96 %**	**-** mono-substitued aromatic compound	**18 %** **2. + 3. ++** impurities	**+** impurities	**++**

Due to low yields induced by oiling out, impurities and massive salt concentrations two further protocols for Hofmann degradations were investigated as outlined in Scheme 15.

The first alternative (Scheme 15**b**) was adapted from previously known literature of De Sousa and Novak[32] for the Hofmann degradation of benzamide to aniline hydrochloride via methyl phenylcarbamate. Applying NBS with 1,8-diazobicyclo[5.4.0]unde-7-ene (DBU) as base for INA **3** resulted in a different product than the desired n-(4-pyridyl) methyl carbamate intermediate. Extraction under basic conditions to avoid water-soluble salt formation of the methyl carbamate, subsequently leading to a migration to the organic phase, revealed the desired compound **4b** after work-up. HCl with reflux-heating was utilized to decarboxylate the intermediate, resulting in low yields of aminopyridine hydrochloride **5b**.

The second alternative (Scheme 15**c**) was tried as proposed by the Chinese patent CN1807415A[53], using I_2, Br_2 and NaOH as catalyst. This route unfortunately led to the formation of a di-brominated 4AP **5c**.

Due to unsatisfying alternatives, optimization efforts for route **a** were resumed. Learning from other trials, the strong affinity of 4AP to water was confronted by utilizing a reverse dean-stark apparatus for continuous liquid-liquid extraction in combination with different solvents and water evaporation (Table 4). Each extraction was challenged by the massive amounts of sodium acetate generated by neutralizing the CH_3COOH with NaOH.

Table 4: overview of optimization efforts of 4-aminopyridine synthesis 2

Aminopyridine 5	10-22	11-11	11-18	11-23
INA	1324	500	750	545
DIPEA [equ]	1.1	1.1	1.1	1.1
PIDA [equ]	1.2	1.2	1.2	1.2
stirring duration [h]	*2 days*	3.5	3.5	4
acid	hydrochloric	hydrochloric	hydrochloric	acetic
stirring duration [min]	120	*overnight*	*overnight*	30
quenching	brine	-	-	-
wash	3x DCM	3x DCM	2x DCM	2x DCM
alkalisation (pH 12)	1 M NaOH	1 M NaOH	NaOH	1 M NaOH
extraction	-	3x DCM	DCM	1. 3x DCM
	-	-	*cont. liqu-liqu*	*2. EtOAc*
water evaporation	*yes*	-	-	-
product	beige solid	white-yellow solid	white-yellow solid	white-yellow solid
yield	**∼60 %**	**12-23 %**	**1. 34 %**	**50 %**
	Na-acetate	Na-acetate	**2. ++** impurities	**2. ++** Na-acetate

Using MeOH as solvent as suggested in embodiment 6[27] and removal of sodium acetate crystals by vacuum filtration prior extraction (protocol section 5.3) finally improved purity and yielded more than 70 % and was implemented later on for the labeled synthesis.

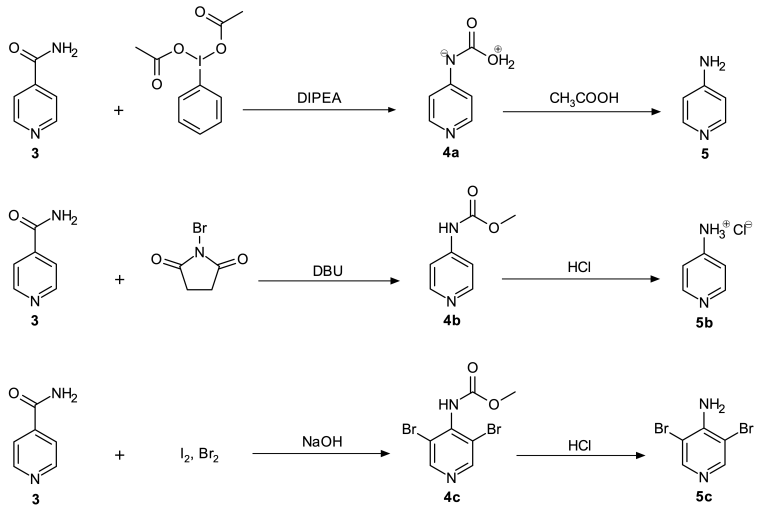

Scheme 15: tested routes to yield 4-aminopyridine

The final step comprised a straightforward aromatic nitration of the amine, inserting a nitro group at ortho position 3 of the pyridine ring (Scheme 16).

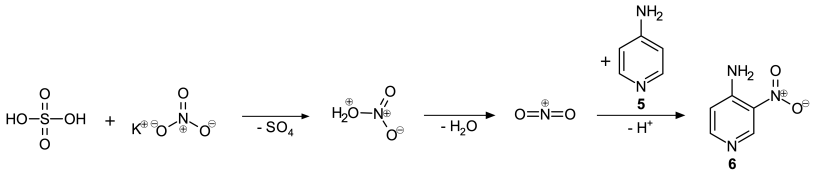

Scheme 16: aromatic nitration

The labeled synthesis of 4-amino-3-nitropyridine was carried out as described in the optimized synthetic protocols in chapter 5 and resulted in 1.63 g of ^{15}N-labeled ANP **6** consuming 5 g of $^{15}NH_4Cl$ and 2 g $K^{15}NO_3$ in overall yield of 17 % via three steps from isonicotinic acid.

Optimization of 4-amino-3-nitropyridine 6 synthesis

Shortened reaction times, as implemented to the synthesis of the *^{15}N-labelled 4-amino-3-nitropyridine*, resulted in similar yields to the reaction times of the literature[1] (44-58 %).

[1] LOBA-MBR VO052901

Chapter 4

Conclusion

The steps of the synthetic route of ^{15}N-labeled ANP **6** were optimized and insight into properties of pyridine derivates was gained. For amidation of isonicotinic acid **1** changes of reactants and reagents did not reveal any improvement. Targeting INA's **3** polarity increased yield and removed impurities. Concerning the Hofmann rearrangement step the reaction was conducted with PIDA. Alternative protocols gave lower (**5b**) or no product (**5c**) yields. Employing embodiment 6[27] with extraction under basic conditions and subsequent removal of sodium acetate resulting from pH adjustments using CH_3COOH and NaOH drastically improved yield (to 72 %). For the introduction of the nitro group via aromatic nitration reaction times could be greatly depleted.
The final synthesis deploying 5 g of nitrogen-15 ammonium chloride and 2 g of nitrogen-15 nitric acid as ^{15}N sources resulted in 1.63 g of [4-^{15}N]amino-[3-^{15}N]nitropyridine **6**, with an overall yield of 17 %.

Chapter 5

Experimental section

5.1 Materials and methods

All solvents were distilled prior to use or purchased from commercial suppliers and used without further purification. Tetrahydrofuran (THF) was dried with MBRAUN solvent purifier MB-SPS-5. Isotope-labeled reagents were purchased from Euriso-top® with following purity grades: ammonium chloride (15N, 99 %) LOT 15ACLG-12-18 and potassium nitrate (15N, 99 %) LOT I-23029H. Other reactants were purchased from further commercial suppliers. Vacuum evaporation was performed on BÜCHI Rotavapor R-210 and R-100 connected to a Recirculating Chiller F-100. Column chromatography was carried out using silica gel 60 (0.040 – 0.063 mm, LOT 040353707) from MACHEREY-NAGEL GmbH & Co. KG. Thin layer chromatography (TLC) was conducted on pre-coated TLC sheets ALUGRAM®Xtra SIL G/UV_{254} from MACHEREY-NAGEL GmbH & Co. KG, layer: 0.20 mm silica gel 60 with fluorescent indicator UV_{254} LOT 802046. TLC was examined using UVAC-60 neolab ultraviolet lamp (254 nm) or by application of aqueous $KMnO_4$ (0.5 %) solution followed by heat treatment via hot-gun. NMR spectra were recorded on Bruker AVANCE NEO spectrometers at 400 MHz and Bruker AVANCE III HD at 176 MHz. Chemical shifts were given in parts per million (ppm). NMR spectra were evaluated with TopSpin™ by Bruker. MS and high resolution mass spectrometry (HRMS) experiments were acquired using Bruker amaZon speed ETD and Bruker maXis with electron ionization (EI, 70 eV) or electrospray ionization (ESI, 3 keV).

5.2 Isonicotin-[^{15}N]amide 3

formula	molecular weight	yield	appearance
$C_6H_6N_2O$	123.12 g/mol	51 %	white solid

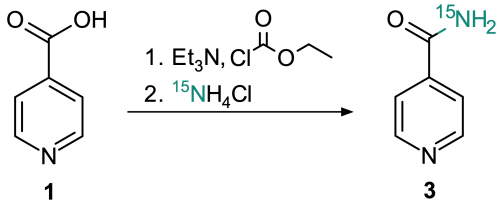

		m[g]	ρ[g/ml]	V[ml]	M[g/mol]	n[mmol]	equivalents
Isonicotinic acid **1**	$C_6H_5NO_2$	7.7		-	123.11	62.55	1
Triethylamine	Et_3N	18.86	0.73	26	101.19	186.41	3
Ethyl chloroformate	$ClCO_2Et$	9.49	1.14	7.33	108.53	87.48	1.4
Ammonium chloride	$^{15}NH_4Cl$	5.0		-	54.48	91.78	1.5

Table 5: reactants and reagents for the synthesis of isonicotin-[^{15}N]amide

Isonicotinic acid was weighed into a dry 1000 ml three-necked flask. After adding 500 ml of dry THF to the white powder, the reaction bulb was set under argon atmosphere. The white suspension was stirred for 10 minutes and then placed in an ice bath. Cooled to 0 °C $ClCO_2Et$ and Et_3N were added drop-wise through syringes and the reaction mixture was stirred for 30 minutes at 0 °C.

^{15}N-labeled NH_4Cl was dissolved in 30 ml of deionised water and added to the vessel over 15 minutes. When the mixture was stirred for another 30 minutes at 0°C, a white solid precipitated within the colourless liquid. The ice bath was removed and the mixture was stirred to room temperature. 40 ml of deionised water were added to the bulb to solubilise the white solid. The liquid mixture was transferred to a separating funnel and extracted five times with 100 ml of EtOAc. The combined organic phase was dried over $MgSO_4$ and the solvents were removed under reduced pressure at 240 mbar and 38 °C until a light beige solid was left in the bulb. The crude product was dissolved in a mixture of EtOAc, MeOH and NH_4 25 % (5 ml : 5 ml : 1 ml) and purified through column chromatography using silica gel as stationary phase and EtOAc, MeOH and NH_4 25 % (77:22:1) as mobile phase. Reaction progress was controlled through TLC using the same solvent mixture. The product fractions were identified using a UV lamp, combined, dried over $MgSO_4$ and transferred to a 1000 ml round-bottomed flask. The solvents were removed under reduced pressure. The white solid was vacuum-dried via oil pump giving a yield of 51 % (3.75 g, 30.48 mmol).

5.3 [4-^{15}N]aminopyridine 5

formula	molecular weight	yield	appearance
$C_5H_6N_2$	95.110 g/mol	72 %	white solid

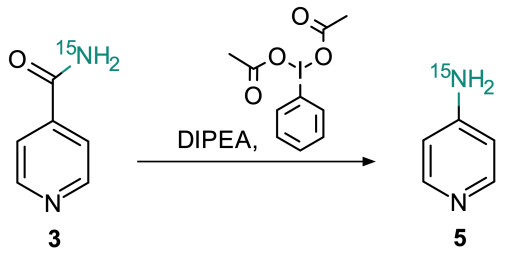

		m[g]	ρ[g/ml]	V[ml]	M[g/mol]	n[mmol]	equivalents
Isonicotin-[^{15}N]amide **3**	INA	3.753		-	123.12	30.48	1
N,N-Diisopropylethylamide	DIPEA	4.526	0.742	6.1	129.24	35.02	1.15
Phenyliodo diacetate	$PhI(OAc)_2$	11.056		-	322.10	34.32	1.13

Table 6: reactants and reagents for the synthesis of [4-^{15}N]aminopyridine

INA **3** was dissolved in a round-bottomed flask with 46 ml of MeOH/H_2O 1:1. N,N-Diisopropyl ethylamine (DIPEA) and phenyliodo diacetate were added during continuous stirring. The slightly yellow suspension was heated in an oil bath to 30 °C, equipped with a reflux condenser and stirred for at least 3.5 hours until the PIDA was completely dissolved. CH_3COOH was added to the reaction mixture to give a pH value of 4 (verified by pH paper). After 30 minutes of stirring MeOH was removed with reduced pressure at 75 mbar and 38 °C. The yellow liquid was transferred to a separation funnel and washed three times with 50 ml of DCM to remove DIPEA. NaOH pellets were dissolved in deionised water and added to the mixture causing an exothermic reaction. Reaching a pH value of 12 the solution turned dull. When the suspension cooled down to room temperature colourless crystals of sodium acetate precipitated and were removed by vacuum filtration with a filter funnel. The yellow filtrate was returned to the separating funnel and extracted five times with 100 ml of EtOAc. The combined organic phases were dried over $MgSO_4$ and EtOAc was removed under reduced pressure. The beige-grey solid was vacuum-dried via oil pump resulting in a yield of 72 % (2.08 g, 21.87 mmol).

5.3.1 Alternative synthesis path of 4-aminopyridine 5b

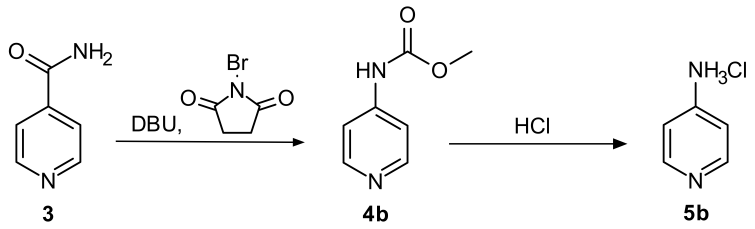

		m[g]	ρ[g/ml]	V[ml]	M[g/mol]	n[mmol]	equivalents
Isonicotinamide **3**	INA	0.26/0.4		-	122.12	2.13/3.28	1
N-bromosuccinimide	NBS	0.754/1.158		-	177.98	4.24/6.51	2
1,8-diazobicyclo[5.4.0]unde-7-ene	DBU	0.733/1.12	1.018	0.72/1.1	152.24	4.81/7.36	2.24

Table 7: reactants and reagents for the alternative synthesis **b** of 4-aminopyridine

In a 250ml three-necked flask INA **3** was dissolved in 60 ml MeOH. After mixing in half of the NBS, the solution turned yellow. During continuous stirring DBU was added and the vessel was reflux heated in an oil bath at 85 °C. After 15 minutes the other half of NBS was added and the reaction mixture was reflux-heated for another 30 minutes. Methanol was removed under reduced pressure of 100 mbar at 37 °C. The yellow viscous liquid was combined with 45 ml of EtOAc and transferred to a separating funnel. The organic layer was washed three times respectively with 20 ml of 6 N HCl, 20 ml of 1 N NaOH and 20 ml of brine. The combined organic phases were dried over $MgSO_4$ and the solvents were evaporated at 37 °C and 175 mbar to obtain 1.2 g of a yellow liquid. The crude product was purified through column chromatography (silica, PE/EE 6:1), dried over $MgSO_4$ and separated from the solvents by rotovap at 37 °C and 5 mbar to yield 37 mg of a yellow solid. The analysis through ^{1}H-NMR (Scheme 40) exposed a different compound than the desired n-(4-pyridyl) methyl carbamate **4b**.

As a consequence the precipitate of the initial aqueous phase was dissolved in 30 ml of 1 N NaOH and extracted three times with 30 ml of EtOAc. The combined organic layers were again dried over $MgSO_4$ and the solvents were evaporated under reduced pressure at 150 mbar and 37 °C to yield 134 mg of a colourless solid. The ^{1}H-NMR (Scheme 41) indicated the desired compound **4b**.

The methyl carbamate was dissolved in its vessel with 3 ml of concentrated HCl. The reaction mixture was reflux-heated at 100 °C overnight. The next day the oil bath was removed and when the mixture reached room temperature, it was quenched with 15 ml of water. The aqueous phase was washed two times with EtOAc and then evaporated under reduced pressure at 60 °C until 15 mg of 4AP **5b**, appearing as light yellow solid were left (Scheme 43).

5.3.2 Alternative synthesis path of 4-aminopyridine 5c

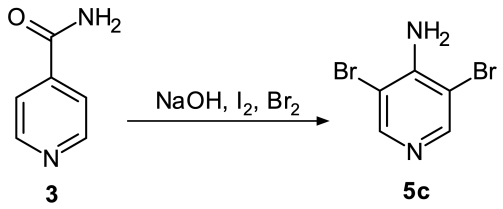

3 **5c**

		m[g]	M[g/mol]	n[mmol]	equivalents
Isonicotinamide **3**	INA	0.488	122.12	4.0	1
Iodine	I_2	0.046	253.808	0.18	0.045
Sodium hydroxide	NaOH	0.4	39.997	10.0	2.5
Bromine	Br_2	0.719	159.81	4.5	1.125

Table 8: reactants and reagents for the alternative synthesis **c** of 4-aminopyridine

In a 50 ml two-necked flask iodine was added to deionised water to create a 1 M iodine solution. When the iodine was fully dissolved the vessel was placed in an ice bath and cooled to 0 °C. During continuous stirring 1.7 ml of 5 M NaOH solution and bromine were slowly added to create the catalyst. INA **3** was subsequently added to the cooled catalyst and the reaction mixture was stirred for 45 minutes at 0 °C until a dark brown solid precipitated. The flask was equipped with a reflux condenser, slowly heated to 80 °C and stirred for 50 minutes. To acquire strong acidity (pH value of 1-2) 1 M HCl solution was added and the reaction solution turned orange-red. The oil bath was removed and when the vessel reached room temperature 1 M NaOH solution was added. At strong alkalinity (pH value of 12-13) a colourless solid precipitated and the liquid turned yellow. After half of the water was evaporated in vacuo at 60 °C, the suspension was cooled to 0 °C. 80 mg of brown crude product were obtained by vacuum filtration via buechner funnel. The analysis through ^{1}H-NMR (Scheme 44) and mass spectrometry (Scheme 77) exposed a di-brominated 4AP **5c**.

5.4 [4-^{15}N]amino-[3-^{15}N]nitropyridine 6

formula	molecular weight	yield	appearance
$C_5H_5N_3O_2$	141.100 g/mol	46 %	orange solid

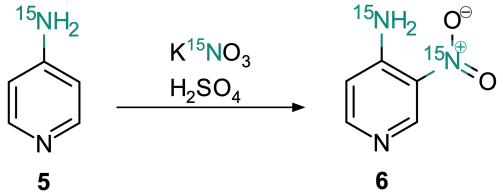

5 **6**

		m[g]	ρ[g/ml]	V[ml]	M[g/mol]	n[mmol]	equivalents
[4-^{15}N]aminopyridine **5**	4AP	1.81		-	95.109	19.03	1
Sulfuric acid	H_2SO_4	32.944	1.83	18	98.08	335.88	17.65
Potassium nitrate	K^{15}NO$_3$	2.0		-	102.097	19.59	1.03

Table 9: reactants and reagents for the synthesis of [4-^{15}N]amino – [3-^{15}N]nitropyridine

In a 250 ml two-necked flask K^{15}NO$_3$ was added to ice-cooled H_2SO_4. The reaction mixture was stirred for 1.5 hours at room temperature to gain a viscous and clear solution. The vessel was cooled in an ice bath when [^{15}N]4AP **5** was slowly added. During continuous stirring at room temperature the reaction mixture turned red as the 4AP **5** dissolved. After 1.5 hours 4AP **5** was completely dissolved and the reaction vessel was equipped with a reflux condenser and heated to 65 °C in an oil bath to conduct the rearrangement. After 2 hours the oil bath and reflux condenser were removed and the ochre-brown reaction mixture was allowed to come to room temperature. The flask was placed in an ice bath and cooled down to 0 °C when 50 ml of ice-cold water were added to quench the reaction. The ice bath was removed and the solution was slowly reheated in an oil bath by stirring for 30 minutes at room temperature and then heating up the oil bath to 60 °C. At 60 °C 25 % NH_4OH were used to neutralise the solution which initiated the precipitation of the crude product. The suspension was stirred for 30 minutes at 60 °C, equipped with a reflux condenser, and then slowly cooled to 6 °C over night to pursue the precipitation. The next day the orange crude product was separated from the yellow-brown liquid through vacuum-filtration using a filter funnel and washed two times with cold, deionised water. The crude product was dissolved in hot EtOAc and recrystallised from heptane to yield 380 mg (28 %, 2.69 mmol) of [4-^{15}N]amino-[3-^{15}N]nitropyridine **6** (a). A second synthesis was conducted with the same implementation yielding 376 mg (28 %, 2.67 mmol) of [4-^{15}N]amino-[3-^{15}N]nitropyridine **6** (b). Two further fractions were isolated from the combined filtrates of the two synthesis' (a+b) after extraction with EtOAc. 520 mg (19%, 3.69 mmol) were obtained from the combined organic layers by drying over $MgSO_4$ and evacuating the solvent under reduced pressure. This fraction showed some impurities in the corresponding NMR spectra. The second fraction revealed 350 mg (13 %, 2.48 mmol) of [4-^{15}N]amino-[3-^{15}N]nitropyridine **6** from the water layer by recrystallising from ethanol and from heptane. Unlabelled implementations (section 3 'optimization') in initial trials under same conditions resulted in higher yields (up to 58 %).

Part II

Fluorinated ^{13}C-compounds for selective protein labeling

Chapter 6

Introduction

Proteins are biological macromolecules consisting of amino acids linked by peptide bonds between the amino and carboxy group. The distinct side chains of the amino acids hold a major impact to their biochemical mode of action. Due to variable peptide lengths, amino acid sequence and building blocks, a high degree of conformational diversity exists, subsequently leading to highly specific configurations.

Peptides are found in every cell where they have diverse physiological and biochemical functions. Oligopeptides may act as signalling substances (e.g. hormones, neurotransmitters), while more than 50 amino acids are essential for enzymatic function[54]. Proteins and peptides play major roles in immune response, metabolism, reproduction etc. thus slight changes within their conformation may lead to pathogenic evolution and disease development. Therefore a profound understanding of their conformational nature, dynamics and interactions is fundamental for suited drug development.

The theory of the chemical structure was first developed by August Kekulé in 1858, who believed that atoms within chemical compounds possess a definite order resulting in a three dimensional structure which can be solved[55]. Nowadays, three-dimensional structure determination is performed mainly by three methods capable of investigating proteins at atomic resolution[56] as illustrated in Table 10 and Scheme 17.

Molecular Type	X-ray	NMR	EM	Multiple methods	Other	Total
Protein (only)	146871	11954	7471	186	104	166586
Protein/Oligosaccharide	8676	31	1306	5	0	10018
Protein/NA	7750	277	2369	3	0	10399
Nucleic acid (only)	2445	1408	62	11	3	3929
Other	154	31	5	0	0	190
Oligosaccharide (only)	11	6	0	1	4	22

Table 10: data export summary PDB[57]

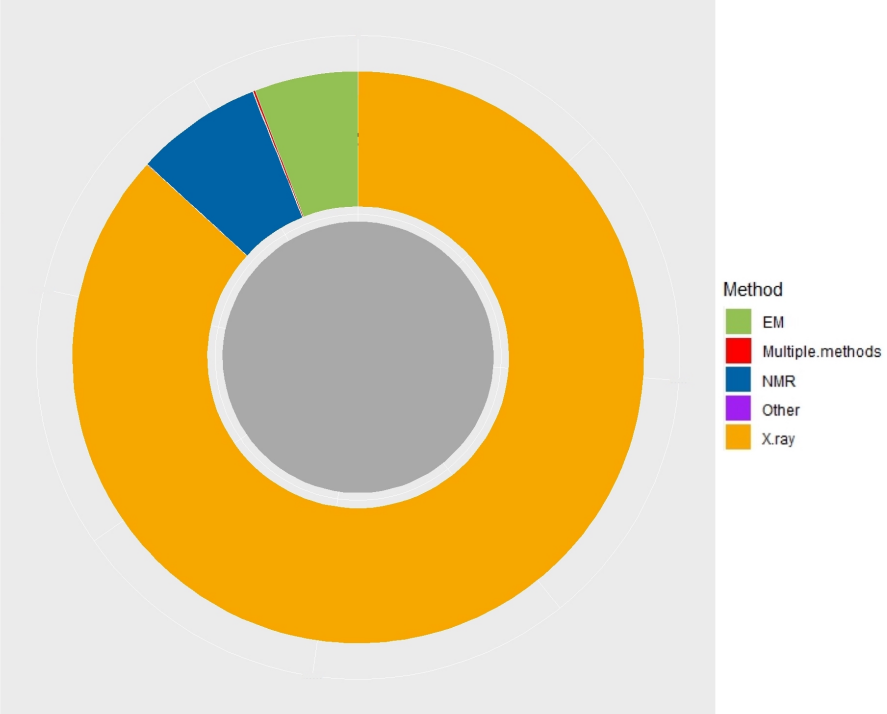

Scheme 17: sunburst chart distribution by experimental methods[57]

Proteins and other biological macromolecules naturally occur in solutions of specific pH and temperature ranges. As for now, NMR spectroscopy is the only method allowing the analysis under these conditions. But as shown in Table 11 and Scheme 18 each of the three methods has its own advantages and disadvantages. Depending on the question referring to the structure to be investigated, the most suited method needs to be chosen.

	X-ray[58]	NMR[56,59]	EM[60]
size limit	20 – 50 µm	< 30 kDa	> 100 kDa
sample preparation	challenging	none	simple
analysis conditions	crystallized	hydrated, rt	frozen
dynamic information	no	yes	no
near native conditions	no	yes	yes
data collection	automatable	automatable challenging at high MW	manual expertise
spatial resolution	∼1 Å	∼2-5 Å	∼6 Å
major disadvantages	static snapshot crystallization	high sample amount high concentration size limit	low resolution technically difficult size limit

Table 11: comparison of the main structure determination methods

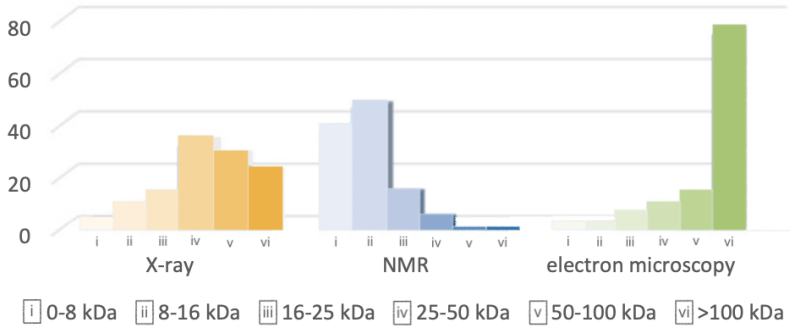

Scheme 18: molecular weight distribution by experimental methods[57]

In 1985 high-resolution NMR spectroscopy was first utilized for structure determination of proteins at atomic resolution[61,62]. At present, structure elucidation of peptides and small proteins is routinely conducted by NMR spectroscopy[54,63] and more than 6 % of the reported protein structures within the protein data bank were solved via NMR (Scheme 17)[57]. Constant progress has been made in hardware (NMR spectrometer, magnetic field, cryo probehead, solid-state NMR), software (automated signal assignment[64,65], data analysis), sample preparation (labeling, protein expression) and experimental techniques (multi-dimensional NMR) to address issues concerning sensitivity (low S/N, high sample amount, sample aggregation) and resolution (complex spectra, signal overlapping, signal broadening through spin diffusion, laborious signal assignment). For structure elucidation of three-dimensional proteins NMR analysis relies on stable isotope labeling with ^{2}H, ^{13}C and ^{15}N[66]. Isotope labeled proteins can be obtained by utilizing the biosynthetic pathway of overexpressing organisms (Scheme 21), cell-free expression systems or solid phase synthesis as explained in more detail in chapter 8, subsection 8.2.2. Target proteins may be labeled uniformly, segmental or site-specific with one or more stable heavy isotopes. Amongst the various NMR methods available, the most appropriate experiment must be wisely chosen to address a specific biomolecular question.

Chapter 7

Aim of the project

This project focused on the synthesis of fluoro-phenylalanine precursor compounds consisting of fluorinated aromatic systems (Scheme 19). By adding ^{15}N-enriched ammonium sources to the minimal medium of an overexpressing system the fluorinated precursor compound will acquire ^{13}C and ^{15}N backbone labeling within protein incorporation. This multi-resonance approach for protein NMR aims to evaluate folding and conformational changes after binding through anticipated NMR spectra simplification due to the ^{19}F nucleus.

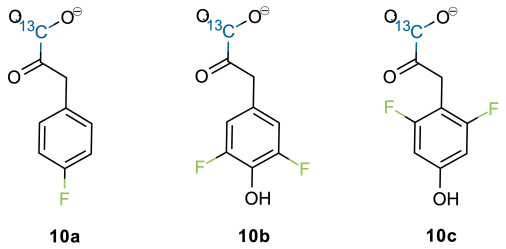

Scheme 19: α-keto pyruvates: fluorinated ^{13}C-labeled phenylalanine precursor compounds

The large spectral dispersion[67,68] and large gyromagnetic ratios of ^{1}H and ^{19}F cores[69] have been proven to be beneficial for the investigation of protein interactions in previous studies[70–72]. Since phenylalanine and other aromatic amino acids are overrepresented within protein binding sites and contribute to hydrophobic and electrostatic π-interactions[73], selective labeling of phenylalanine for the study of binding interactions is reasonable[74]. The design of further labeling patterns based on the fluorination of the synthesized compounds **10a-c** is demonstrated in Scheme 20 **10a*-c***. The alternating ^{12}C – ^{2}H and ^{13}C – ^{19}F spin systems are feasible to attain defined relaxation pathways due to the demand of NMR experiments.

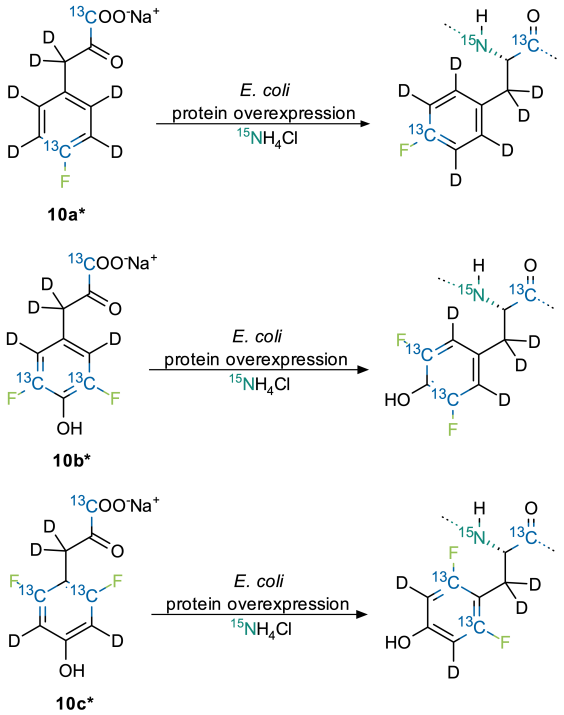

Scheme 20: labeling patterns with alternating ^{12}C-^{2}H and ^{13}C-^{19}F spin systems, adapted from unfluorinated sodium [1-^{13}C]phenylpyruvate[75]

For protein incorporation of the synthesized compounds, *E. coli* will be assessed as overexpression system. Therefore another part of this project was to synthesize corresponding amino acids to address the question which method directs to the highest incorporation rates, the labeled α-keto acid supplemented culture medium, the supplemented culture medium with N-phosphonomethylglycine (glyphosate)[76] to inhibit the endogenous shikimic acid pathway or the straightforward addition of the labeled amino acid without utilizing the overexpression system's biosynthetic pathway[77–79].

The successful synthesis of para-fluorophenyl-[1-^{13}C]pyruvate **10a**; 3,5-difluoro-4-hydroxyphenyl-[1-^{13}C]pyruvate **10b**; 2,6-difluoro-4-hydroxyphenyl-[1-^{13}C]pyruvate **10c**; and para-fluorophenylalanine targets to evaluate the incorporation of fluorinated amino acids, particularly how much fluorinated compound needs to be added to a culture medium to obtain sufficient protein labeling. Protein incorporation of these unnatural amino acids may lead to diverse labeling variations of fluorinated phenylalanine addressing further research questions, especially the investigation of aromatic ring system dynamics via ^{13}C-^{19}F TROSY.

Chapter 8

Theoretical background

Protein labeling

NMR spectra simplification is commonly obtained by isotope labeling of amino acids, which has led to great progress in structure elucidation of large proteins (> 25 kDa) and the study of biological macromolecules[80]. Protein nuclei are selectively enriched (e.g. ^{13}C, ^{15}N) or depleted (e.g. replacing ^{1}H by ^{2}H) to induce scalar couplings or signal eliminations[81]. ^{19}F is another way to obtain NMR spectra simplification resulting from its favourable physico-chemical properties. To address specific biomolecular questions of large molecules, a suitaible isotope pattern of the protein sample must therefore be chosen and optimized due to the demand of the intended NMR application.

8.1 Stable heavy isotope labeling

8.1.1 Deuteration

A perturbation of nuclear spin orientation, followed by the emission of electromagnetic signals, only occurs when the frequency of the applied oscillating magnetic field is approximately matching the Larmor precession frequency of the nuclear magnetization[82]. Since the Larmor precession frequency of deuterium is more than six-fold lower compared to ^{1}H, replacing carbon-bonded hydrogens with deuterium leads to proton signal elimination and reduced linewidths in NMR spectra. Deuteration of proteins is commonly achieved by uniform or random fractional labeling strategies, ranging from total proton substitution to moderate replacements.[66] These methods have been used for structural studies of high molecular weight proteins, TROSY applications (decreased ^{1}H–^{1}H spin flip rate)[83,84], nuclear Overhauser effect spectroscopy (NOESY) experiments (reduced linewidths)[85,86], 2D ^{1}H-^{1}H homonuclear spectra (reduction of dipolar relaxation pathways, spin-diffusion and passive scalar couplings)[85,86], ^{15}N-^{1}H heteronuclear single quantum coherence (HSQC) experiments (improved sensitivity and resolution)[87], triple-resonance and multi-dimensional experiments (improved sensitivity)[88,89] etc. However, unspecific deuterated substitution patterns or complete elimination of all except for exchangeable proton signals may reveal further difficulties in NMR signal assignment and structural studies based on conventional NOE approaches[81].

8.1.2 Enrichment via Carbon-13 and Nitrogen-15

Commercially available simple sources of Carbon-13 (a), i.e. isotopologues of acetone and glycine, are used as starting material to synthesize ^{13}C-labeled metabolic precursor compounds of amino acids (b) to obtain the desired labeled protein (e) after cell-based overexpression (c) as illustrated in Scheme 21[75,90]. Uniform ^{15}N-labeling through adding ^{15}N-salts to the expression media leads to protein backbone labeling of the peptide bond's amide function and may be utilized for structure and conformation studies[66].

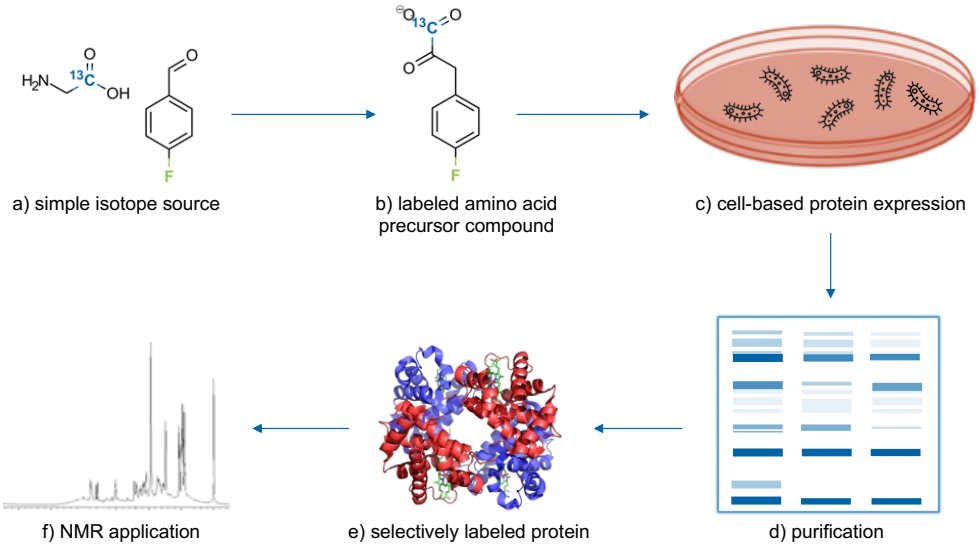

Scheme 21: stable heavy isotope protein labeling

Uniform labeling with/incorporation of ^{13}C and/or ^{15}N nuclei exhibit ^{13}C – ^{1}H or ^{15}N – ^{1}H spin pairs lead to multiple large one-bond scalar and dipolar coupling interactions resulting in multiexponential relaxation pathways[91]. NMR spectra may be simplified through the deprivation of one-bond ^{13}C – ^{13}C or three-bond ^{13}C – ^{1}H by alternating – ^{13}C – ^{12}C – ^{13}C – labeling patterns/isotopic enrichment[92,93]. The resulting isolated spin pairs reveal defined relaxation pathways for the interpretation of protein dynamics[92].

8.2 Fluorine labeling

8.2.1 NMR properties of Fluorine-19

Fluorine-19 is the only natural occurring and stable fluorine isotope, it exists in 100 % natural abundance. Natural biological systems contain no fluorine, which makes the spin-½ fluorine nucleus an interesting NMR probe, especially in studies with low proton signal intensity. ^{19}F is used as replacement of the ^{1}H nucleus due to its strong scalar couplings which offer efficient magnetization transfer to ^{13}C or ^{1}H nuclei and a large magnetogyric ratio of 83 %[69], providing high sensitivity for NMR observations, strong dipolar couplings[94] and measurements at field strengths consistent with ^{1}H resonance frequencies of 600 MHz or lower. The fluorine chemical shift is sensitive to local van der Waals interactions and electrostatic fields[95,96] owing to its large paramagnetic component of the chemical shielding term, derived from its unpaired valence electron. Compared to ^{1}H, ^{13}C and ^{15}N spin probes, ^{19}F bears a wide range of chemical shifts associated with unique local electronic environments in folded proteins[67,68].

Fluorine chemical shifts therefore enable the separation of resonances in 1D NMR and are particularly suitable for the study of protein conformational changes and dynamics[70–72]. Fluorinated amino acids are readily incorporated biosynthetically, accomplished by non-auxotrophic bacterial strains[97] or via induced auxotrophy approaches leading to uniformly labeled proteins[76,98]. The aim of spectroscopic studies of protein interactions is to observe proteins most undistorted, ideally involving non-perturbing probes. Fluorinated amino acids are assumed to be isosteric with their native counterparts and the van der Waals radius of ^{19}F is less than 20 % larger compared to ^{1}H, anticipating weak perturbations. However, varying degrees of probe-induced perturbations arising from fluorinated aromatics have been observed previously[99–101]. Fluorinated aromatics and aliphatics have shown to stabilize protein folding[102] due to the fluorophobic effect (increased hydrophobicity of fluorocarbon species, selective fluorine self-association)[103]. Therefore examination of protein stability, structural and functional perturbations arising from fluorine labeling is essential.

nucleus	natural abundance	spin *I*	magnetogyric ratio γ [10^7·rad·T^{-1}·s^{-1}]	NMR frequency [MHz]	vdW radius [pm]	EN
^{1}H	99.98 %	½	26.8	100	120	2.10
^{2}H	0.01 %	1	4.11	15.35		
^{12}C	98.9 %	0	-	-	170	2.50
^{13}C	1.07 %	½	6.73	25.15		
^{19}F	100 %	½	25.2	94.09	147	4.17

Table 12: comparison of nuclear spin and other nuclear properties[104]

8.2.2 Fluorine labeling strategies

In fluorine labeled proteins native amino acids are substituted with fluorinated amino acids[105] or fluorine tags. Fluorinated probes may be incorporated into proteins by chemical modification or biosynthetically to achieve site-specific fluorine labeling[106,107]. Also the preparation of fusion proteins for studying complex or large systems, consisting of a biosynthetically produced native domain and a chemically synthesized fluorine-labeled fragment, is possible by chemical ligation strategies[108].

Chemical synthesis may be applied for incorporating unnatural amino acids into peptides or small proteins which are difficult to express in bacteria. Solution- or solid-phase peptide synthesis[109] (Scheme 22) offer site-specific labeling of peptides consisting of less than 50 amino acids[110]. Longer polypeptides suffer from accumulation of byproducts and reduced product solubility. Large peptides and full-length proteins may be attained by fragment condensation of synthesized protein fragments or native chemical ligation strategies[108].

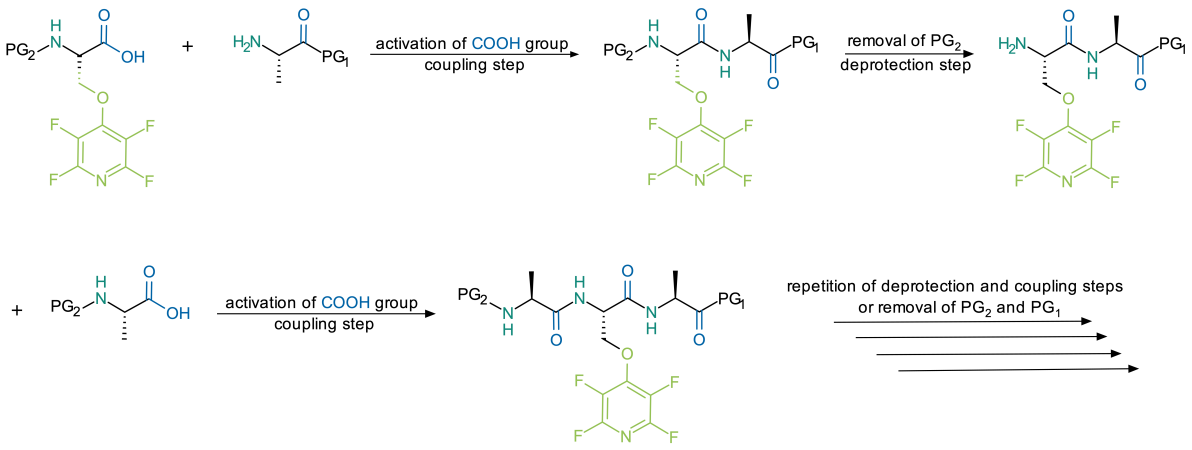

Scheme 22: peptide synthesis[110] of fluoropyridine-containing tripeptide alanine-fluoropyridine-alanine[111]. PG_1 benzyl ester protecting group, PG_2 Boc protecting group

Protein tagging by chemical modification is usually applied for polar and positively charged amino acids. Amino acids less soluble in aqueous solutions would require the addition of apolar or aprotic polar solvents, which may unfold the desired protein[112]. Protein tagging is achieved by adding an excess of fluorine labeling reagent into a dilute protein solution, followed by purification via gel-filtration chromatography, centrifugal filtering or dialysis[113].

Biosynthetic incorporation of fluorinated amino acid analogs is achieved by employing bacterial strains which are auxotrophic for the desired amino acid probe[114] or possess induced auxotrophy[79,115]. Enzymes causing dilution or scrambling of the label[116] have been knocked out within these strains to obtain adequate label distribution in the isolated protein and avoid mutations causing interfering cell growth[114]. Fluorine probes are added to the expression media together with their native counterpart to maintain bacterial growth and efficient protein expression despite fluorine's toxicity[76]. Some fluorinated amino acids additionally require the over-expression of their native aminoacyl-transfer RNA (tRNA) synthetase to promote adequate levels of incorporation. Supplementation with glyphosate[117], a competitive inhibitor of 5-enolpyruvylshikimik acid-3-phosphate synthetase (Scheme 26 aroA; enzyme code (EC) 2.5.1.19)[76], intercepts endogenous aromatic amino acid synthesis and may help to increase the uptake of the fluorine probe[118]. In Scheme 23 an example of a uniformly-labeled peptide chain is illustrated, pointing out the substitution of endogenous phenylalanine by a labeled variant.

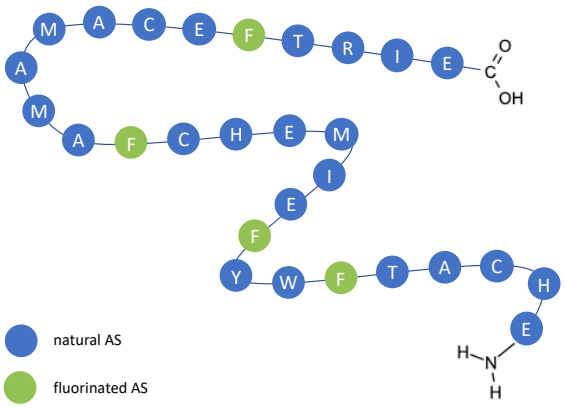

Scheme 23: peptide chain with labeled phenylalanine (F)

Site-specific labeling is often more favourable in large proteins than uniform labeling, which might lead to structural disruption and spectral overcrowding[119]. Site-specific incorporation of fluorinated amino acid analogues is accomplished by adding the substituting fluorinated amino acid to the culture medium of an expressing species, which is unable to metabolize this particular analogue. In Scheme 24, a codon programming the position to be substituted and its corresponding suppressor tRNA, which will decode this position, are utilized together with a substrate-specific aminoacyl-tRNA synthetase for the analogue and for the suppressor tRNA[120]. This approach may allow the substitution of any amino acid position within a protein with a labeled amino acid[121].

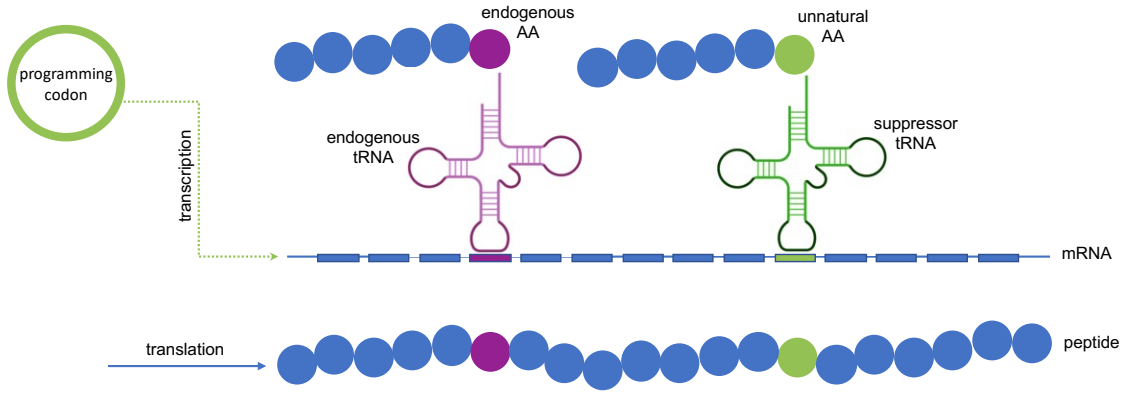

Scheme 24: site-specific incorporation of unnatural amino acids into proteins of interest

8.3 *Escherichia coli*

E. coli is a facultative anaerobic bacterium and is endemic in the gastrointestinal tract of warm-blooded organisms. Because of its well-known bacteria genetics and its capability of amino acid biosynthesis and biodegradation for all 20 amino acids[116] as displayed in Scheme 25, *E. coli* is the most commonly used expression system organism for cell-based protein overexpression[122].

8.3.1 Phenylalanine biosynthetic pathway[123]

Since the aromatic amino acids, phenylalanine, tyrosine and tryptophan, arise from a joint pathway, the shikimic acid pathway, this endogenous pathway of an overexpressing species (e.g. *E. coli*) may be utilized for protein incorporation of isotope-labeled and unnatural phenylalanine. As illustrated in Scheme 26, the the shikimic acid pathway starts with the condensation of PEP and E4P, mediated by three isoenzymes AroG, AroF, and AroH (EC 2.5.1.54) respectively. The built C7 sugar, 3-deoxy-D-arabino-heptulosonic acid 7-phosphate (DAHP), is oxidized by 3-dehydroquinate synthase (aroB, EC 4.2.3.4) and drops its phosphoryl group to cycle to 3-dehydrochinate. Dehydration by 3-dehydroquinate hydrolase (EC 4.2.1.10) leads to 3-dehydro shikimate, which will be reduced to shikimate using nicotinamide adenine dinucleotide phosphate (NADPH). Phosphorylation of shikimate using adenosine triphosphate (ATP) results in shikimate-3-phosphate, which is condensated with a second molecule. The resulting 5-enolpyruvyl-3-phosphoshikimate loses its phosphate group through chorismate synthase (EC 4.2.3.5) and becomes chorismate, the joint precursor of all three aromatic amino acids. Chorismate mutase (PheA, EC 5.4.99.5)

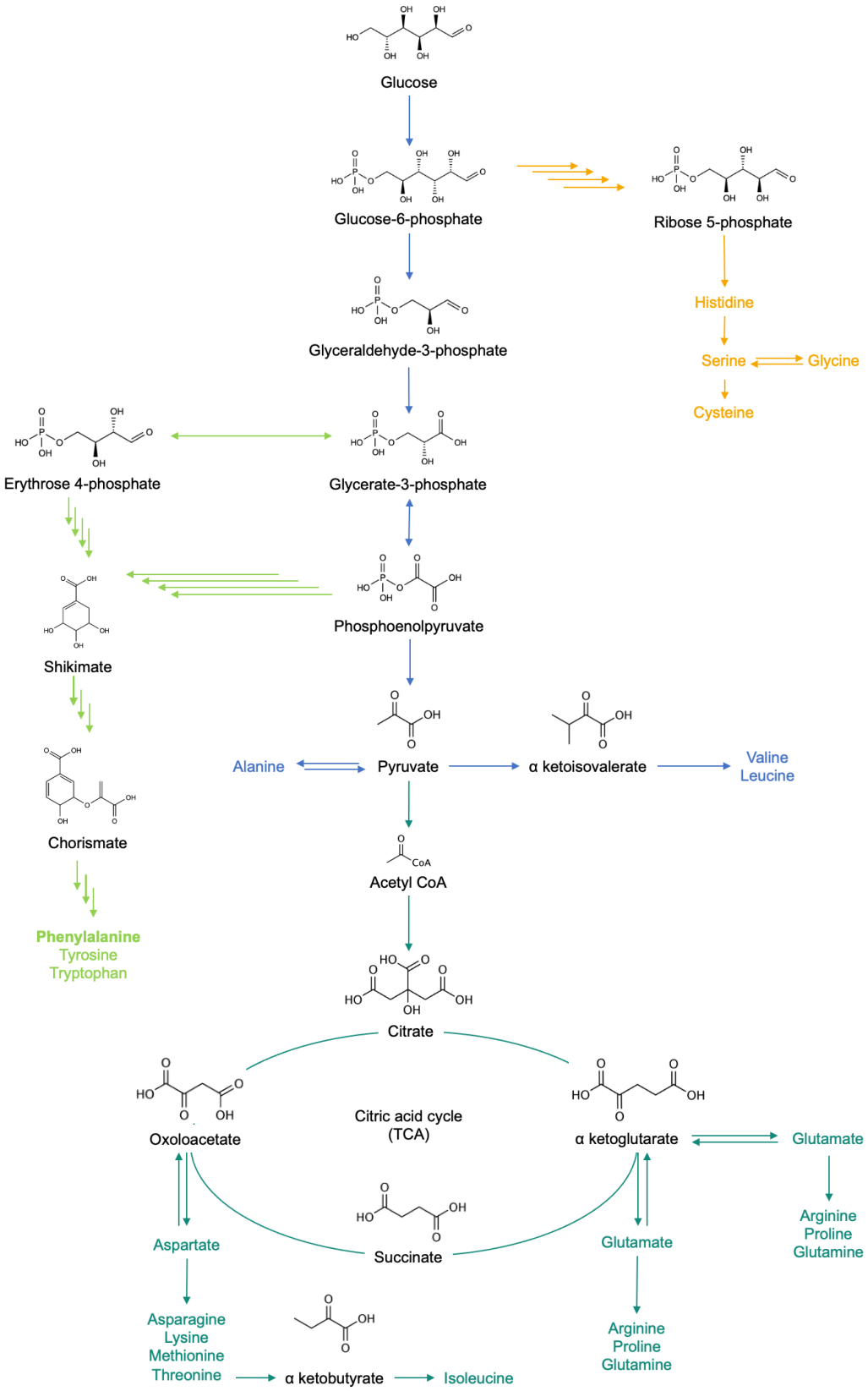

Scheme 25: biosynthesis of amino acids including glycolysis, pentose phosphate pathway, shikimic acid pathway and citric acid cycle

converts chorismate into prephenate by an electro-cyclic reaction. Phenylpyruvate, the amino-acid-specific precursor of phenylalanine, arises after dehydration and decarboxylation mediated by phenylalanine prephenate dehydrogenase (PheA, EC 4.2.1.51). In the final step, the keto acid is transaminated through phenylalanine transaminase (EC 2.6.1.58) to give L-phenylalanine.

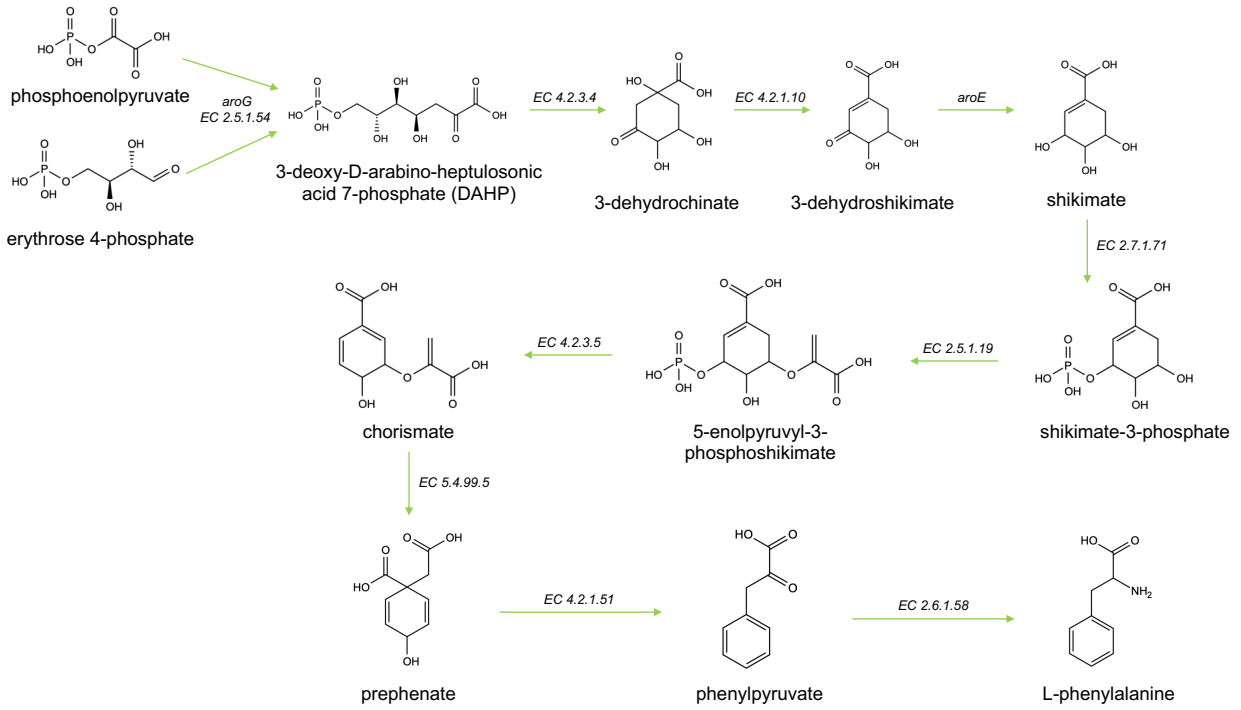

Scheme 26: phenylalanine metabolism in *E. coli* starting from PEP and E4P (shikimic acid pathway)

Chapter 9

Results

For the synthesis of the respective fluorophenyl-[1-^{13}C]pyruvates **10a-c** a three-step synthetic route (Scheme 27, **7-10**) was followed, established by Billek, G. in 1961[124] and modified by Lichtenecker *et al.* in 2013[125] for the synthesis of unfluorinated sodium [1-^{13}C]phenylpyruvate.

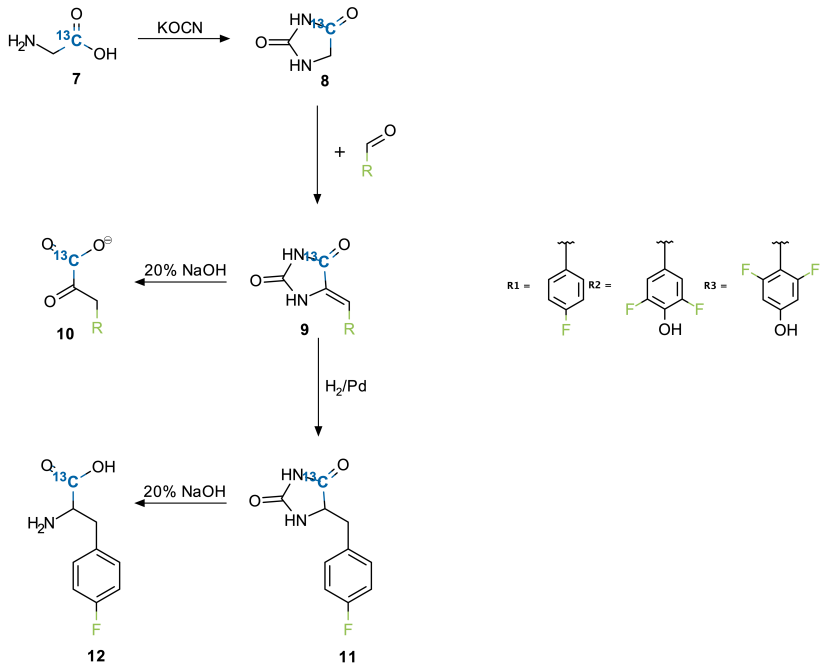

Scheme 27: synthesis path of fluorinated phenylalanine residue precursor compounds

[1-^{13}C]glycine **7** by Euriso-top® was used as ^{13}C-labeled source and starting material. In a one-pot reaction, as reported previously[126,127], [^{13}C]hydantoin **8** was obtained in good yields by utilizing potassium cyanate (KOCN), subsequently leading to cyclization under acidic conditions (Scheme 28).

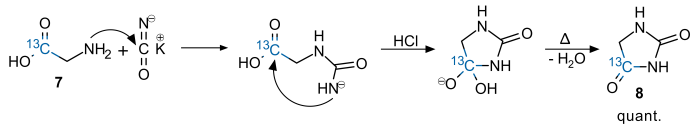

Scheme 28: Urech hydantoin synthesis

In presence of ethanolamine, aldol condensation of [^{13}C]hydantoin **8** with the corresponding fluorinated benzaldehydes (Scheme 31) led to the formation of **9a-c** respectively (Scheme 29). While **9a-b** were gained by recrystallization in high purity, the red compound **9c** required purification by column chromatography.

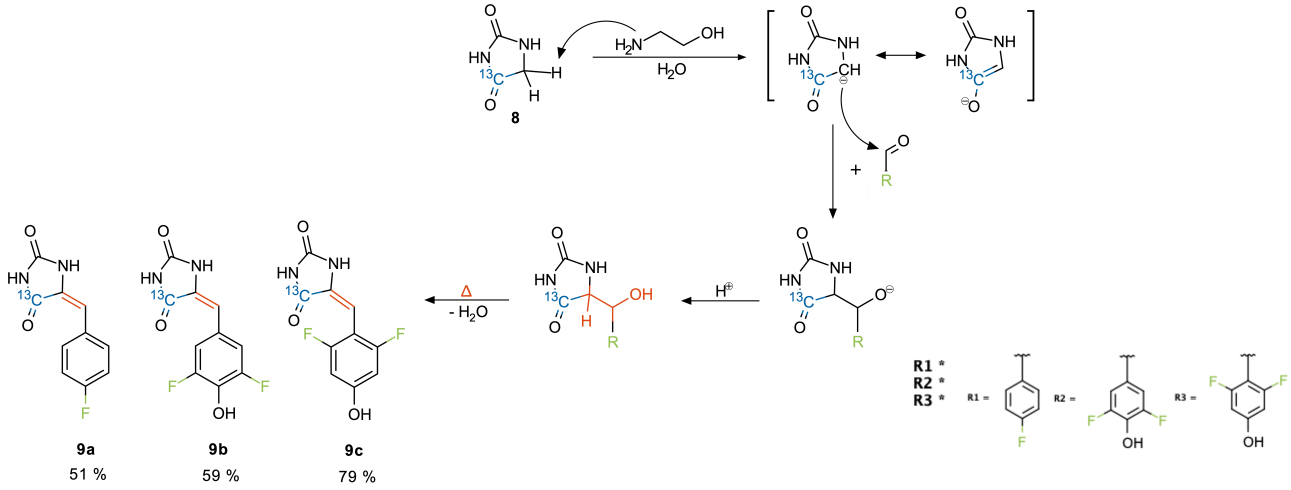

Scheme 29: condensation: [1-^{13}C]hydantoin ⟶ fluorinated benzal – [1-^{13}C]hydantoin

In the final step, hydrolysis of **9a-c** was performed under basic conditions and argon atmosphere to conduct the opening of the hydantoin ring, leading to the target α-keto acids. Subsequent lyophilisation yielded the respective sodium-salts **10a-b** in high purity and **10c** with unsatisfying purity (section 11.6).

The racemic para-fluorophenylalanine **12** was pursued to explore whether its bacterial uptake might be favoured upon the respective α-keto acid. The synthesis was performed as outlined in Scheme 27 (**7-9, 11-12**) without ^{13}C-labeling, starting from unlabeled glycine **7**. To obtain para-fluoro phenylalanine **12** para-fluorinated compound **9a** was reduced by hydrogen in presence of palladium on activated carbon 10 % (Pd/C) (**9, 11**) prior to hydrolysis. While compound **11** could be determined via NMR (Scheme 73) with impurities, after hydrolysis of **11** the corresponding product **12** could not be identified via NMR analysis. Since salts as NaCl do not comprise any NMR-active nuclei, high concentrations of NaCl within the NMR sample might lead to compound concentrations below the detection limit. In assumption this was the reason of missing product peaks within the measured NMR spectra, an ion exchange column was carried out to remove interfering salts. The NMR spectra of the fractions eluated under basic conditions revealed traces of the expected ammonium-salt of para-fluorophenylalanine including side products. Also the acidic eluate potentially contained fractions of the desired compound due to its odour and colour. Hence further strategies need to be considered to remove unwanted salts and isolate the compound within the fractions.

Chapter 10

Conclusion and Outlook

^{13}C-labeled phenylpyruvates, para-fluorophenyl pyruvate **10a** and 3,5-difluoro-4-hydroxyphenyl pyruvate **10b** were successfully synthesized starting from low-cost [1-^{13}C]glycine. 2,6-difluoro-4-hydroxyphenyl pyruvate **10c** and para-fluorinated phenylalanine **12** were synthesized with impurities, thus need further optimization of the synthetic protocols. Future studies using these compounds will reveal if incorporation via the shikimic acid pathway of *E. coli* leads to ^{13}C and ^{15}N backbone labeling combined with fluorinated aromatic ring systems (Scheme 30) and will be assessed by adding different concentrations of the fluorinated phenylalanine precursors to the culture medium.

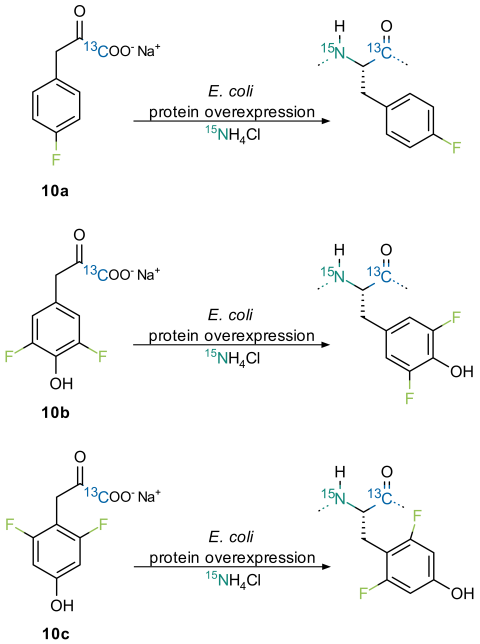

Scheme 30: *E. coli*-based overexpression leading to specific isotope-labeling patterns in target proteins, adapted from unfluorinated sodium [1-^{13}C]phenylpyruvate[75]

The synthesis of para-fluoro phenylalanine was carried out to determine the most efficient way for protein incorporation of fluorinated phenylalanine despite fluorine's toxicity towards *E. coli*. Addition of α-keto acids to the growth medium of overexpressing systems supplemented with glyphosate[76] as well as the straight-forward addition of amino acids has previously been conducted for diversely-labeled analogs[77–79] and may be adapted for the

synthesized compounds.

The synthesis' of fluorinated phenylpyruvates **10a-c** were accomplished by employing fluoro-benzaldehydes as fluorine sources (Scheme 31). Therefore customizing aromatic labeling patterns to the demand of NMR experiments may be accomplished by deploying suitable isotope-labeled fluoro-benzaldehydes. In particular alternating $^{12}C - ^{2}H$ and $^{13}C - ^{19}F$ spin systems are feasible to attain defined relaxation pathways for $^{13}C - ^{19}F$ TROSY experiments investigating the dynamics of aromatic rings.

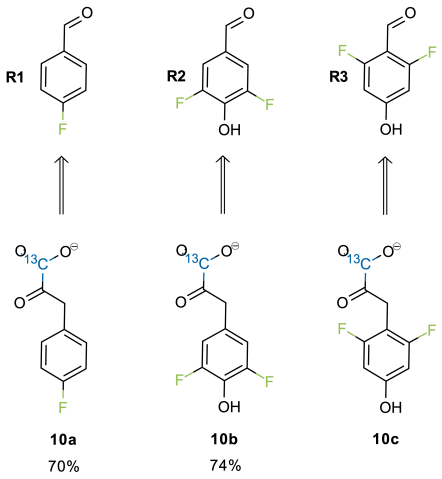

Scheme 31: α-keto pyruvates: fluorinated synthesis products deriving from fluoro-benzaldehydes

The three-dimensional protein structure is crucial for its functional interactions. Protein folding is well-defined and determined by the characteristics of amino acid side chains and their interplay. Thus, globally-substitued proteins with fluorinated amino acids may differ in stability, structural and functional properties[99–103]. Therefore probe-induced perturbations arising from the fluorine atoms chemical behaviour need to be explicitly investigated.

Chapter 11

Experimental section

11.1 Materials and methods

All solvents were distilled prior to use or purchased from commercial suppliers and used without further purification. Isotope-labeled glycine (1-13C, 99 %) LOT PR-28181 was purchased from Euriso-top®. Fluorinated reagents were purchased from Alfa Aesar with following purity grades: 4-fluorobenzaldehyde (98 %) LOT 10212616, 2,6-difluoro-4-hydroxybenzaldehyde (95 %) LOT 10167329, 3,5-difluoro-4-hydroxybenzaldehyde (97 %) LOT 10169226. 3,5-difluoro-4-hydroxybenzaldehyde (99 %) LOT AS473452 was additionally purchased from Apollo Scientific Ltd. Other reactants were purchased from further commercial suppliers. Vacuum evaporation was performed on BÜCHI Rotavapor R-210 and R-100 connected to a Recirculating Chiller F-100. Column chromatography was carried out using silica gel 60 (0.040 – 0.063 mm, LOT 040353707) from MACHEREY-NAGEL GmbH & Co. KG. TLC was conducted on pre-coated TLC sheets ALUGRAM®Xtra SIL G/UV_{254} from MACHEREY-NAGEL GmbH & Co. KG, layer: 0.20 mm silica gel 60 with fluorescent indicator UV_{254} LOT 802046. TLC was examined using UVAC-60 neolab ultraviolet lamp (254 nm) or by application of aqueous $KMnO_4$ (0.5 %) solution followed by heat treatment via hot-gun. NMR spectra were recorded on Bruker AVANCE NEO spectrometers at 400 MHz and Bruker AVANCE III HD at 176 MHz. Chemical shifts were given in parts per million (ppm). NMR spectra were evaluated with TopSpin™ by Bruker. Lyophilisation was conducted with Christ™ Gefriertrocknungsanlage ALPHA 1-2 LDplus. Freeze-drying was done via liquid nitrogen and subsequent water removal by inducing high vacuum on CRVpro6 oil pump.

11.2 [1-^{13}C]hydantoin 8

formula	molecular weight	yield	appearance
$C_3H_4N_2O_2$	101.069 g/mol	quantitative	white solid

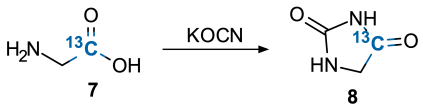

		m[mg]	M[g/mol]	n[mmol]	equivalents
[1-^{13}C]glycine **7**	$C_2H_5NO_2$	500	76.07	6.57	1
potassium cyanate	KOCN	800	81.12	9.86	1.5

Table 13: reactants and reagents for the synthesis of [1-^{13}C]hydantoin

[1-^{13}C]glycine **7** and KOCN were weighed into a 25 ml round-bottomed flask. 4.2 ml of water were added to the white solids and the reaction mixture was heated in an oil bath to 100 °C, equipped with a reflux condenser. The solids dissolved and after two hours of stirring the flask was cooled in an ice bath. At 0 °C 1.6 ml of concentrated HCl were slowly added to conduct the ring closure. Upon addition, a white solid precipitated. The vessel was returned to the oil bath, equipped with a reflux condenser and heated to 120 °C. After one hour of stirring the white solid was dissolved and the colourless suspension was again placed in an ice bath. After precipitation of the white hydantoin, the liquid was removed by vacuum-filtration with a filter funnel. Additional fractions were collected by evaporating the filtrate under reduced pressure, cooling it and separating further precipitated solids by vacuum-filtration. Over-all 800 mg of [^{13}C]hydantoin **8** (6.5 mmol; quantitative) were obtained.

11.3 Para-fluorobenzal-[1-^{13}C]hydantoin 9a

formula	molecular weight	yield	appearance
$C_{10}H_7FN_2O_2$	207.17 g/mol	51 %	yellow solid

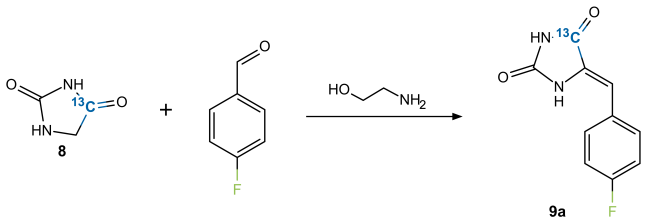

		m[mg]	ρ[g/ml]	V[μl]	M[g/mol]	n[mmol]	equivalents
[1-^{13}C]hydantoin **8**	$C_3H_4N_2O_2$	546		-	101.069	5.4	1
ethanol amine	C_2H_7NO	530	1.02	520	61.08	8.68	1.6
4-fluorobenzaldehyde	C_7H_5FO	940	1.175	800	124.11	7.57	1.4

Table 14: reactants and reagents for the synthesis of para-fluorobenzal-[1-^{13}C]hydantoin

In a 25 ml two-necked flask, equipped with a reflux condenser and glass plug, [^{13}C]hydantoin **8** was dissolved with 2.5 ml of water at 70 °C. To give a pH-value of 7 0.5 ml of saturated $NaHCO_3$ were added to the solution. Then ethanol amine was added and the reaction mixture was heated to 90 °C. 4-fluorobenzaldehyde was dissolved in 3 ml of ethanol and slowly added to the vessel. The aldol condensation was conducted over night at 120 °C. The following day the yellow reaction mixture was cooled down to 0 °C to induce the precipitation of the crude product. The yellow solid was separated from the fluid by vacuum-filtration and recrystallised from EtOH. 170 mg (0.82 mmol, 15 %) of grey-yellow solid were yielded and 400 mg (1.93 mmol, 36 %) of bright yellow solid with slight impurities were obtained after solvent evacuation under reduced pressure, cooling and vacuum-filtration.

11.4 3,5-difluoro-4-hydroxybenzal-[1-^{13}C]hydantoin 9b

formula	molecular weight	yield	appearance
$C_{10}H_6F_2N_2O_3$	241.158 g/mol	59 %	yellow solid

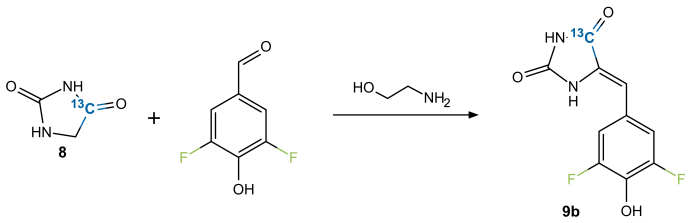

		m[mg]	ρ[g/ml]	V[ml]	M[g/mol]	n[mmol]	equ
[1-^{13}C]hydantoin **8**	$C_3H_4N_2O_2$	182		-	101.069	1.8	1.9
ethanol amine	C_2H_7NO	151	1.02	0.148	61.08	2.47	2.6
3,5-difluoro-4-hydroxybenzaldehyde	$C_7H_4F_2O_2$	150		-	158.10	0.95	1

Table 15: reactants and reagents for the synthesis of 3,5-difluoro-4-hydroxybenzal-[1-^{13}C]hydantoin

In a 25 ml two-necked flask, equipped with a reflux condenser and glass plug, [^{13}C]hydantoin **8** was dissolved with 2.5 ml of water at 70 °C. To give a pH-value of 7 0.5 ml of saturated $NaHCO_3$ were added to the solution. Then ethanol amine was added and the reaction mixture was heated to 90 °C. 3,5-difluoro-4-hydroxybenzaldehyde was dissolved in 3 ml of EtOH and slowly added to the vessel. The aldol condensation was conducted over night at 120 °C. The following day the yellow-brown reaction mixture was evaporated under reduced pressure and EtOAc/heptane/MeOH 5:5:1 was added to induce the precipitation of the crude product. The yellow solid was separated from the fluid by vacuum-filtration to yield 135 mg (0.56 mmol, 59 %) of yellow solid.

11.5 2,6-difluoro-4-hydroxybenzal-[1-^{13}C]hydantoin 9c

formula	molecular weight	yield	appearance
$C_{10}H_6F_2N_2O_3$	241.158 g/mol	79 %	red solid

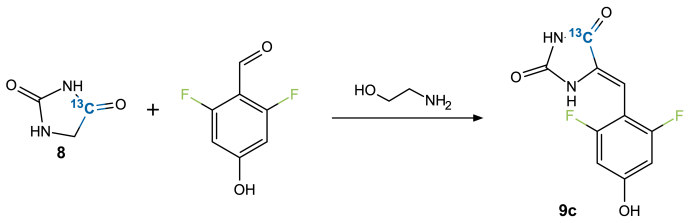

		m[mg]	ρ[g/ml]	V[ml]	M[g/mol]	n[mmol]	equ
[1-^{13}C]hydantoin **8**	$C_3H_4N_2O_2$	80		-	101.0869	0.79	1
ethanol amine	C_2H_7NO	80	1.02	0.078	61.08	1.3	1.65
2,6-difluoro-4-hydroxybenzaldehyde	$C_7H_4F_2O_2$	150		-	158.10	0.95	1.2

Table 16: reactants and reagents for the synthesis of 2,6-difluoro-4-hydroxybenzal-[1-^{13}C]hydantoin

In a 25 ml two-necked flask, equipped with a reflux condenser and glass plug, [^{13}C]hydantoin **8** was dissolved with 2.5 ml of water at 70 °C. To give a pH-value of 7 0.5 ml of saturated $NaHCO_3$ were added to the solution. Then ethanol amine was added and the reaction mixture was heated to 90 °C. 2,6-difluoro-4-hydroxybenzaldehyde was dissolved in 3 ml of EtOH and slowly added to the vessel. The aldol condensation was conducted over night at 120 °C. The following day the red reaction mixture was evaporated under reduced pressure and purified by column chromatography (silica gel, EtOAc/heptane/MeOH 5:5:1) to obtain 150 mg (0.62 mmol, 79 %) of red solid.

11.6 Fluorophenyl-[1-^{13}C]pyruvate 10

	formula	molecular weight	yield	appearance
para-fluorophenyl-[1-^{13}C]pyruvate **10a**	$C_9H_6FO_3$	182.135 g/mol	70 %	grey solid
3,5-difluoro-4-hydroxyphenyl-[1-^{13}C]pyruvate **10b**	$C_9H_5F_2O_4$	216.125 g/mol	74 %	orange solid
2,6-difluoro-4-hydroxyphenyl-[1-^{13}C]pyruvate **10c**	$C_9H_5F_2O_4$	216.125 g/mol	60 %	red solid

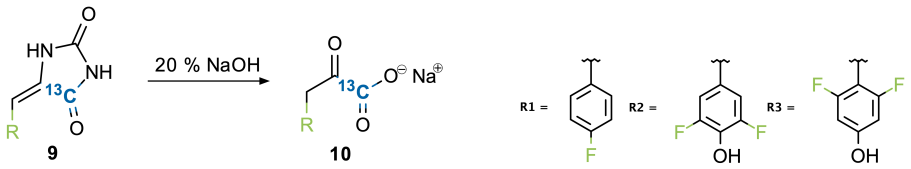

		m[mg]	M[g/mol]	n[mmol]	equ
para-fluorobenzal-[1-^{13}C]hydantoin **9a**	pFBH	150	207.169	0.72	1
3,5-difluoro-4-hydroxybenzal-[1-^{13}C]hydantoin **9b**	3,5 – FHBH	135	241.158	0.56	1
2,6-difluoro-4-hydroxybenzal-[1-^{13}C]hydantoin **9c**	2,6 – FHBH	120	241.158	0.5	1

Table 17: reactants and reagents for the synthesis of fluorinated phenylalanine precursors

The substrates were weighted into a 25 ml two-necked flask respectively. Then the vessels were equipped with a septum and reflux condenser and put in an oil bath. After continuous argon flow was applied, 5 ml of NaOH 20 % were slowly added with a syringe through the septum. To conduct the hydrolysis, argon purging was continued throughout the reaction for 3 hours at 110 °C. The oil bath and argon line were removed and the solutions were extracted two times with Et_2O under argon atmosphere constituted by a balloon to avoid degradation of the crude products. Adding half concentrated HCl the α-keto acids precipitated upon reaching a strong acidic pH value. The flasks were removed from the argon atmosphere and the suspensions were transferred to a separating funnel. They were extracted five times with Et_2O, the combined organic layers were dried over $MgSO_4$ and Et_2O was evaporated under reduced pressure in a 100 ml round-bottomed flask. The corresponding NMR spectra of 3,5-difluoro-4-hydroxyphenyl-[1-^{13}C]pyruvic acid **10b** (Scheme 65, 66) and 2,6-difluoro-4-hydroxyphenyl-[1-^{13}C]pyruvic acid **10c** (Scheme 70, 71) revealed impurities. 20 ml of water were added to each free α-keto acid respectively and 1 N NaOH was utilized to give pH values of 7 which dissolved the precipitates. The solutions were lyophilised to yield 92 mg (0.51 mmol, 70 %) of grey sodium para-fluorophenyl-[1-^{13}C]pyruvate **10a**, 89 mg (0.41 mmol, 74 %) of orange sodium 3,5-difluoro-4-hydroxyohenyl-[1-^{13}C]pyruvate **10b** and 65 mg (0.3 mmol, 60 %) of impure red sodium 2,6-difluoro-4-hydroxyphenyl-[1-^{13}C]pyruvate **10c**, respectively.

11.7 5-[(para-fluorophenyl)methyl]hydantoin 11

formula	molecular weight	yield	appearance
$C_{10}H_9FN_2O_2$	208.192 g/mol	73 %	grey solid

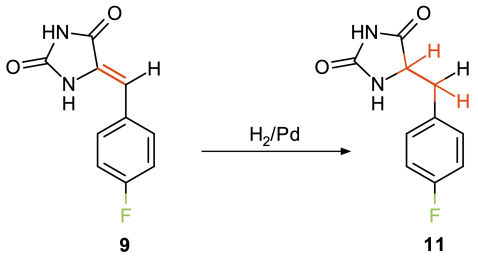

9 **11**

		m[mg]	M[g/mol]	n[mmol]	equivalents
para-fluorobenzal-hydantoin **9a**	$C_{10}H_7FN_2O_2$	75	206.176	0.36	1
10 % palladium on charcoal	Pd/C	40	106.42	0.38	1.03

Table 18: reactants and reagents for the synthesis of 5-[(4-fluorophenyl)methyl]hydantoin

In a 50 ml two-necked flask para-fluorobenzal-hydantoin was solved in 6 ml of MeOH. After adding the catalyst, the reaction bulb was equipped with a double-layered H_2-balloon. The hydrogenation was conducted over night during vigorous stirring under atmospheric pressure. The following day the H_2-balloon was detached and the Pd/C was removed in a funnel by Celite filtration. MeOH was evaporated under reduced pressure to yield 55 mg (0.26 mmol, 73 %) of grey compound **11**.

11.8 Para-fluorophenylalanine 12

formula	molecular weight	appearance
$C_9H_9FNO_2$	182.18 g/mol	white-yellow solid

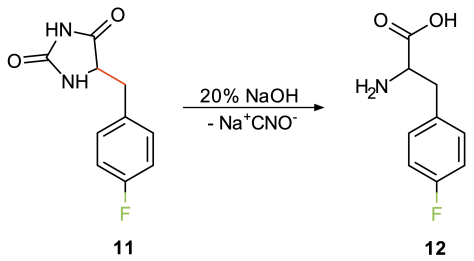

11 **12**

		m[mg]	M[g/mol]	n[mmol]	equivalents
5-[(para-fluorophenyl)methyl]hydantoin **11**	$C_{10}H_9FN_2O_2$	55	208.192	0.26	1

Table 19: reactants and reagents for the synthesis of racemic p-fluorophenylalanine

The substrate was weighted into a 25 ml two-necked flask. Then the vessel was equipped with a septum and reflux condenser and put in an oil bath. After continuous argon flow was applied, 10 ml of 20% NaOH were slowly added with a syringe through the septum. To conduct the hydrolysis, argon purging was continued throughout the reaction for 3.5 hours at 130 °C. The oil bath and argon line were removed and half concentrated HCl was added until the crude product precipitated whilst reaching strong acidic pH value. The flask was removed from the argon atmosphere and the white solid was separated from the fluid and dried by vacuum-filtration with a filter funnel. In the corresponding NMR spectra only solvent peaks were visible. As a consequence, bulk NaCl was tried to remove via ion exchanger revealing traces of para-fluorophenylalanine ammonium-salt together with an unidentified side product.

Bibliography

1. Adams, R. & Ulich, L. H. The use of Oxalyl Chloride and Bromide for producing Acid Chlorides, Acid Bromides or Anhydrides. III. *Journal of the American Chemical Society* **42,** 599–611 (Mar. 1920).
2. Jursic, B. S. & Zdravkovski, Z. A Simple Preparation of Amides from Acids and Amines by Heating of Their Mixture. *Synthetic Communications* **23,** 2761–2770 (Nov. 1993).
3. Vaughan, J. R. & Osato, R. L. The Preparation of Peptides Using Mixed Carbonic-Carboxylic Acid Anhydrides. *Journal of the American Chemical Society* **74,** 676–678 (Feb. 1952).
4. Ezawa, T., Kawashima, Y., Noguchi, T., Jung, S. & Imai, N. Amidation of carboxylic acids via the mixed carbonic carboxylic anhydrides and its application to synthesis of antidepressant (1S, 2R)-tranylcypromine. *Tetrahedron: Asymmetry* **28,** 1690–1699 (Dec. 2017).
5. Katritzky, A. R., He, H.-Y. & Suzuki, K. N-Acylbenzotriazoles: Neutral Acylating Reagents for the Preparation of Primary, Secondary, and Tertiary Amides. *The Journal of Organic Chemistry* **65,** 8210–8213 (Oct. 2000).
6. Neises, B. & Steglich, W. Simple Method for the Esterification of Carboxylic Acids. *Angewandte Chemie International Edition in English* **17,** 522–524 (July 1978).
7. Shioiri, T., Ninomiya, K. & Yamada, S. Diphenylphosphoryl azide. New convenient reagent for a modified Curtius reaction and for peptide synthesis. *Journal of the American Chemical Society* **94,** 6203–6205 (Aug. 1972).
8. Mizuhara, T. *et al.* Direct Preparation of Primary Amides by Reaction of Carboxylic Acids and Ammonia in Alcohols Using DMT-MM. *Chemistry Letters* **37,** 1190–1191 (Dec. 2008).
9. Kunishima, M., Kawachi, C., Hioki, K., Terao, K. & Tani, S. Formation of carboxamides by direct condensation of carboxylic acids and amines in alcohols using a new alcohol- and water-soluble condensing agent: DMT-MM. *Tetrahedron* **57,** 1551–1558 (Feb. 2001).
10. Hall, J. H. & Gisler, M. A simple method for converting nitriles to amides. Hydrolysis with potassium hydroxide in tert-butyl alcohol. *The Journal of Organic Chemistry* **41,** 3769–3770 (Nov. 1976).
11. Moorthy, J. N. & Singhal, N. Facile and Highly Selective Conversion of Nitriles to Amides via Indirect Acid-Catalyzed Hydration Using TFA or AcOH-2SO4. *The Journal of Organic Chemistry* **70,** 1926–1929 (Jan. 2005).
12. Goto, A., Endo, K. & Saito, S. RhI-Catalyzed Hydration of Organonitriles under Ambient Conditions. *Angewandte Chemie International Edition* **47,** 3607–3609 (Apr. 2008).

13. Gawley, R. E. *The Beckmann Reactions: Rearrangements, Elimination-Additions, Fragmentations, and Rearrangement-Cyclizations* May 1988.

14. Owston, N. A., Parker, A. J. & Williams, J. M. J. Highly Efficient Ruthenium-Catalyzed Oxime to Amide Rearrangement. *Organic Letters* **9,** 3599–3601 (Aug. 2007).

15. Park, S., Choi, Y.-a., Han, H., Yang, S. H. & Chang, S. Rh-Catalyzed one-pot and practical transformation of aldoximes to amides. *Chemical Communications,* 1936 (2003).

16. Smith, P. A. S. *The Curtius Reaction* Mar. 2011.

17. Wallis, E. S. & Lane, J. F. *The Hofmann Reaction* Mar. 2011.

18. Wolff, H. *The Schmidt Reaction* Mar. 2011.

19. Kurti, L. & Czako, B. *Strategic Applications of Named Reactions in Organic Synthesis* 758. ISBN: 9780124297852 (Academic Press, 2005).

20. Shioiri, T. in *Comprehensive Organic Synthesis* 795–828 (Elsevier, 1991).

21. Gogoi, P. & Konwar, D. An efficient modification of the Hofmann rearrangement: synthesis of methyl carbamates. *Tetrahedron Letters* **48,** 531–533 (Jan. 2007).

22. Chen, M. *et al.* Synthesis and evaluation of 2-(4-[4-acetylpiperazine-1-carbonyl] phenyl)- 1H-benzo[d]imidazole-4-carboxamide derivatives as potential PARP-1 inhibitors and preliminary study on structure-activity relationship. *Drug Development Research* **83,** 55–63 (June 2021).

23. Zagulyaeva, A. A., Banek, C. T., Yusubov, M. S. & Zhdankin, V. V. Hofmann Rearrangement of Carboxamides Mediated by Hypervalent Iodine Species Generated in Situ from Iodobenzene and Oxone: Reaction Scope and Limitations. *Organic Letters* **12,** 4644–4647 (Sept. 2010).

24. Miyamoto, K. *et al.* Iodoarene-catalyzed oxidative transformations using molecular oxygen. *Chemical Communications* **53,** 9781–9784 (2017).

25. Liu, P., Wang, Z. & Hu, X. Highly Efficient Synthesis of Ureas and Carbamates from Amides by Iodosylbenzene-Induced Hofmann Rearrangement. *European Journal of Organic Chemistry* **2012,** 1994–2000 (Feb. 2012).

26. Reboul, V. *et al.* A Straightforward Synthesis of N-Substituted Ureas from Primary Amides. *Synthesis* **52,** 2099–2105 (Apr. 2020).

27. *The preparation method of 4AP* Chinese patent CN106554306A (Hybio Pharmaceutical Co Ltd, Sept. 2015). https://patents.google.com/patent/CN106554306A/en (2021).

28. Silva, L. F., Siqueira, F. A., Pedrozo, E. C., Vieira, F. Y. M. & Doriguetto, A. C. Iodine(III)-Promoted Ring Contraction of 1,2-Dihydronaphthalenes: A Diastereoselective Total Synthesis of p-Indatraline. *Organic Letters* **9,** 1433–1436 (Mar. 2007).

29. Yusubov, M. S. & Zhdankin, V. V. Development of new recyclable reagents and catalytic systems based on hypervalent iodine compounds. *Mendeleev Communications* **20,** 185–191 (July 2010).

30. Borah, A. J. & Phukan, P. Efficient synthesis of methyl carbamate via Hofmann rearrangement in the presence of TsNBr2. *Tetrahedron Letters* **53,** 3035–3037 (June 2012).

31. Huang, X. & Keillor, J. W. Preparation of methyl carbamates via a modified Hofmann rearrangement. *Tetrahedron Letters* **38,** 313–316 (Jan. 1997).

32. DeSousa, J. D. & Novak, B. M. Resolving the Regioregularity of Poly(N-n-hexyl-N'-phenylcarbodiimide) via Nitrogen-15 Labeling. *ACS Macro Letters* **1,** 672–675 (May 2012).

33. Jew, S.-s., Park, H. G., Park, H.-J., Park, M.-s. & Cho, Y.-s. New method for Hofmann rearrangement. *Tetrahedron Letters* **31,** 1559–1562 (Jan. 1990).

34. Ivanovic, M., Jevtic, I., Dosen-Micovic, L. & Ivanovic, E. Hofmann Rearrangement of Carboxamides Mediated by N-Bromo-acetamide. *Synthesis* **48,** 1550–1560 (Mar. 2016).

35. Bastos, G. A. & de Mattos, M. C. S. A convenient Hofmann reaction of carboxamides and cyclic imides mediated by trihaloisocyanuric acids. *Tetrahedron Letters* **83,** 153422 (Oct. 2021).

36. Gambacorta, G. & Baxendale, I. R. Continuous-Flow Hofmann Rearrangement Using Trichloroisocyanuric Acid for the Preparation of 2-Benzoxazolinone. *Organic Process Research and Development* **26,** 422–430 (Jan. 2022).

37. Acott, B., with A. Hassanali, A. L. J. B. & Redmond, J. W. Reaction of lead tetra-acetate with primary amides. Formation of alkyl carbamates. *Tetrahedron Letters* **6,** 4039–4045 (Jan. 1965).

38. Olah, G. A. Aromatic substitution. XXVIII. Mechanism of electrophilic aromatic substitutions. *Accounts of Chemical Research* **4,** 240–248 (July 1971).

39. Ridd, J. H. Mechanism of aromatic nitration. *Accounts of Chemical Research* **4,** 248–253 (July 1971).

40. Brinck, T. & Liljenberg, M. *Arene Chemistry* (ed Mortier, J.) (John Wiley and Sons, Inc, Dec. 2015).

41. Olah, G. A., Malhotra, R. & Narang, S. C. in *World Scientific Series in 20th Century Chemistry* 975–979 (World Scientific Publishing Company, Jan. 2003).

42. Nakatani, K. *et al.* Solvation in nitration of benzene and the valence electronic structure of the Wheland intermediate. *Physical Chemistry Chemical Physics* **24,** 16453–16461 (2022).

43. *Encyclopedia of Reagents for Organic Synthesis* (ed Paquette, L. A.) 2nd ed. (Wiley, 2009). ISBN: 978-0-470-01754-8.

44. Galabov, B. *et al.* Arenium ions are not obligatory intermediates in electrophilic aromatic substitution. *Proceedings of the National Academy of Sciences* **111,** 10067–10072 (June 2014).

45. Galabov, B., Nalbantova, D., von R. Schleyer, P. & Schaefer, H. F. Electrophilic Aromatic Substitution: New Insights into an Old Class of Reactions. *Accounts of Chemical Research* **49,** 1191–1199 (June 2016).

46. Stuyver, T., Danovich, D., Proft, F. D. & Shaik, S. Electrophilic Aromatic Substitution Reactions: Mechanistic Landscape, Electrostatic and Electric-Field Control of Reaction Rates, and Mechanistic Crossovers. *Journal of the American Chemical Society* **141,** 9719–9730 (May 2019).

47. Katritzky, A. R. *et al.* Preparation of nitropyridines by nitration of pyridines with nitric acid. *Organic and Biomolecular Chemistry* **3,** 538 (2005).

48. Katritzky, A. R. & Fan, W.-Q. Mechanisms and Rates of the Electrophilic Substitution Reactions of Heterocycles. *Heterocycles* **34,** 2179 (1992).

49. Bakke, J. M. & Ranes, E. A New Efficient Synthesis of 3-Nitropyridine and Substituted Derivatives. *Synthesis* **1997,** 281–283 (Mar. 1997).

50. Ege, S. N. *Organic Chemistry* 1827. ISBN: 9780669076387 (Houghton Mifflin Harcourt Trade Reference Publishers, 1984).

51. Kirpal, A. & Reiter, E. 3-Nitro-pyridin und seine Derivate. *Berichte der deutschen chemischen Gesellschaft (A and B Series)* **58,** 699–701 (Apr. 1925).

52. Bakke, J. M. *et al.* Nitration of Aromatic and Heteroaromatic Compounds by Dinitrogen Pentaoxide. *Acta Chemica Scandinavica* **48,** 1001–1006 (1994).

53. *4-aminopyridine preparation method* Chinese patent CN1807415A (Beijing University of Chemical Technology, Jan. 2005). https://patents.google.com/patent/CN1807415A/en (2021).

54. Sewald, N. & Jakubke10.1038/755, H.-D. *Peptides: Chemistry and Biology* 2nd ed. (WILEY-VCH Verlag GmbH Co. KGaA, Weinheim, 2009).

55. Kekulé, A. *Lehrbuch der Organischen Chemie, oder der Chemie der Kohlenstoffverbindungen* (1859).

56. Banci, L., Bertini, I., Luchinat, C. & Mori, M. NMR in structural proteomics and beyond. *Progress in Nuclear Magnetic Resonance Spectroscopy* **56,** 247–266 (Apr. 2010).

57. PDB, R. *PDB Data Distribution by Experimental Method and Molecular Type* https://www.rcsb.org/stats/summary.

58. McPherson, A. & Gavira, J. A. Introduction to protein crystallization. *Acta Crystallographica Section F Structural Biology Communications* **70,** 2–20 (Dec. 2013).

59. Kainosho, M. *et al.* Optimal isotope labelling for NMR protein structure determinations. *Nature* **440,** 52–57 (Mar. 2006).

60. Bhella, D. Cryo-electron microscopy: an introduction to the technique, and considerations when working to establish a national facility. *Biophysical Reviews* **11,** 515–519 (July 2019).

61. Williamson, M. P., Havel, T. F. & Wuethrich, K. Solution conformation of proteinase inhibitor IIA from bull seminal plasma by 1H nuclear magnetic resonance and distance geometry. *Journal of Molecular Biology* **182,** 295–315 (Mar. 1985).

62. Boelens, R., Scheek, R. M., Dijkstra, K. & Kaptein, R. Sequential assignment of imino- and amino-proton resonances in 1H NMR spectra of oligonucleotides by two-dimensional NMR spectroscopy. Application to a lac operator fragment. *Journal of Magnetic Resonance (1969)* **62,** 378–386 (May 1985).

63. Montelione, G. T., Zheng, D., Huang, Y. J., Gunsalus, K. C. & Szyperski, T. Protein NMR spectroscopy in structural genomics. *Nature Structural Biology* **7,** 982–985 (Nov. 2000).

64. Croft, D., Kemmink, J., Neidig, K.-P. & Oschkinat, H. Tools for the automated assignment of high-resolution three-dimensional protein NMR spectra based on pattern recognition techniques. *Journal of Biomolecular NMR* **10,** 207–219 (1997).

65. Guentert, P. Automated structure determination from NMR spectra. *European Biophysics Journal* **38,** 129–143 (Sept. 2008).

66. Gardner, K. H. & Kay, L. E. The use of 2H, 13C, 15N multidimensional NMR to study the structure and dynamics of proteins. *Annual Review of Biophysics and Biomolecular Structure* **27,** 357–406 (June 1998).

67. Frieden, C. The Kinetics of Side Chain Stabilization during Protein Folding. *Biochemistry* **42,** 12439–12446 (Oct. 2003).

68. Luchette, P. A., Prosser, R. S. & Sanders, C. R. Oxygen as a Paramagnetic Probe of Membrane Protein Structure by Cysteine Mutagenesis and 19F NMR Spectroscopy. *Journal of the American Chemical Society* **124,** 1778–1781 (Jan. 2002).

69. Gakh, Y. G., Gakh, A. A. & Gronenborn, A. M. Fluorine as an NMR probe for structural studies of chemical and biological systems. *Magnetic Resonance in Chemistry* **38,** 551–558 (2000).

70. Horng, J.-C. & Raleigh, D. P. Φ-Values beyond the Ribosomally Encoded Amino Acids: Kinetic and Thermodynamic Consequences of Incorporating Trifluoromethyl Amino Acids in a Globular Protein. *Journal of the American Chemical Society* **125,** 9286–9287 (2003).

71. Li, H. & Frieden, C. Fluorine-19 NMR Studies on the Acid State of the Intestinal Fatty Acid Binding Protein. *Biochemistry* **45,** 6272–6278 (Apr. 2006).

72. Peng, J. W. Cross-Correlated 19F Relaxation Measurements for the Study of Fluorinated Ligand-Receptor Interactions. *Journal of Magnetic Resonance* **153,** 32–47 (Nov. 2001).

73. Conte, L. L., Chothia, C. & Janin, J. The atomic structure of protein-protein recognition sites. *Journal of Molecular Biology* **285** (ed Fersht, A. R.) 2177–2198 (Feb. 1999).

74. Weininger, U., Diehl, C. & Akke, M. 13C relaxation experiments for aromatic side chains employing longitudinal- and transverse-relaxation optimized NMR spectroscopy. *Journal of Biomolecular NMR* **53,** 181–190 (July 2012).

75. Lichtenecker, R. J. Synthesis of aromatic 13C/2H-alpha-ketoacid precursors to be used in selective phenylalanine and tyrosine protein labelling. *Org. Biomol. Chem.* **12,** 7551–7560 (2014).

76. Kim, H.-W., Perez, J. A., Ferguson, S. J. & Campbell, I. D. The specific incorporation of labelled aromatic amino acids into proteins through growth of bacteria in the presence of glyphosate. *FEBS Letters* **272,** 34–36 (Oct. 1990).

77. Ong, S.-E. *et al.* Stable Isotope Labeling by Amino Acids in Cell Culture, SILAC, as a Simple and Accurate Approach to Expression Proteomics. *Molecular &amp Cellular Proteomics* **1,** 376–386 (May 2002).

78. Ibarrola, N., Molina, H., Iwahori, A. & Pandey, A. A Novel Proteomic Approach for Specific Identification of Tyrosine Kinase Substrates Using [13C]Tyrosine. *Journal of Biological Chemistry* **279,** 15805–15813 (Apr. 2004).

79. Ramaraju, B., McFeeters, H., Vogler, B. & McFeeters, R. L. Bacterial production of site specific 13C labeled phenylalanine and methodology for high level incorporation into bacterially expressed recombinant proteins. *Journal of Biomolecular NMR* **67,** 23–34 (Dec. 2016).

80. Kigawa, T., Muto, Y. & Yokoyama, S. Cell-free synthesis and amino acid-selective stable isotope labeling of proteins for NMR analysis. *Journal of Biomolecular NMR* **6,** 129–134 (Sept. 1995).

81. Goto, N. K. & Kay, L. E. New developments in isotope labeling strategies for protein solution NMR spectroscopy. *Current Opinion in Structural Biology* **10,** 585–592 (Oct. 2000).

82. Tampieri, A., Szabó, M., Medina, F. & Gulyás, H. A brief introduction to the basics of NMR spectroscopy and selected examples of its applications to materials characterization. *Physical Sciences Reviews* **6** (June 2020).

83. Pervushin, K., Riek, R., Wider, G. & Wuethrich, K. Attenuated T2 relaxation by mutual cancellation of dipole-dipole coupling and chemical shift anisotropy indicates an avenue to NMR structures of very large biological macromolecules in solution. *Proceedings of the National Academy of Sciences* **94,** 12366–12371 (Nov. 1997).

84. Pervushin, K., Riek, R., Wider, G. & Wuethrich, K. Transverse Relaxation-Optimized Spectroscopy (TROSY) for NMR Studies of Aromatic Spin Systems in 13C-Labeled Proteins. *Journal of the American Chemical Society* **120,** 6394–6400 (June 1998).

85. LeMaster, D. M. & Richards, F. M. NMR sequential assignment of Escherichia coli thioredoxin utilizing random fractional deuteriation. *Biochemistry* **27,** 142–150 (Jan. 1988).

86. Torchia, D. A., Sparks, S. W. & Bax, A. NMR signal assignments of amide protons in the alpha-helical domains of staphylococcal nuclease. *Biochemistry* **27,** 5135–5141 (July 1988).

87. Garrett, D. S. *et al.* Solution Structure of the 30 kDa N-Terminal Domain of Enzyme I of the Escherichia coli Phosphoenolpyruvate: Sugar Phosphotransferase System by Multidimensional NMR. *Biochemistry* **36,** 2517–2530 (Mar. 1997).

88. Bax, A. Multidimensional nuclear magnetic resonance methods for protein studies. *Current Opinion in Structural Biology* **4,** 738–744 (Oct. 1994).

89. Clore, G. M. & Gronenborn, A. M. Multidimensional heteronuclear nuclear magnetic resonance of proteins, 349–363 (1994).

90. Lichtenecker, R., Schoerghuber, J. & Bisaccia, M. Synthesis of Metabolic Amino acid Precursors: Tools for Selective Isotope Labeling in Cell-Based Protein Overexpression. *Synlett* **26,** 2611–2616 (Aug. 2015).

91. Vold, R. R. & Vold, R. L. Transverse relaxation in heteronuclear coupled spin systems: AX, AX2 AX3, and AXY. *The Journal of Chemical Physics* **64,** 320–332 (Jan. 1976).

92. LeMaster, D. M. & Kushlan, D. M. Dynamical Mapping of E. coli Thioredoxin via 13C NMR Relaxation Analysis. *Journal of the American Chemical Society* **118,** 9255–9264 (Jan. 1996).

93. Kay, L. E. Protein dynamics from NMR. *Nature Structural Biology* **5,** 513–517 (July 1998).

94. Loewen, M. C. *et al.* Solution 19F nuclear Overhauser effects in structural studies of the cytoplasmic domain of mammalian rhodopsin. *Proceedings of the National Academy of Sciences* **98,** 4888–4892 (Apr. 2001).

95. Chambers, S. E., Lau, E. Y. & Gerig, J. T. Origins of Fluorine Chemical Shifts in Proteins. *Journal of the American Chemical Society* **116,** 3603–3604 (Apr. 1994).

96. Gerig, J. T. Fluorine NMR of proteins. *Progress in Nuclear Magnetic Resonance Spectroscopy* **26,** 293–370 (Jan. 1994).

97. Frieden, C., Hoeltzli, S. D. & Bann, J. G. in *Methods in Enzymology* 400–415 (Elsevier, 2004).

98. Evanics, F., Kitevski, J. L., Bezsonova, I., Forman-Kay, J. & Prosser, R. S. 19F NMR studies of solvent exposure and peptide binding to an SH3 domain. *Biochimica et Biophysica Acta (BBA) - General Subjects* **1770,** 221–230 (Feb. 2007).

99. Duewel, H. S., Daub, E., Robinson, V. & Honek, J. F. Elucidation of Solvent Exposure, Side-Chain Reactivity, and Steric Demands of the Trifluoromethionine Residue in a Recombinant Protein. *Biochemistry* **40,** 13167–13176 (Oct. 2001).

100. Luck, L. A. & Falke, J. J. Fluorine-19 NMR studies of the D-galactose chemosensory receptor. 2. Calcium binding yields a local structural change. *Biochemistry* **30,** 4257–4261 (Apr. 1991).

101. Xiao, G., Parsons, J. F., Tesh, K., Armstrong, R. N. & Gilliland, G. L. Conformational changes in the crystal structure of rat glutathione transferase M1-1 with global substitution of 3-fluorotyrosine for tyrosine. *Journal of Molecular Biology* **281,** 323–339 (Aug. 1998).

102. Woll, M. G., Hadley, E. B., Mecozzi, S. & Gellman, S. H. Stabilizing and Destabilizing Effects of Phenylalanine F5-Phenylalanine Mutations on the Folding of a Small Protein. *Journal of the American Chemical Society* **128,** 15932–15933 (Nov. 2006).

103. Chiu, H.-P. *et al.* Helix Propensity of Highly Fluorinated Amino Acids. *Journal of the American Chemical Society* **128,** 15556–15557 (Nov. 2006).

104. Friebolin, H. *Ein- und zweidimensionale NMR-Spektroskopie: Eine Einführung* 5th ed. (Wiley-VCH Verlag WILEY-VCH Verlag GmbH, Feb. 2013).

105. Campos-Olivas, R., Aziz, R., Helms, G. L., Evans, J. N. S. & Gronenborn, A. M. Placement of 19F into the center of GB1: effects on structure and stability. *FEBS Letters* **517,** 55–60 (Mar. 2002).

106. Cellitti, S. E. *et al.* Incorporation of Unnatural Amino Acids to Probe Structure, Dynamics, and Ligand Binding in a Large Protein by Nuclear Magnetic Resonance Spectroscopy. *Journal of the American Chemical Society* **130,** 9268–9281 (June 2008).

107. Didenko, T., Liu, J. J., Horst, R., Stevens, R. C. & Wüthrich, K. Fluorine-19 NMR of integral membrane proteins illustrated with studies of GPCRs. *Current Opinion in Structural Biology* **23,** 740–747 (Oct. 2013).

108. Dawson, P. E. & Kent, S. B. H. Synthesis of Native Proteins by Chemical Ligation. *Annual Review of Biochemistry* **69,** 923–960 (June 2000).

109. Merrifield, R. B. Solid Phase Peptide Synthesis. I. The Synthesis of a Tetrapeptide. *Journal of the American Chemical Society* **85,** 2149–2154 (July 1963).

110. Jaradat, D. M. M. Thirteen decades of peptide synthesis: key developments in solid phase peptide synthesis and amide bond formation utilized in peptide ligation. *Amino Acids* **50,** 39–68 (Nov. 2017).

111. Hudson, A. S., Hoose, A., Coxon, C. R., Sandford, G. & Cobb, S. L. Synthesis of a novel tetrafluoropyridine-containing amino acid and tripeptide. *Tetrahedron Letters* **54,** 4865–4867 (Sept. 2013).

112. Shriver, J. W. & Sykes, B. D. Energetics of the equilibrium between two nucleotide-free myosin subfragment 1 states using fluorine-19 NMR. *Biochemistry* **21,** 3022–3028 (June 1982).

113. Kalbitzer, H. R. *et al.* A new high sensitivity 19F probe for labeling cysteine groups of proteins. *NMR in Biomedicine* **5,** 347–350 (Nov. 1992).

114. Lin, M. T. *et al.* in *Isotope Labeling of Biomolecules - Labeling Methods* 45–66 (Elsevier, 2015).

115. Salopek-Sondi, B., Vaughan, M. D., Skeels, M. C., Honek, J. F. & Luck, L. A. 19F NMR Studies of the Leucine-Isoleucine-Valine Binding Protein: Evidence That a Closed Conformation Exists in Solution. *Journal of Biomolecular Structure and Dynamics* **21,** 235–246 (Oct. 2003).

116. Waugh, D. S. Genetic tools for selective labeling of proteins with alpha-15N-amino acids. *Journal of Biomolecular NMR* **8** (Sept. 1996).

117. Franz, J. E., Mao, M. K. & Sikorski, J. A. Glyphosate, a Unique Global Herbicide. *ACS Monograph* **189,** 653 pp. (1997).

118. Kitevski-LeBlanc, J. L., Evanics, F. & Prosser, R. S. Approaches for the measurement of solvent exposure in proteins by 19F NMR. *Journal of Biomolecular NMR* **45,** 255–264 (Aug. 2009).

119. Marsh, E. N. G. & Suzuki, Y. Using 19F NMR to Probe Biological Interactions of Proteins and Peptides. *ACS Chemical Biology* **9,** 1242–1250 (May 2014).

120. Smolskaya, S. & Andreev, Y. Site-Specific Incorporation of Unnatural Amino Acids into Escherichia coli Recombinant Protein: Methodology Development and Recent Achievement. *Biomolecules* **9,** 255 (June 2019).

121. Furter, R. Expansion of the genetic code: Site-directed p-fluoro-phenylalanine incorporation in Escherichia coli. *Protein Science* **7,** 419–426 (Feb. 1998).

122. PDB, R. *PDB Data Distribution by Expression System Organism* https://www.rcsb.org/stats/distribution-expression-organism-gene.

123. Herrmann, K. M. & Weaver, L. M. The Shikimate Pathway. *Annual Review of Plant Physiology and Plant Molecular Biology* **50,** 473–503 (June 1999).

124. Billek, G. Zur Synthese der Phenylbrenztraubensäure. *Mitt Monatsheft Chemie* **3.** 343–351 (92 1961).

125. Lichtenecker, R. J., Weinhaeupl, K., Schmid, W. & Konrat, R. Alpha-Ketoacids as precursors for phenylalanine and tyrosine labelling in cell-based protein overexpression. *Journal of Biomolecular NMR* **57,** 327–331 (Nov. 2013).

126. Ware, E. The Chemistry of the Hydantoins. *Chemical Reviews* **46,** 403–470 (June 1950).

127. Lichtenecker, R. J., Coudevylle, N., Konrat, R. & Schmid, W. Selective Isotope Labelling of Leucine Residues by Using alpha-Ketoacid Precursor Compounds. *ChemBioChem* **14,** 818–821 (Apr. 2013).

Abbreviations

PIDA phenyliodo diacetate. 6, 11, 13–19, 22

$TsNBr_2$ N,N-dibromo-p-toluensulfonamide. 6

^{15}N-labeled ANP [4-^{15}N]amino-[3-^{15}N]nitropyridine. viii, xiv, 2, 9, 12, 19, 25

E. coli *Escherichia coli*. vi, xi, xv, 31, 36, 41

EN electro negativity. 34

vdW van der Waals. 34

EM electron microscopy. 27, 28

4AP 4-aminopyridine. vi, xiv, 10–12, 23–25, 66

ACN acetonitrile. 11, 13–18

ATP adenosine triphosphate. 36

Bn benzyl ester protecting group. 35

Boc *tert*-butyloxycarbonyl. 35

DAHP 3-deoxy-D-arabino-heptulosonic acid 7-phosphate. 36

DBU 1,8-diazobicyclo[5.4.0]unde-7-ene. 11, 23

DCC dicyclohexylcarbodiimide. 5

DIPEA N,N-Diisopropyl ethylamine. 11, 13–18, 22

DMSO-d_6 deuterated dimethyl sulfoxide. vi, xv, 61–65, 67–75

DMT-MM 4-(4,6-dimethoxy-1,3,5-triazin-2-yl)-4-methylmorpholinium chloride. 5

DPPA diphenylphosphoryl azide. 5

E4P D-erythrose-4-phosphate. xiv, 36, 38

EC enzyme code. 35, 36, 38

glyphosate N-phosphonomethylglycine. 31, 35, 41

HSQC heteronuclear single quantum coherence. 32

INA isonicotinamide. 9–11, 13, 14, 16–19, 22–24

MS mass spectroscopy. vii, 2, 20, 84–92

MW molecular weight. 28

NADPH nicotinamide adenine dinucleotide phosphate. 36

NBS N-bromosuccinimide. 6, 11, 23

NMR nuclear magnetic resonance. vi, vii, ix, xi–xiii, xv, xvi, 2, 20, 23–25, 28–30, 32–34, 40, 42, 43, 48, 50, 61–83

NOESY nuclear Overhauser effect spectroscopy. 32

Nu^- nucleophile. 3

Oxone® potassium peroxymonosulfate. 6

PDB protein data bank. xii, 27

PEP phosphoenolepyruvate. xiv, 36, 38

PhIO iodosylbenzene. 6

S_EAr electrophilic aromatic substitution. v, xii, 7, 8

TEA triethylamine. 13, 17

THF tetrahydrofuran. 10, 20, 21

TLC thin layer chromatography. 13, 17, 20, 21, 43

tRNA transfer RNA. 35, 36

TROSY transverse relaxation-optimized spectroscopy. ix, xi, 31, 32, 42

US ultrasound. 11, 13, 14

Z atom or group which is bound to the acyl group. 3

Appendix A

Spectral analysis: nuclear magnetic resonance

solvent	^{1}H-NMR absorption δ [ppm]	H_2O or HDO δ [ppm]
DMSO – d_6	2.49	3.3
$CDCl_3$	7.24	1.5
D_2O	4.65	4.8

Table 20: solvent peaks of ^{1}H-NMR spectra (400 MHz)

A.1 NMR spectra of [4-^{15}N]amino-[3-^{15}N]nitropyridine 6 synthesis

A.1.1 ^{1}H-NMR (400MHz) of isonicotin-[^{15}N]amide 3

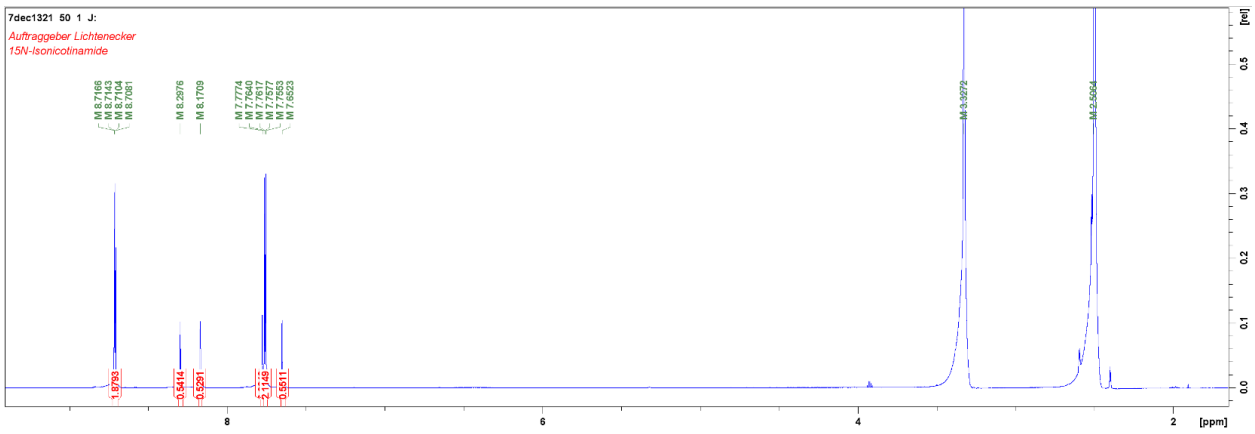

Scheme 32: overview ^{1}H-NMR 400 MHz (DMSO-d_6) of [^{15}N]isonicotinamide

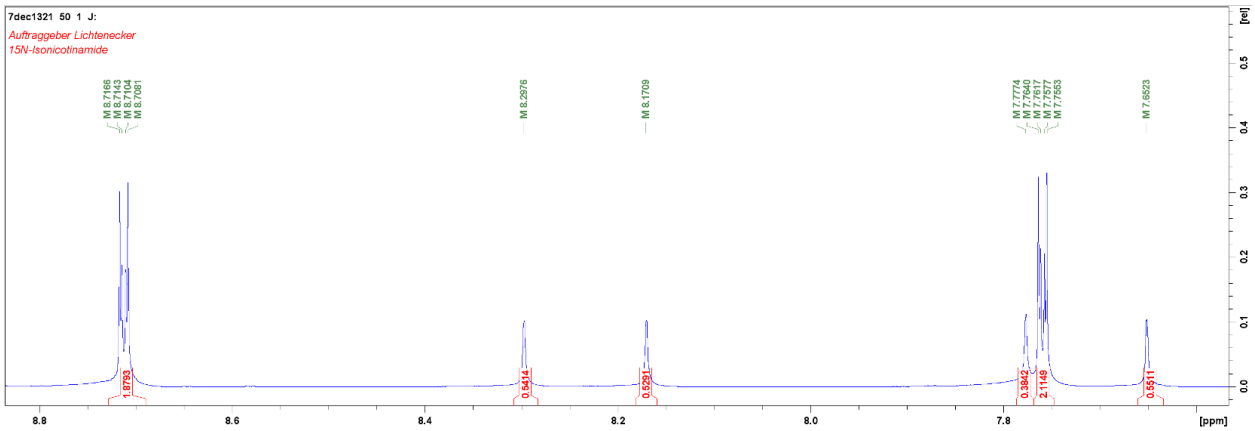

Scheme 33: ROI ^{1}H-NMR 400 MHz (DMSO-d_6) of [^{15}N]isonicotinamide

Chemical shift [ppm]	Multiplicity	Integration	Coupling [Hz]	Assignment	Atom no.
7.65, 7.78	singlet, singlet	1 H	J_{NH} = 1.3	-^{15}N**H$_A$**	2
7.76	doublet of doublets	2 H	J_{HH} = 5.0, 5.0	-pyridyl C**H**	4, 8
8.17, 8.30	singlet, singlet	1 H	J_{NH} = 1.3	-^{15}N**H$_B$**	2
8.71	doublet of doublets	2 H	J_{HH} = 5.0, 5.0	-pyridyl C**H**	5, 7

Table 21: ^{1}H-NMR of [^{15}N]isonicotinamide

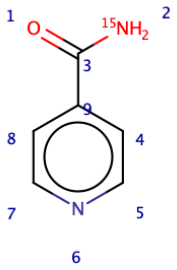

Scheme 34: peak assignment of ^{1}H-NMR of [^{15}N]isonicotinamide

A.1.2 ^{13}C-NMR (176 MHz) of [^{15}N]isonicotinamide 3

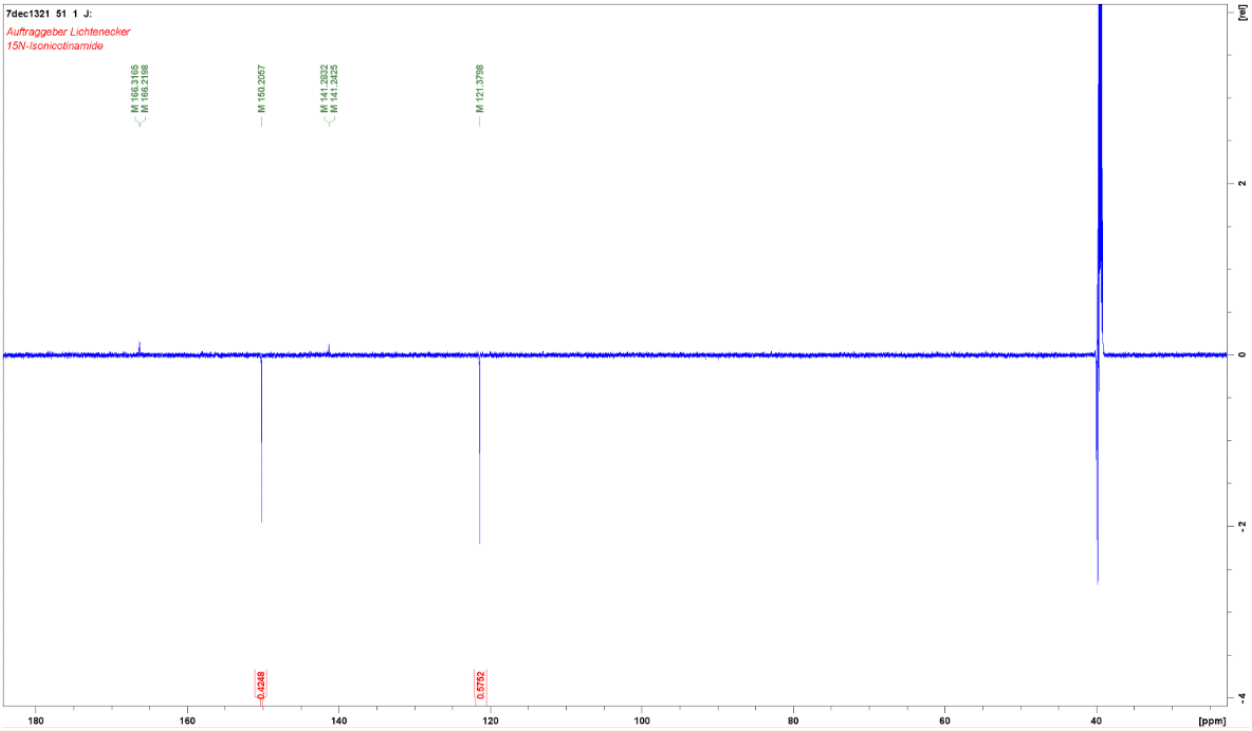

Scheme 35: ^{13}C-NMR 176 MHz (DMSO-d$_6$) of [^{15}N]isonicotinamide

Chemical shift [ppm]	Integration	Assignment	Atom no.
121.38	2 C	– pyridyl **C**(– C)	4, 8
141.26	1 C	– pyridyl **C**(– C = O)	9
150.21	2 C	– pyridyl **C**(– N)	5, 7
166.27	1 C	– **C** = O	3

Table 22: ^{13}C-NMR of [^{15}N]isonicotinamide

A.1.3 ^{1}H-NMR (400 MHz) of [4-^{15}N]aminopyridine 5

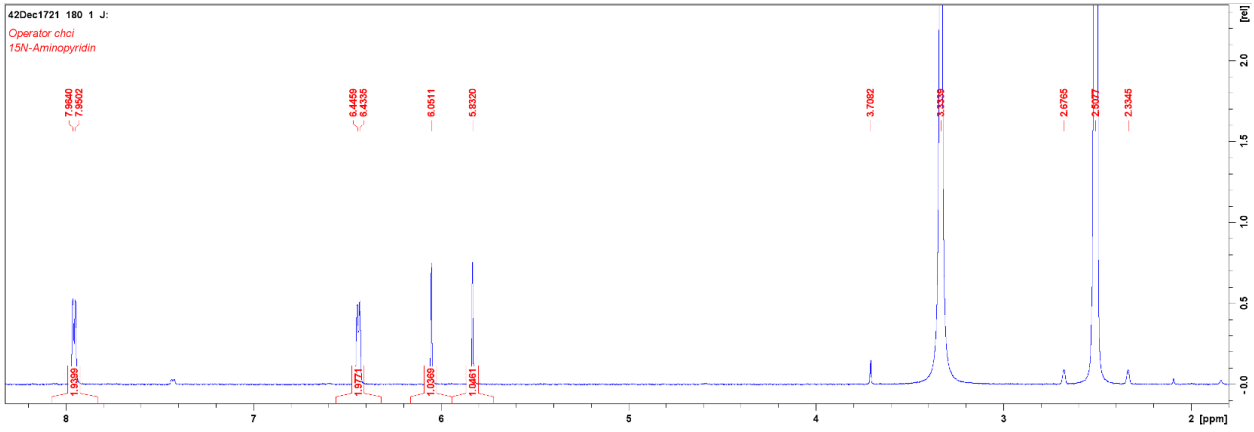

Scheme 36: overview ^{1}H-NMR 400 MHz (DMSO-d_6) of [4-^{15}N]aminopyridine

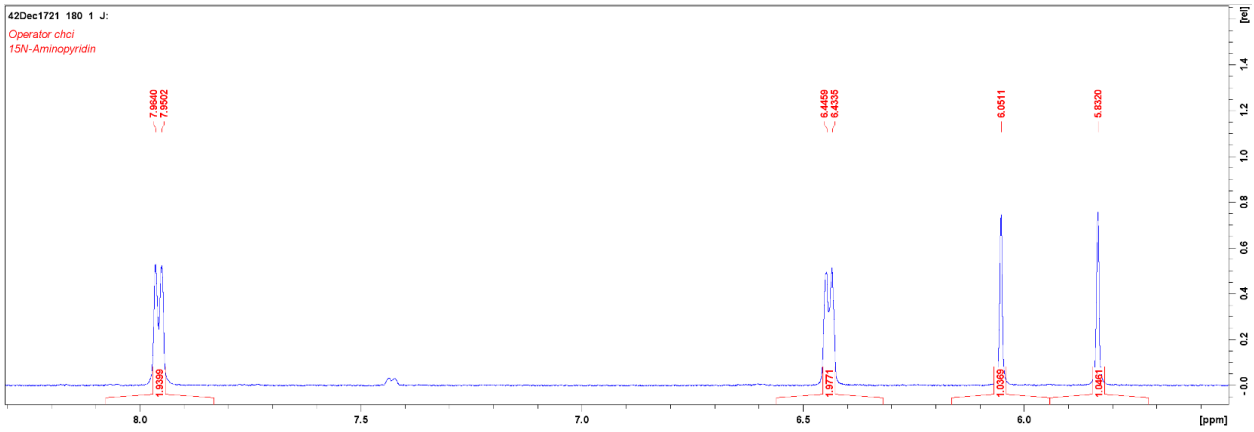

Scheme 37: ROI ^{1}H-NMR 400 MHz (DMSO-d_6) of [4-^{15}N]aminopyridine

Chemical shift [ppm]	Multiplicity	Integration	Coupling [Hz]	Assignment	Atom no.
7.96	doublet	2 H	$^{3}J_{HH}$ = 1.4	– N – pyridyl C**H$_2$**	3, 5
6.44	doublet	2 H	$^{3}J_{HH}$ = 1.2	– C – pyridyl C**H$_2$**	2, 6
5.83, 6.05	singlet, singlet	2 H	$^{1}J_{NH}$ = 2.2	-^{15}N**H$_2$**	1, 1

Table 23: ^{1}H-NMR of [4-^{15}N]aminopyridine

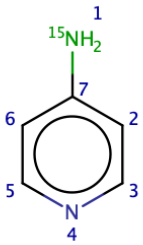

Scheme 38: peak assignment for ^{1}H-NMR of [4-^{15}N]aminopyridine

A.1.4 ^{13}C-NMR (176 MHz) of [4-^{15}N]aminopyridine 5

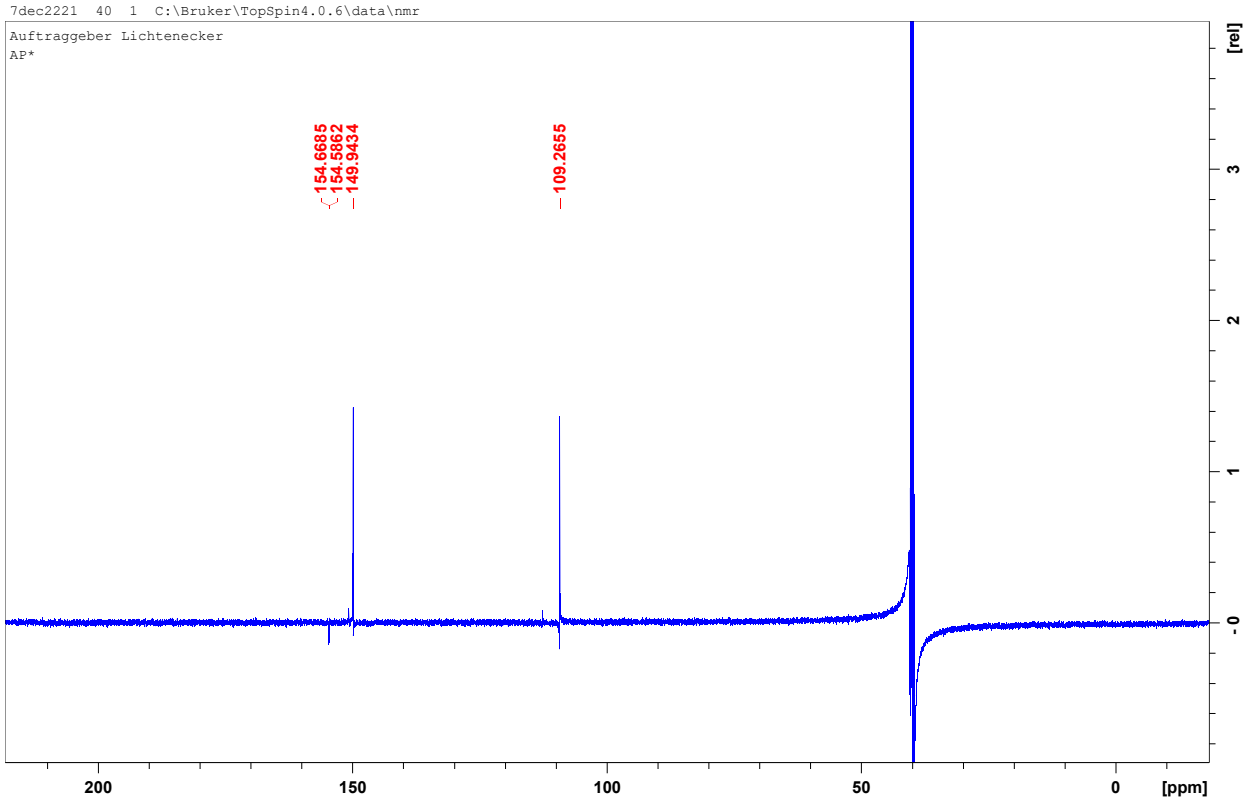

Scheme 39: ^{13}C-NMR 176 MHz (DMSO-d$_6$) of [4-^{15}N]aminopyridine

Chemical shift [ppm]	Integration	Assignment	Atom no.
109.3	2 C	– pyridyl **C**(– C)	2, 6
149.4	2 C	– pyridyl **C**(– N)	3, 5
154.6	1 C	– pyridyl **C**(– ^{15}N)	7

Table 24: ^{13}C-NMR of [4-^{15}N]aminopyridine

A.1.5 ^{1}H-NMR (400 MHz) of compounds resulting from alternative 4AP 5 synthesis'

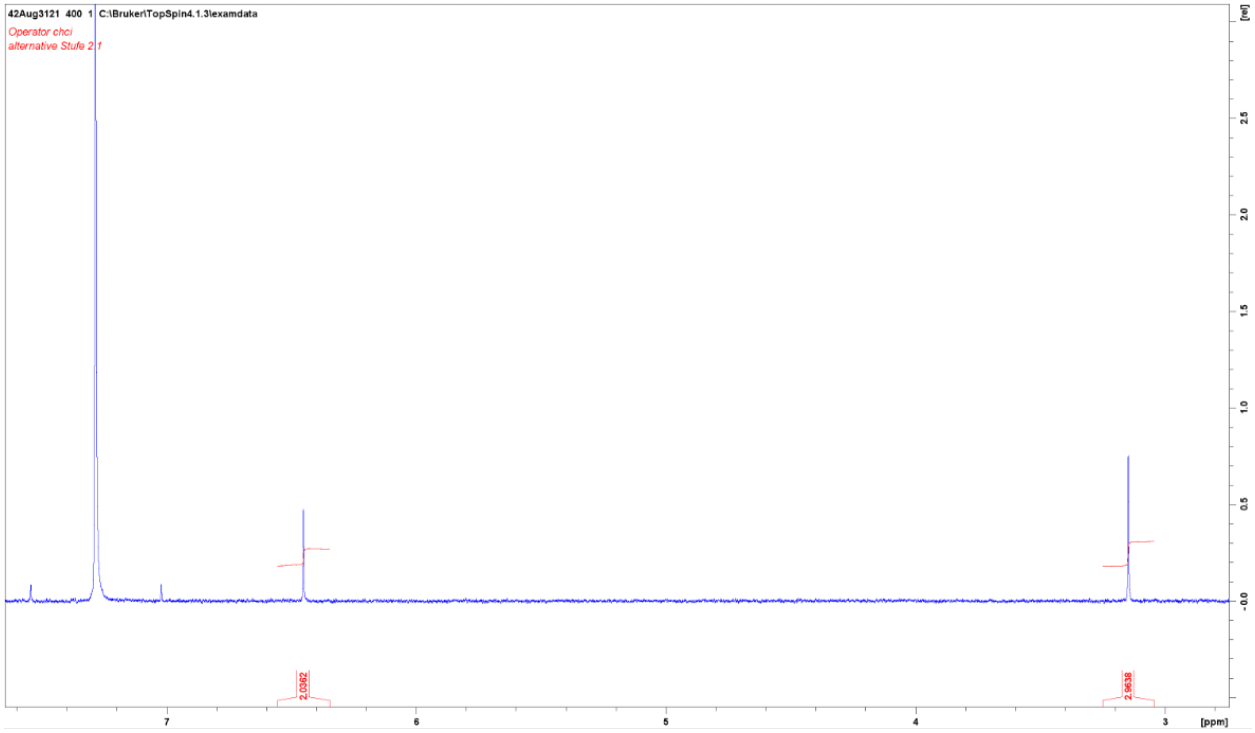

Scheme 40: ^{1}H-NMR 400 MHz ($CDCl_3$) of compound resulting from alternative path **b**

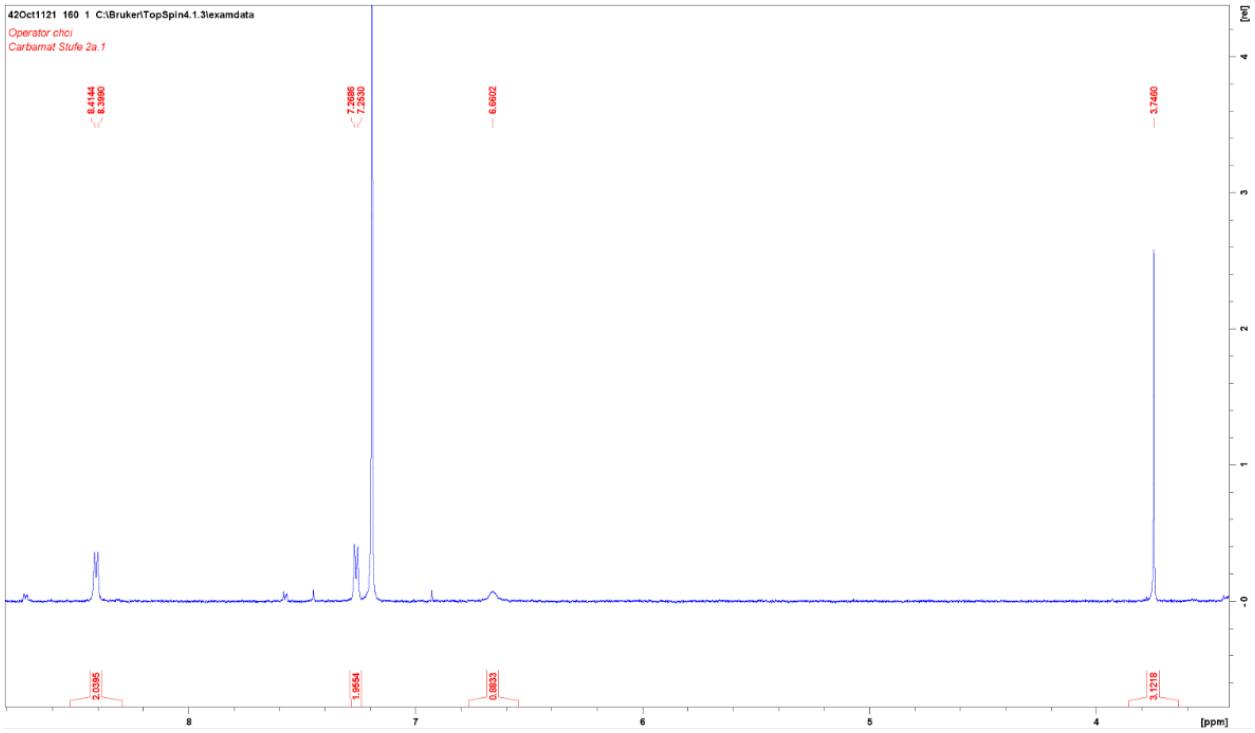

Scheme 41: ^{1}H-NMR 400 MHz ($CDCl_3$) of n-(4-pyridyl) methyl carbamate **4b**

Chemical shift [ppm]	Multiplicity	Integration	Coupling [Hz]	Assignment	Atom no.
3.75	singlet	3 H	-	– C**H**$_3$	11
6.66	singlet	1 H	-	– N**H** – CO –	7
7.3	doublet	2 H	$^3J_{HH}$ = 1.54	– C – pyridyl C**H**	2, 6
8.4	doublet	2 H	$^3J_{HH}$ = 1.56	– N – pyridyl C**H**	3, 5

Table 25: ^{1}H-NMR of n-(4-pyridyl) methyl carbamate **4b**

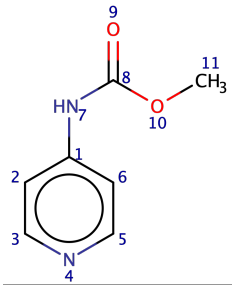

Scheme 42: peak assignment for ^{1}H-NMR of n-(4-pyridyl) methyl carbamate **4b**

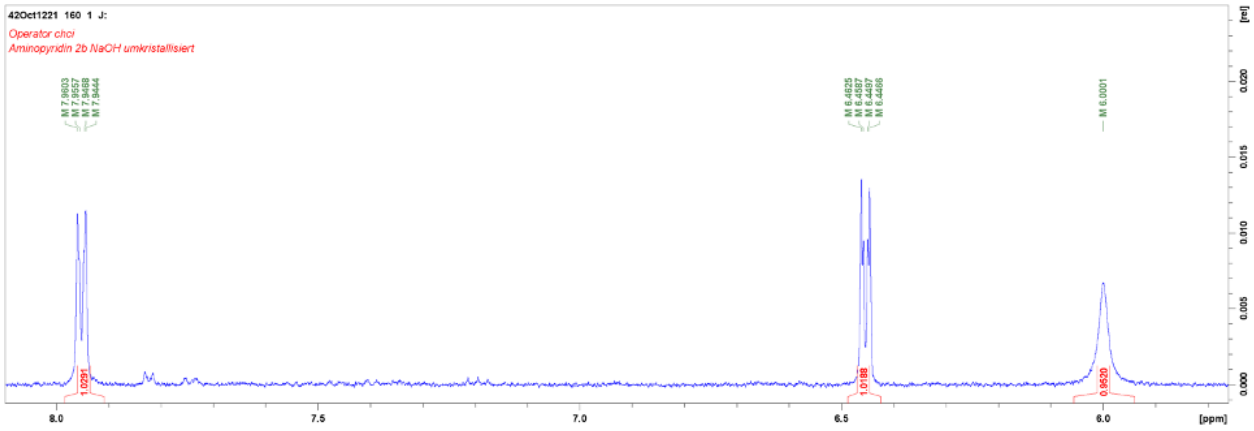

Scheme 43: ^{1}H-NMR 400 MHz (DMSO-d_6) of 4-aminopyridine hydrochloride **5b**

Chemical shift [ppm]	Multiplicity	Integration	Coupling [Hz]	Assignment	Atom no.[38]
6.0	singlet	2 H	-	– C – N**H$_2$**	1, 1
6.45	doublet of doublets	2 H	$^3J_{HH}$ = 15.9	– C – pyridyl C**H$_2$**	2, 6
7.95	doublet	2 H	$^3J_{HH}$ = 15.9	– N – pyridyl C**H$_2$**	3, 5

Table 26: ^{1}H-NMR of [4-^{15}N]aminopyridine

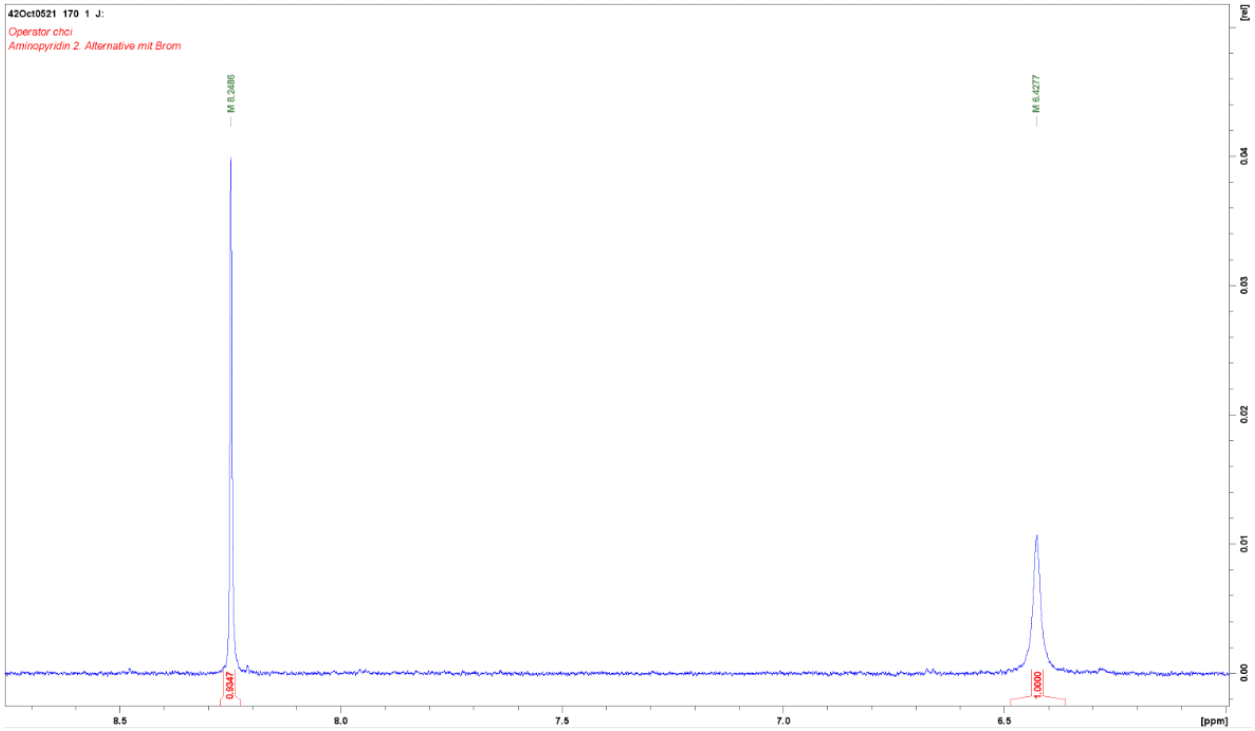

Scheme 44: ^{1}H-NMR 400 MHz (DMSO-d_6) of brominated 4-aminopyridine **5c**

Chemical shift [ppm]	Multiplicity	Integration	Coupling [Hz]	Assignment	Atom no.
6.43	singlet	2 H	-	– C – N**H$_2$**	7, 7
8.25	singlet	2 H	-	– N – pyridyl C**H**	3, 5

Table 27: ^{1}H-NMR of brominated 4-aminopyridine **5c**

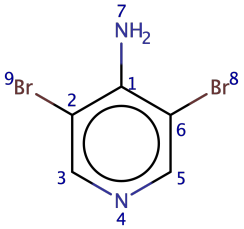

Scheme 45: peak assignment for ^{1}H-NMR 400 MHz (DMSO-d_6) of brominated 4-aminopyridine **5c**

A.1.6 ^{1}H-NMR (400 MHz) of [4-^{15}N]amino – [3-^{15}N]nitropyridine 6

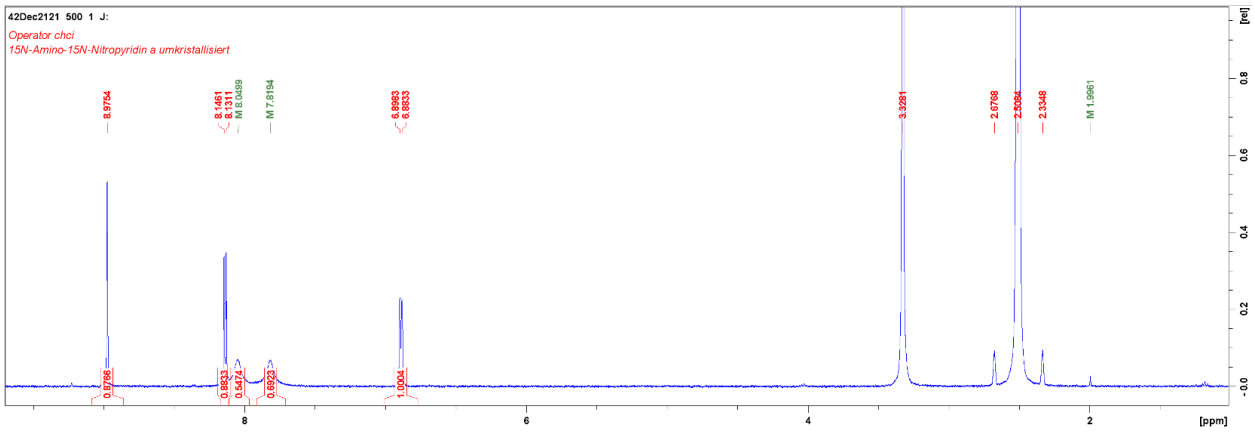

Scheme 46: overview ^{1}H-NMR 400 MHz (DMSO-d$_6$) of [4-^{15}N]amino-[3-^{15}N]nitropyridine (a)

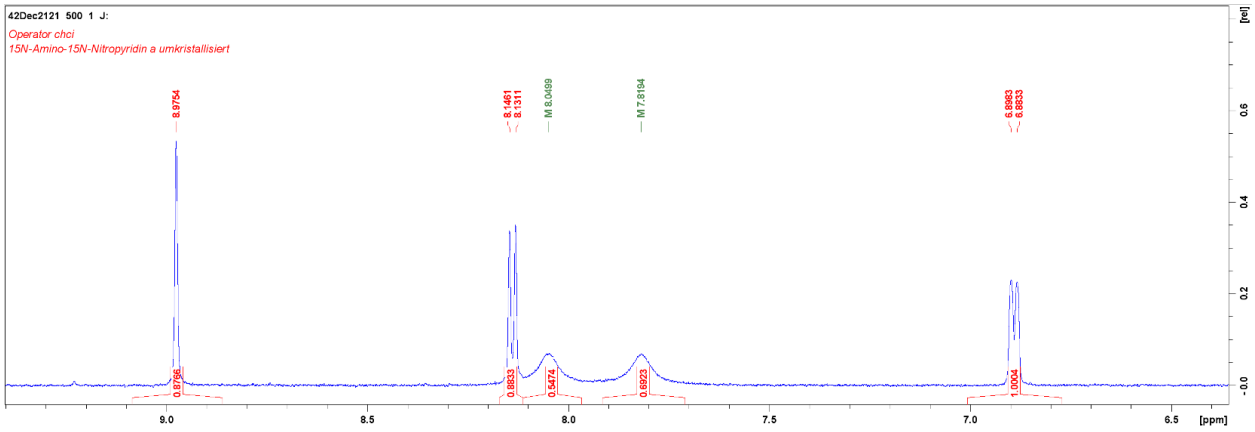

Scheme 47: ROI ^{1}H-NMR 400 MHz (DMSO-d$_6$) of [4-^{15}N]amino-[3-^{15}N]nitropyridine (a)

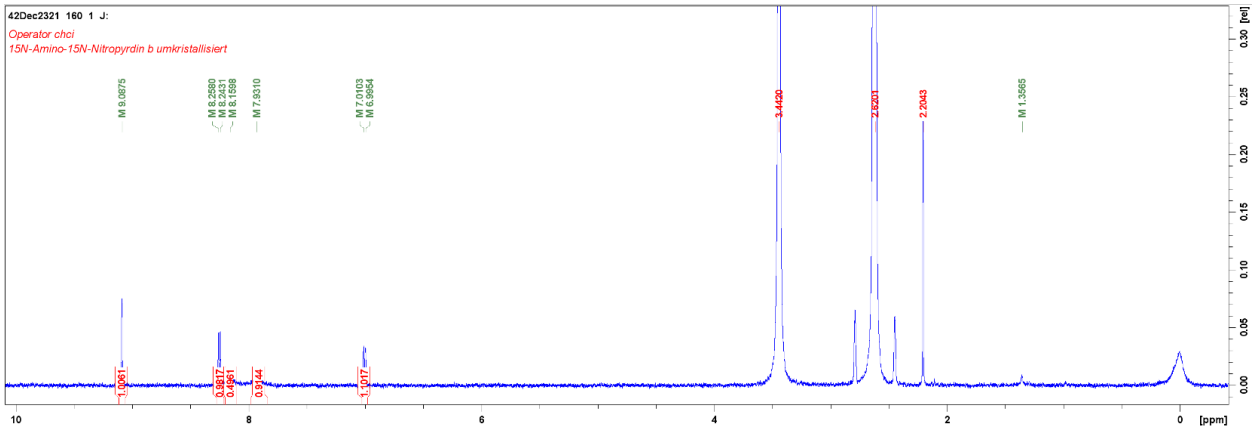

Scheme 48: overview ^{1}H-NMR 400 MHz (DMSO-d$_6$) of [4-^{15}N]amino-[3-^{15}N]nitropyridine (b)

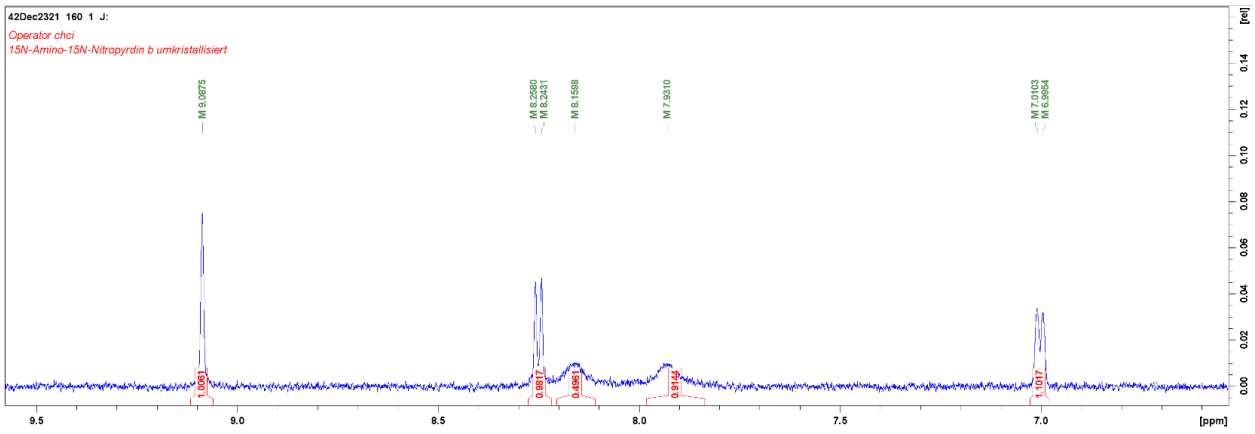

Scheme 49: ROI ^{1}H-NMR 400 MHz (DMSO-d_6) of [4-^{15}N]amino-[3-^{15}N]nitropyridine (b)

Chemical shift [ppm]	Multiplicity	Integration	Coupling [Hz]	Assignment	Atom no.
8.98	singlet	1 H	-	– N – pyridyl C**H** – CNO_2	5
8.14	doublet	1 H	$^{3}J_{HH}$ = 1.5	– N – pyridyl C**H** – CH	3
8.05, 7.82	singlet, singlet	1 H	$^{1}J_{NH}$ = 2.2	– C – ^{15}N**H$_2$**	7, 7
6.89	doublet	1 H	$^{3}J_{HH}$ = 1.5	– C pyridyl C**H** – CNH_2	2

Table 28: ^{1}H-NMR of [4-^{15}N]amino – [3-^{15}N]nitropyridine

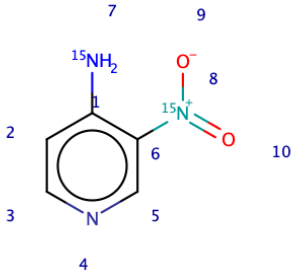

Scheme 50: peak assignment for ^{1}H-NMR of [4-^{15}N]amino – [3-^{15}N]nitropyridine

A.1.7 ^{13}C-NMR (176 MHz) of [4-^{15}N]amino – [3-^{15}N]nitropyridine 6

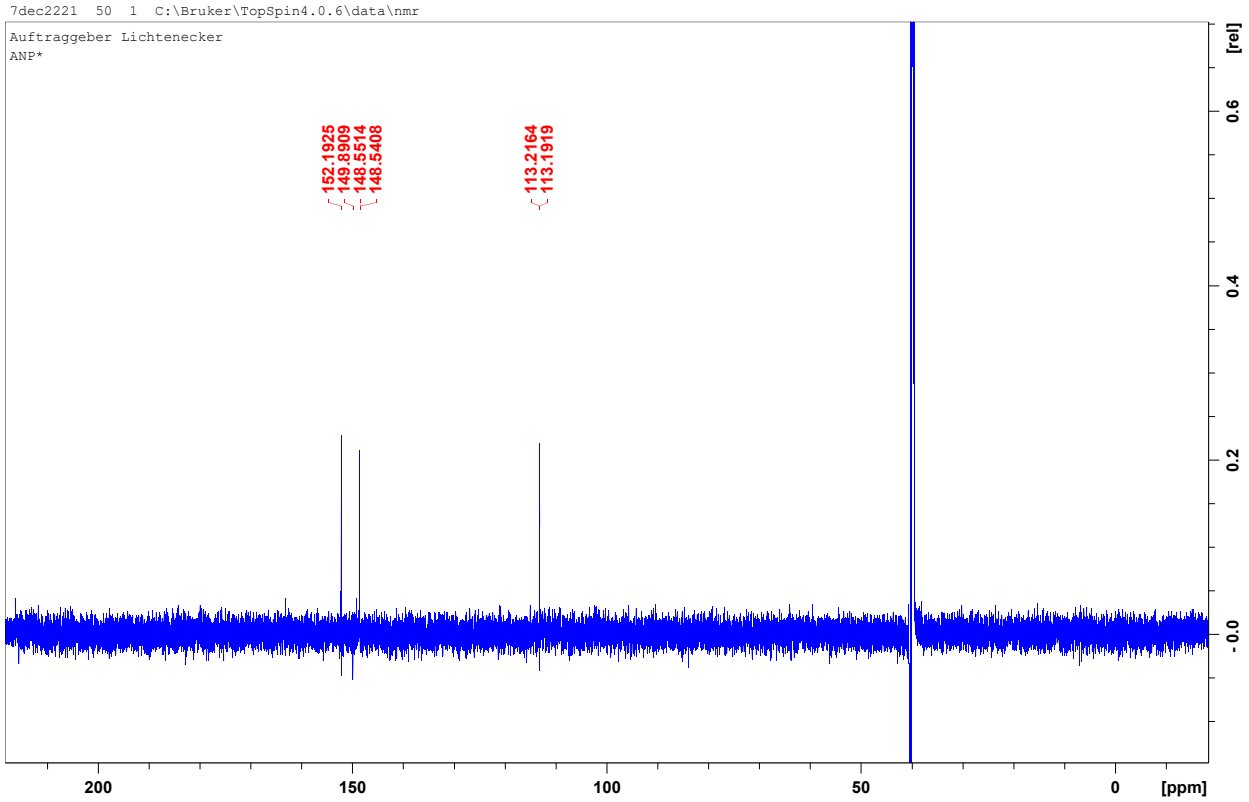

Scheme 51: ^{13}C-NMR 176 MHz (DMSO-d_6) of [4-^{15}N]amino – [3-^{15}N]nitropyridine

Chemical shift [ppm]	Integration	Assignment	Atom no.
113.2	1 C	– pyridyl **C**(– C)	2
148.54	1 C	– pyridyl **C**(– $^{15}NO_2$)	6
148.55	1 C	– pyridyl **C**(– $^{15}NH_2$)	1
149.89	1 C	– pyridyl **C**(– N)	5
152.19	1 C	– pyridyl **C**(– N)	3

Table 29: ^{13}C-NMR of [4-^{15}N]amino – [3-^{15}N]nitropyridine

A.2 NMR spectra of fluorinated phenylalanine precursor compounds

A.2.1 ^{1}H-NMR (DMSO-d_6) of [1-^{13}C]hydantoin 8

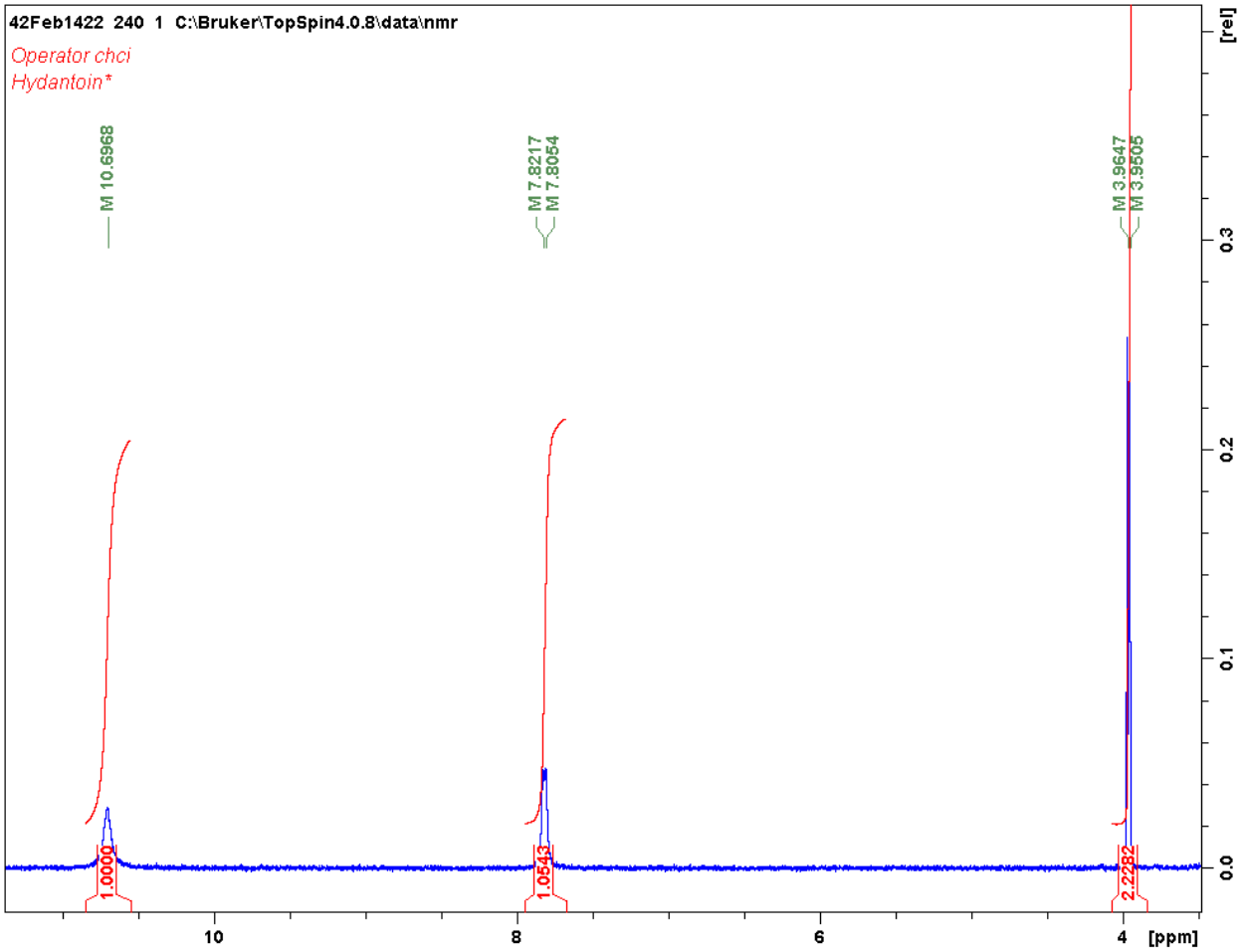

Scheme 52: ^{1}H-NMR 400 MHz (DMSO-d_6) of [1-^{13}C]hydantoin

Chemical shift [ppm]	Multiplicity	Integration	Coupling [Hz]	Assignment	Atom no.
4.0	doublet	2 H	$^{2}J_{HH}$ = 14.2	– NH – C**H$_2$** – CO –	10, 11
7.8	doublet	1 H	$^{2}J_{^{13}CH}$ = 16.3	– CO – N**H** – CO –	8
10.7	singlet	1 H	-	– CH_2 – N**H** – CO –	9

Table 30: ^{1}H-NMR of [1-^{13}C]hydantoin

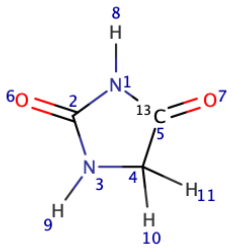

Scheme 53: peak assignment for ^{1}H-NMR of [1-^{13}C]hydantoin

A.2.2 ^{1}H-NMR (DMSO-d$_6$) of para-fluorobenzal-[1-^{13}C]hydantoin 9a

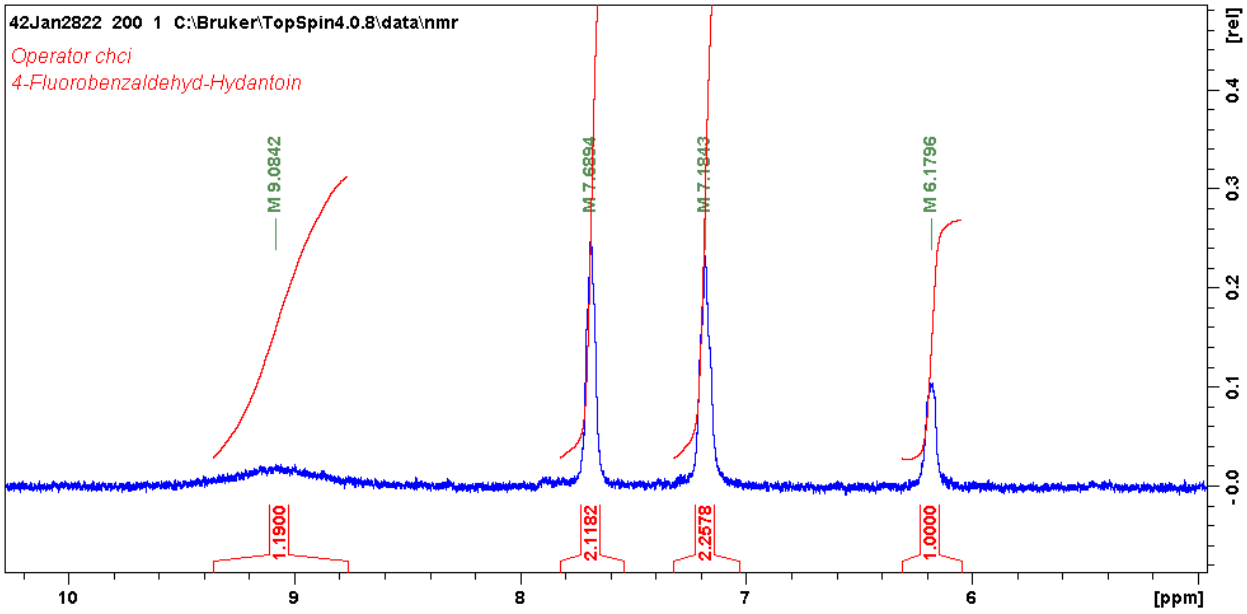

Scheme 54: ^{1}H-NMR 400 MHz (DMSO-d$_6$) of para-fluorobenzal-[1-^{13}C]hydantoin

Chemical shift [ppm]	Multiplicity	Integration	Coupling [Hz]	Assignment	Atom no.
6.18	singlet	1 H	-	– C**H** =	18
7.18	singlet	2 H	-	– phenyl C**H**	11, 13
7.69	singlet	2 H	-	– phenyl C**H**	10, 14
9.08	broad	1 H	-	– CO – N**H** – CO –	16

Table 31: ^{1}H-NMR of para-fluorobenzal-[1-^{13}C]hydantoin

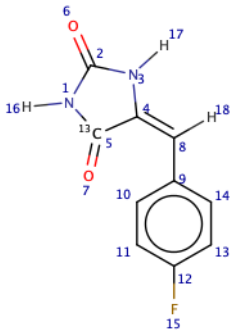

Scheme 55: peak assignment for ^{1}H-NMR of para-fluorobenzal-[1-^{13}C]hydantoin

A.2.3 ^{1}H-NMR (DMSO-d_6) of 3,5-difluoro-4-hydroxybenzal-[1-^{13}C]hydantoin 9b

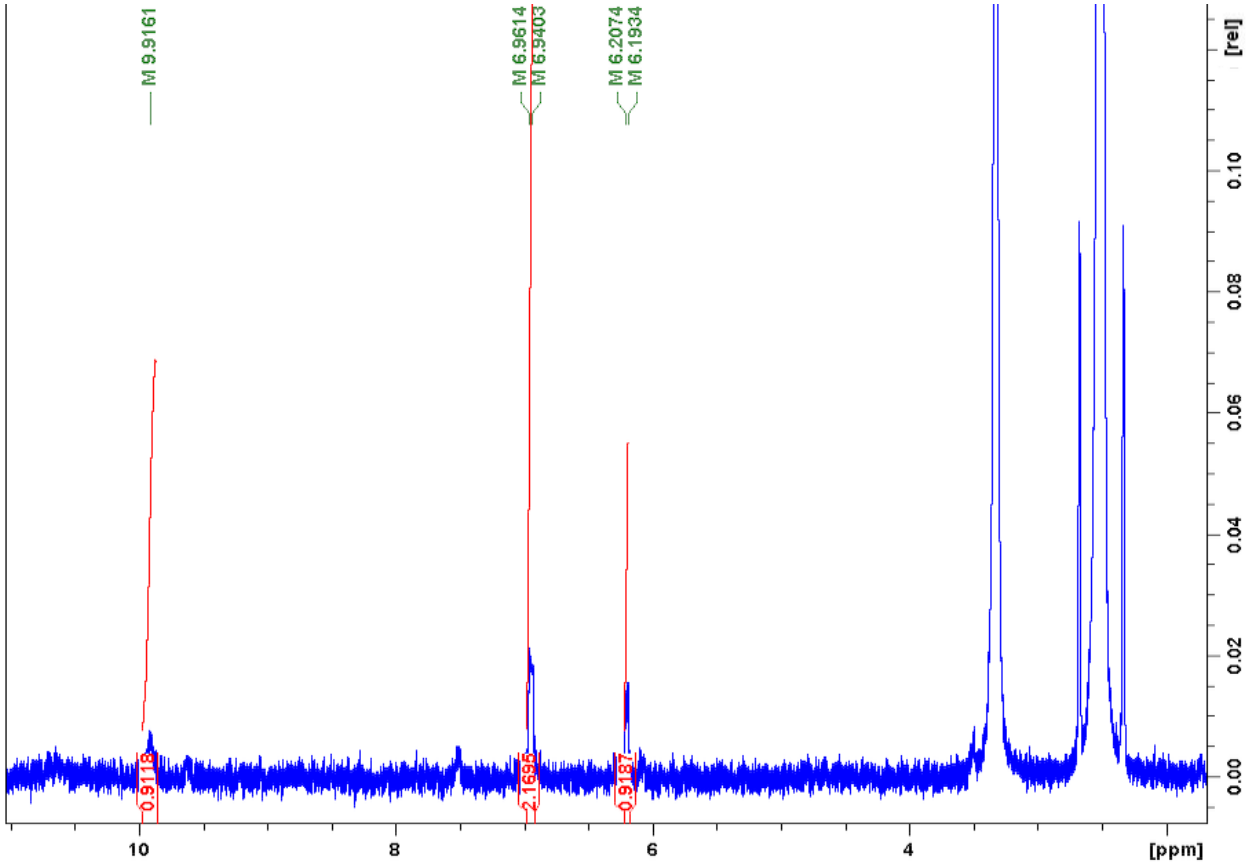

Scheme 56: ^{1}H-NMR of 3,5-difluoro-4-hydroxybenzal-[1-^{13}C]hydantoin

Chemical shift [ppm]	Multiplicity	Integration	Coupling [Hz]	Assignment	Atom no.
6.20	doublet	1 H	$^{3}J_{^{13}CH}$ = 1.4	– C**H** =	18
6.95	quartet	2 H	$^{3}J_{FH}$ = 21.1	– phenyl C**H**	2, 6
9.92	singlet	1 H	-	– CO – N**H** – CO –	19

Table 32: ^{1}H-NMR of 3,5-difluoro-4-hydroxybenzal-[1-^{13}C]hydantoin

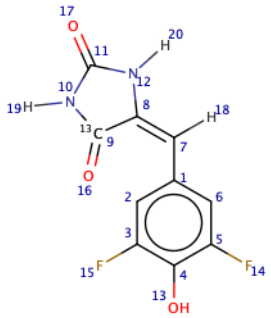

Scheme 57: peak assignment for ^{1}H-NMR of 3,5-difluoro-4-hydroxybenzal-[1-^{13}C]hydantoin

A.2.4 ^{1}H-NMR (DMSO-d$_6$) of 2,6-difluoro-4-hydroxybenzal-[1-^{13}C]hydantoin 9c

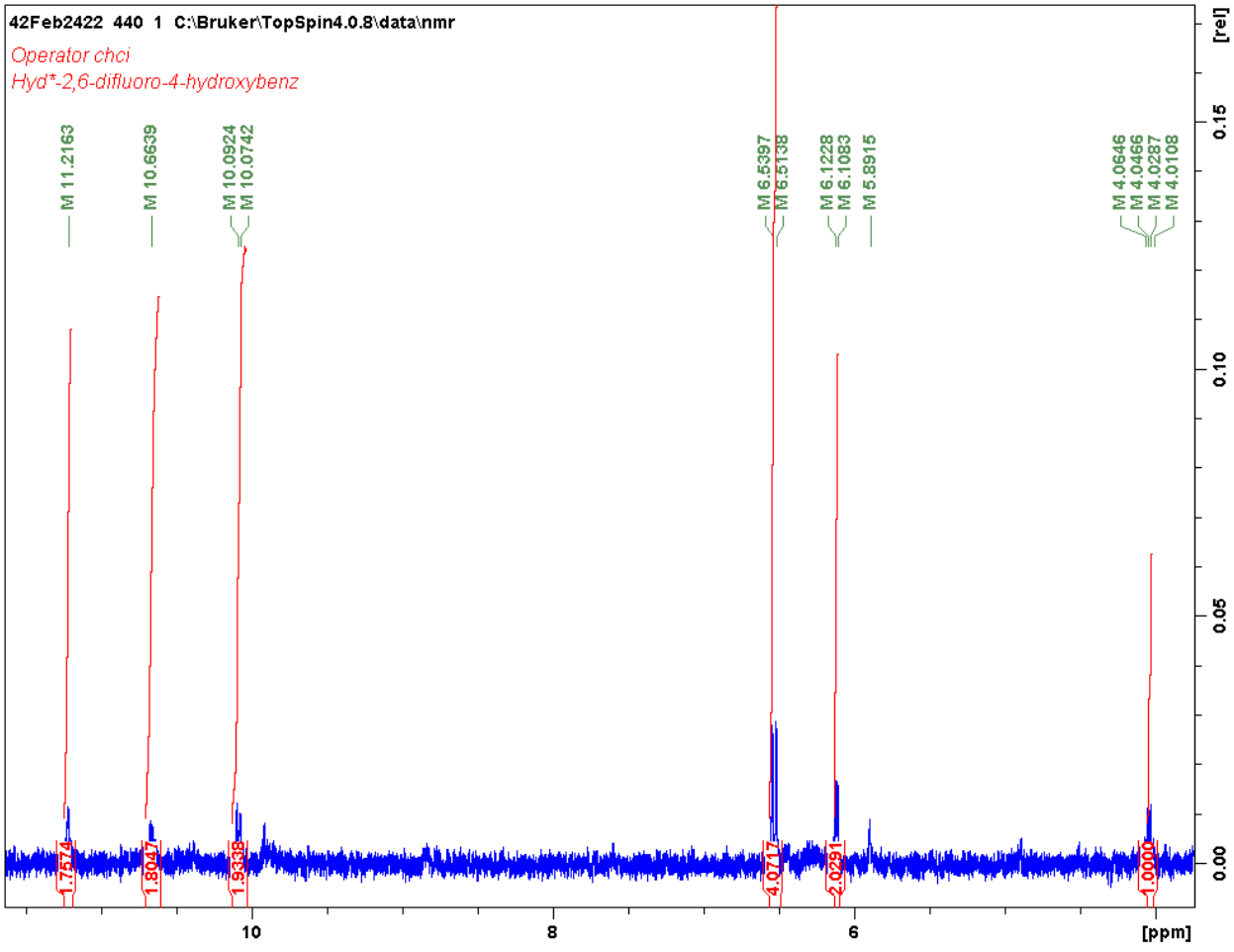

Scheme 58: ^{1}H-NMR 400 MHz (DMSO-d$_6$) of 2,6-difluoro-4-hydroxybenzal-[1-^{13}C]hydantoin

Chemical shift [ppm]	Multiplicity	Integration	Coupling [Hz]	Assignment	Atom no.
6.11	doublet	1 H	$^{3}J_{HH}$ = 14.5	– O**H**	15
6.52	doublet	2 H	$^{3}J_{FH}$ = 25.9	– phenyl C**H**	11, 13
10.08	doublet	1 H	$^{3}J_{^{13}CH}$ = 18.2	– C**H** =	20
10.66	singlet	1 H	-	– C – N**H** – CO –	19
11.22	singlet	1 H	-	– ^{13}CO – N**H** – CO –	18

Table 33: ^{1}H-NMR of 2,6-difluoro-4-hydroxybenzal-[1-^{13}C]hydantoin

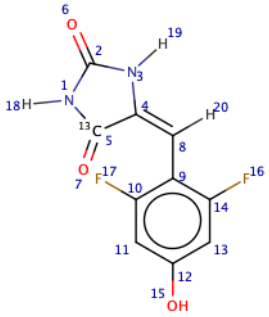

Scheme 59: peak assignment for ^{1}H-NMR of 2,6-difluoro-4-hydroxybenzal-[1-^{13}C]hydantoin

A.2.5 ^{1}H-NMR ($CDCl_3$) of p-fluorophenyl-[1-^{13}C]pyruvic acid 10a

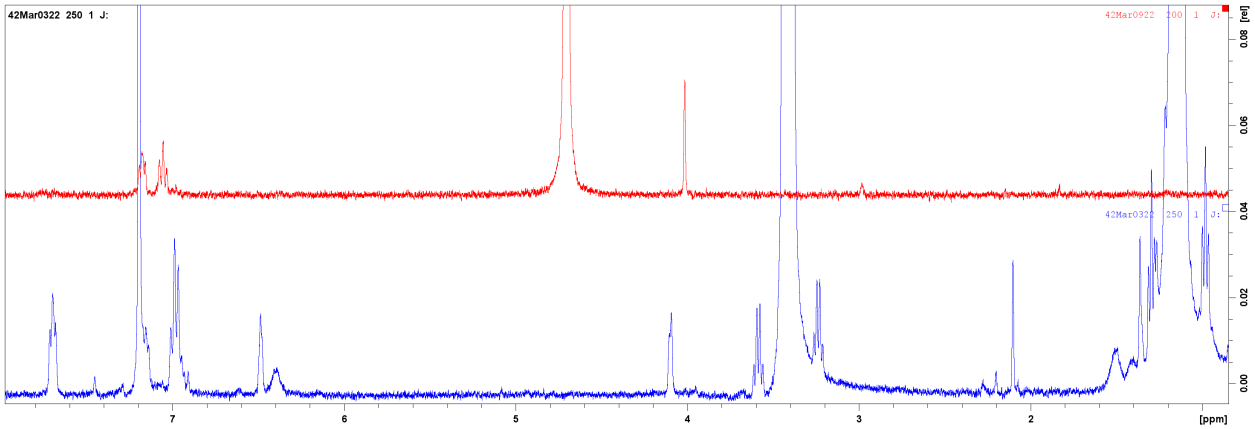

Scheme 60: comparison ^{1}H-NMR 400 MHz of p-fluorophenyl-[1-^{13}C]pyruvic acid prior and p-fluorophenyl-[1-^{13}C]pyruvate after lyophilization

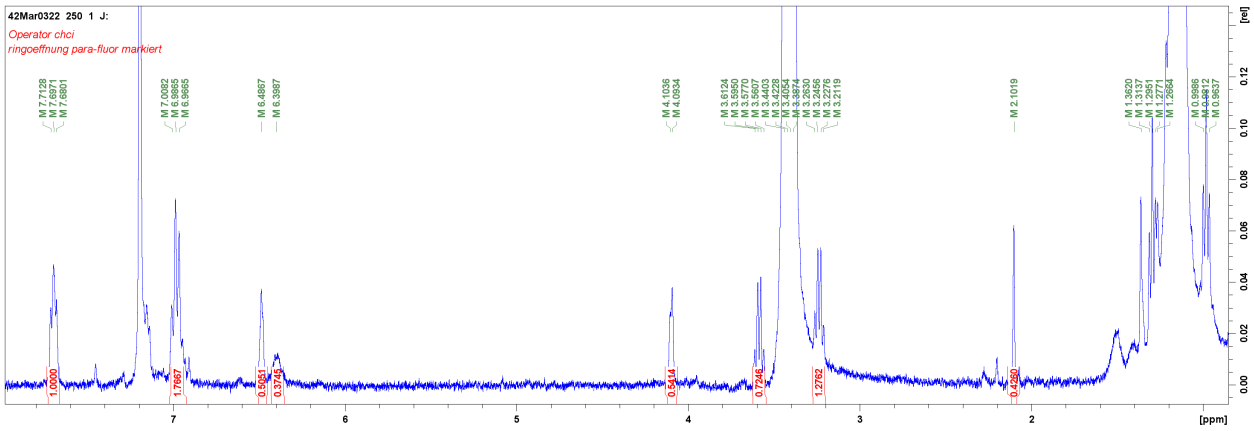

Scheme 61: ^{1}H-NMR 400 MHz ($CDCl_3$) of p-fluorophenyl-[1-^{13}C]pyruvic acid

Chemical shift [ppm]	Multiplicity	Integration	Coupling [Hz]	Assignment	Atom no.
4.1	singlet	2 H	-	– C**H$_2$** – CO –	7
6.5	singlet	1 H	-	– C**H** =	27
6.97 - 7.01	multiplet	4 H	-	– phenyl C**H**	3,5, 8,16
7.16 - 7.19	multiplet	2 H	-	– phenyl C**H**	2, 6
7.68 - 7.71	multiplet	2 H	-	– phenyl C**H**	15, 19

Table 34: ^{1}H-NMR of p-fluorophenyl-[1-^{13}C]pyruvic acid

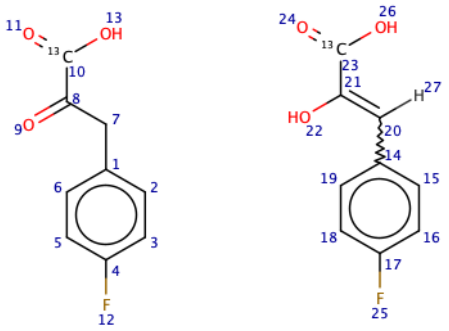

Scheme 62: peak assignment for ^{1}H-NMR of p-fluorophenyl-[1-^{13}C]pyruvic acid keto $\longleftrightarrow$ enol form

A.2.6 ^{1}H-NMR (D_2O) of p-fluorophenyl-[1-^{13}C]pyruvate 10a

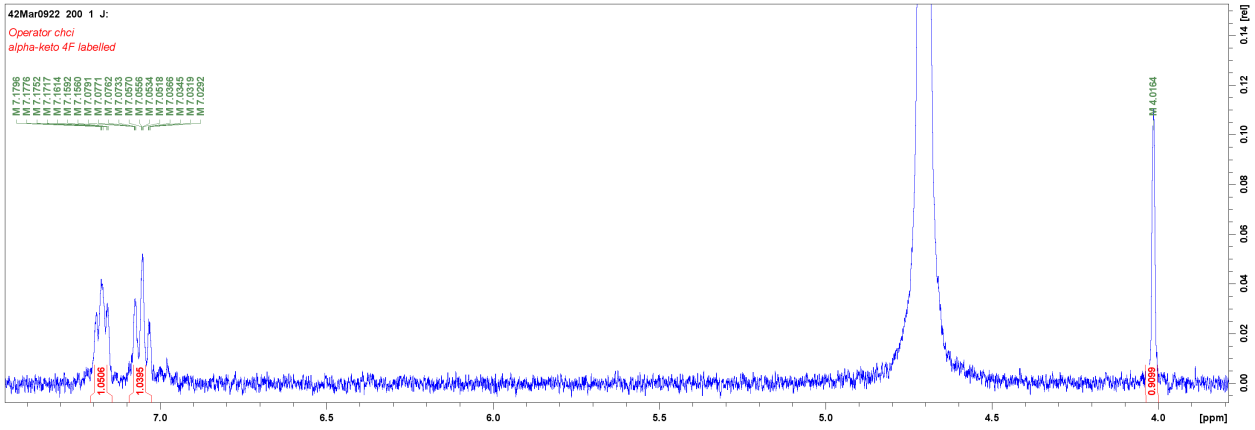

Scheme 63: ^{1}H-NMR 400 MHz (D_2O) of p-fluorophenyl-[1-^{13}C]pyruvate

Chemical shift [ppm]	Multiplicity	Integration	Coupling [Hz]	Assignment	Atom no.
4.02	singlet	2 H	-	– C**H$_2$** – CO –	7
7.03	doublet of doublets	2 H	$^{3}J_{FH}$ = 7.4	– phenyl C**H**	10, 12
7.05 - 7.18	multiplet	2 H	-	– phenyl C**H**	9, 13

Table 35: ^{1}H-NMR of p-fluorophenyl-[1-^{13}C]pyruvate

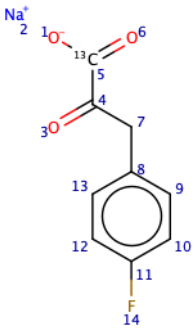

Scheme 64: peak assignment for ^{1}H-NMR of p-fluorophenyl-[1-^{13}C]pyruvate

A.2.7 ^{1}H-NMR ($CDCl_3$) of 3,5-difluoro-4-hydroxyphenyl-[1-^{13}C]pyruvic acid 10b

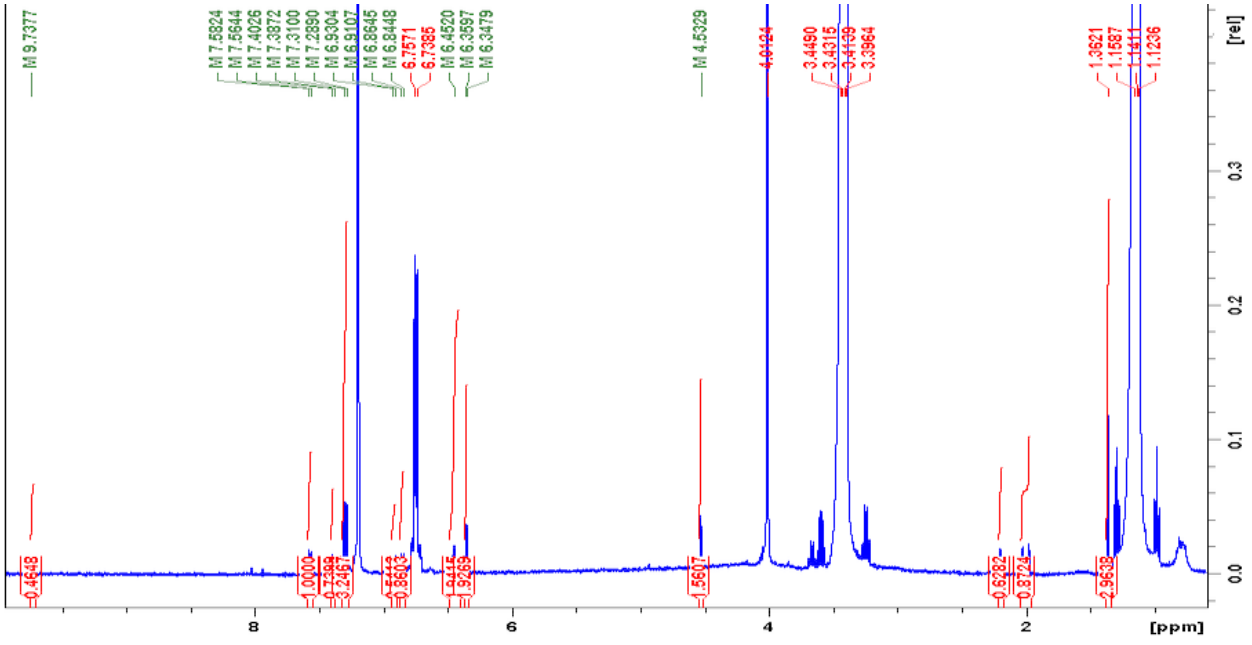

Scheme 65: overview ^{1}H-NMR 400 MHz ($CDCl_3$) of (3,5-difluoro-4-hydroxyphenyl)[1-^{13}C]pyruvic acid

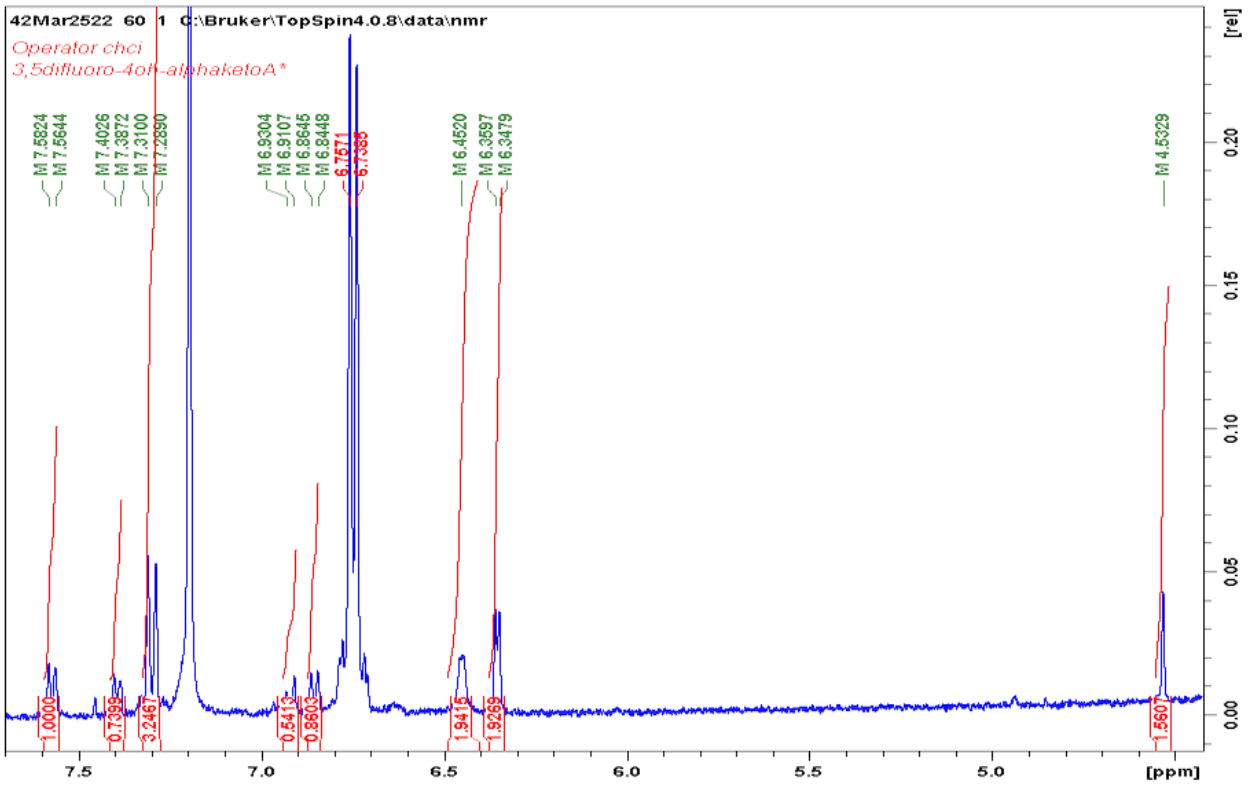

Scheme 66: ROI ^{1}H-NMR 400 MHz ($CDCl_3$) of (3,5-difluoro-4-hydroxyphenyl)[1-^{13}C]pyruvic acid

Chemical shift [ppm]	Multiplicity	Integration	Coupling [Hz]	Assignment	Atom no.
4.53	singlet	2 H	-	– C**H$_2$** – CO –	8
6.3	doublet of doublet	2 H	$^3J_{FH}$ = 11.8	– phenyl C**H**	2, 6
6.5	doublet of doublet	2 H	$^3J_{FH}$ =	– phenyl C**H**	15, 19
6.8	singlet	1 H	-	– phenyl C – O**H**	20
6.9	singlet	1 H	-	– phenyl C – O**H**	7
7.4	doublet	1 H	$^3J_{^{13}CH}$ = 15.4	– C**H** =	31
7.6	doublet	1 H	$^3J_{^{13}CH}$ = 18	– CH = C – O**H** –	23
9.74	singlet	2 H	-	– ^{13}COO**H**	13, 26

Table 36: ^{1}H-NMR of (3,5-difluoro-4-hydroxyphenyl)pyruvic acid

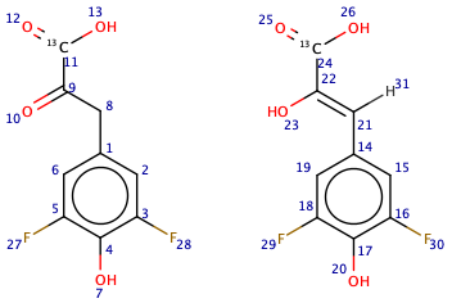

Scheme 67: peak assignment for ^{1}H-NMR of (3,5-difluoro-4-hydroxyphenyl)[1-^{13}C]pyruvic acid keto ⟷ enol form

A.2.8 ^{1}H-NMR (D_2O)of 3,5-difluoro-4-hydroxyphenyl-[1-^{13}C]pyruvate 10b

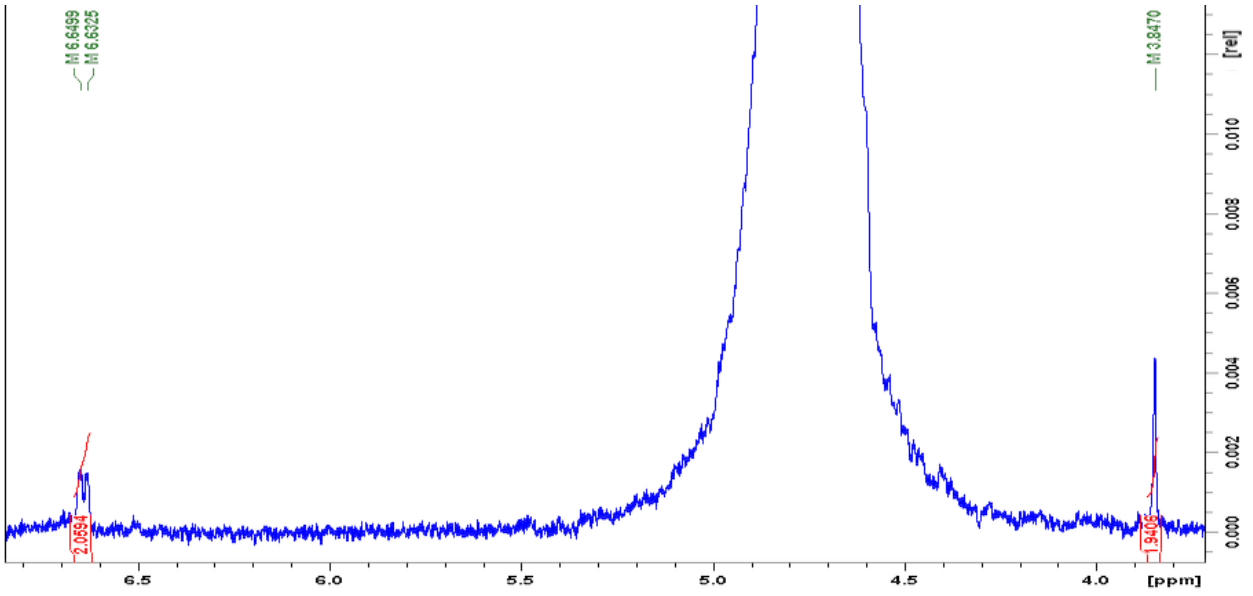

Scheme 68: ^{1}H-NMR 400 MHz (D_2O) of (3,5-difluoro-4-hydroxyphenyl)[1-^{13}C]pyruvate

Chemical shift [ppm]	Multiplicity	Integration	Coupling [Hz]	Assignment	Atom no.
3.85	singlet	2 H	-	– C**H$_2$** – CO –	6
6.63 - 6.65	multiplet	2 H	-	– phenyl C**H**	8, 12

Table 37: ^{1}H-NMR of 3,5-difluoro-4-hydroxyphenyl-[1-^{13}C]pyruvate

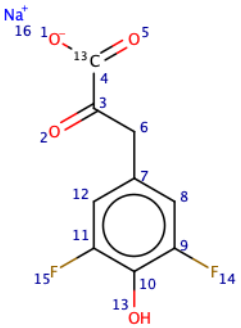

Scheme 69: peak assignment for ^{1}H-NMR of 3,5-difluoro-4-hydroxyphenyl-[1-^{13}C]pyruvate

A.2.9 ^{1}H-NMR ($CDCl_3$) of 2,6-difluoro-4-hydroxyphenyl-[1-^{13}C]pyruvic acid 10c

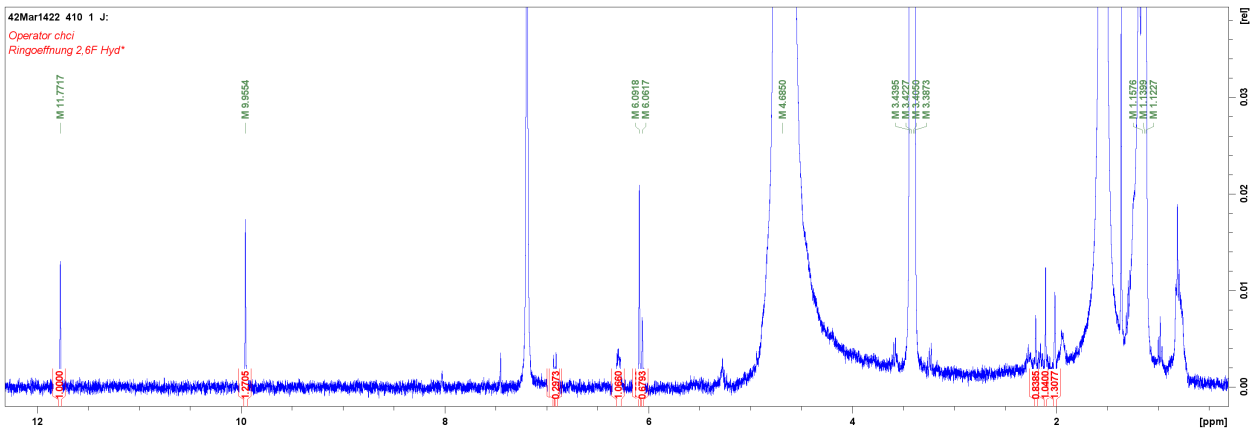

Scheme 70: ^{1}H-NMR 400 MHz ($CDCl_3$) of 2,6-difluoro-4-hydroxyphenyl-[1-^{13}C]pyruvic acid

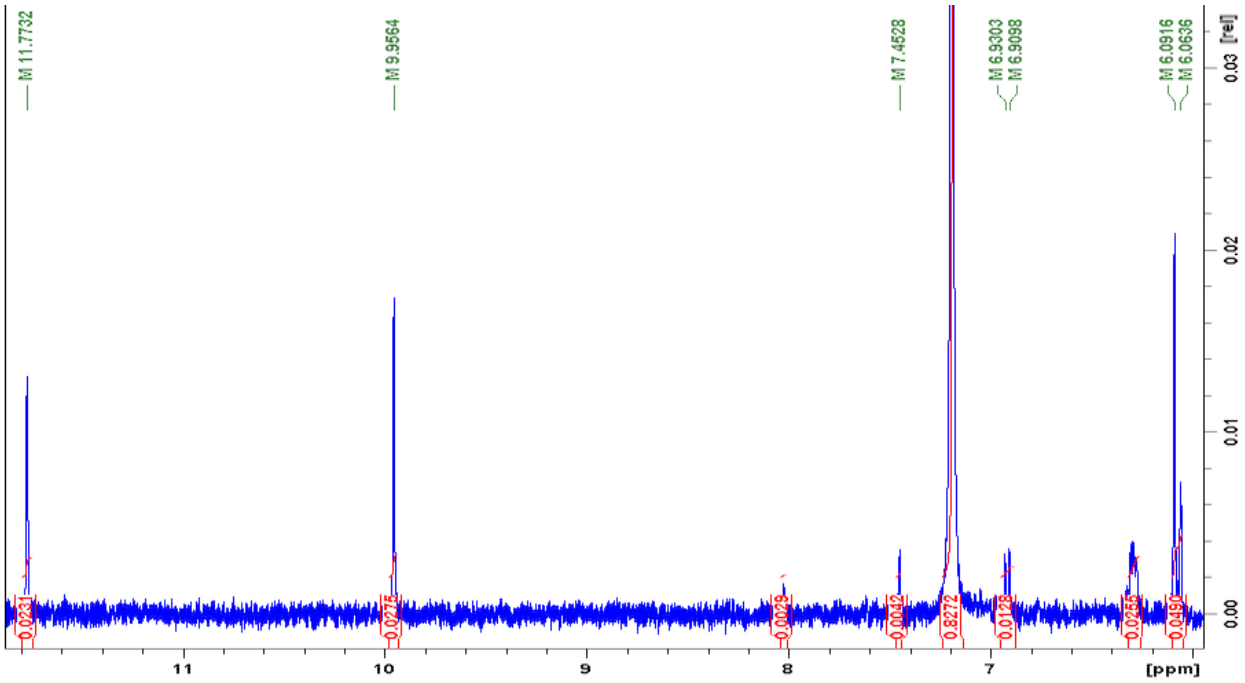

Scheme 71: ROI ^{1}H-NMR 400 MHz ($CDCl_3$) of (2,6-difluoro-4-hydroxyphenyl)[1-^{13}C]pyruvic acid

Chemical shift [ppm]	Multiplicity	Integration	Coupling [Hz]	Assignment	Atom no.
6.06	singlet	1 H	-	phenyl C – O**H**	22
6.09	singlet	1 H	-	phenyl C – O**H**	7
6.3	doublet of doublets	2 H	$^{3}J_{FH}$ = 20.6	– phenyl C**H**	18, 20
6.9	doublet of doublets	2 H	$^{3}J_{FH}$ = 20.5	– phenyl C**H**	3, 5
7.4	singlet	1 H	-	– C**H** =	31
8.0	singlet	1 H	-	= C – O**H**	27
10.0	singlet	1 H	-	– CO – O**H**	15
11.8	singlet	1 H	-	– CO – O**H**	30

Table 38: ^{1}H-NMR of (2,6-difluoro-4-hydroxyphenyl)[1-^{13}C]pyruvic acid

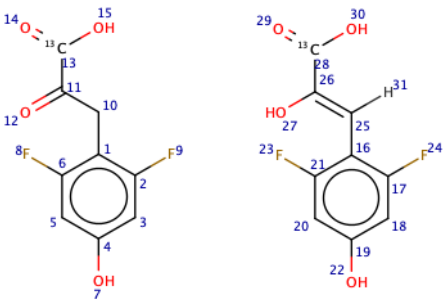

Scheme 72: peak assignment for ^{1}H-NMR of (2,6-difluoro-4-hydroxyphenyl)[1-^{13}C]pyruvic acid keto $\longleftrightarrow$ enol form

A.2.10 ^{1}H-NMR ($CDCl_3$) of 5-[(4-fluorophenyl)methyl]hydantoin 11

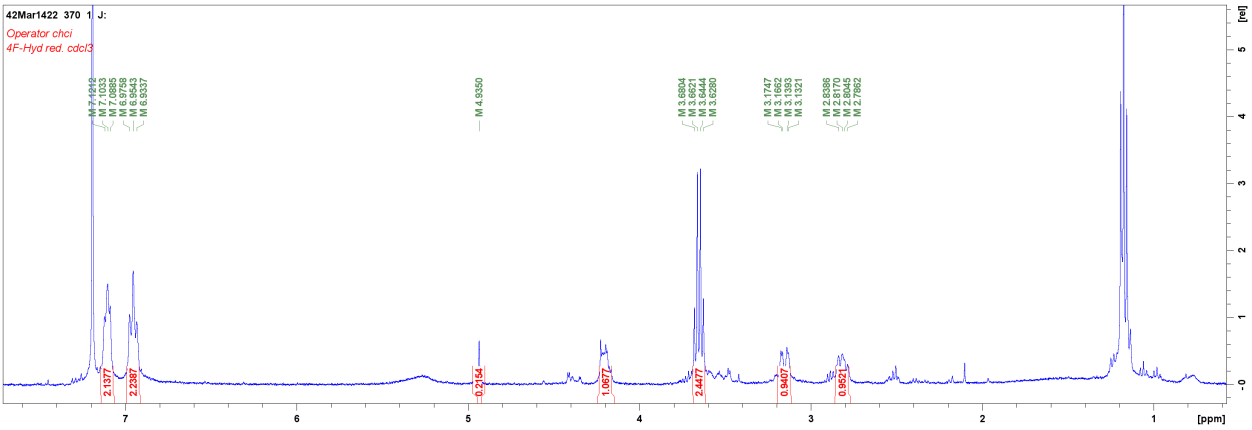

Scheme 73: ^{1}H-NMR 400 MHz ($CDCl_3$) of 5-[(4-fluorophenyl)methyl]hydantoin

Chemical shift [ppm]	Multiplicity	Integration	Coupling [Hz]	Assignment	Atom no.
2.79 - 2.84	multiplet	1 H	$^{3}J_{HH}$ = 54.4	– C**H**$_2$ –	16
3.13 - 3.17	multiplet	1 H	$^{3}J_{HH}$ = 42.6	– C**H**$_2$ –	17
4.10 - 4.22	multiplet	1 H	-	– CH_2 – C**H** –	18
6.95	doublet of doublets	2 H	$^{3}J_{FH}$ = 2.1	– phenyl C**H**	3, 5
7.10	doublet of doublets	2 H	J_{HH} = 2.7	– phenyl C**H**	2, 6

Table 39: ^{1}H-NMR of 5-[(4-fluorophenyl)methyl]hydantoin

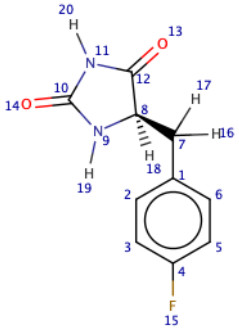

Scheme 74: peak assignment for ^{1}H-NMR of 5-[(4-fluorophenyl)methyl]hydantoin

Appendix B

Spectral analysis: mass spectroscopy

B.1 MS of [4-^{15}N]amino-[3-^{15}N]nitropyridine 6 synthesis

B.1.1 High-resolution MS of [^{15}N]isonicotinamide 3

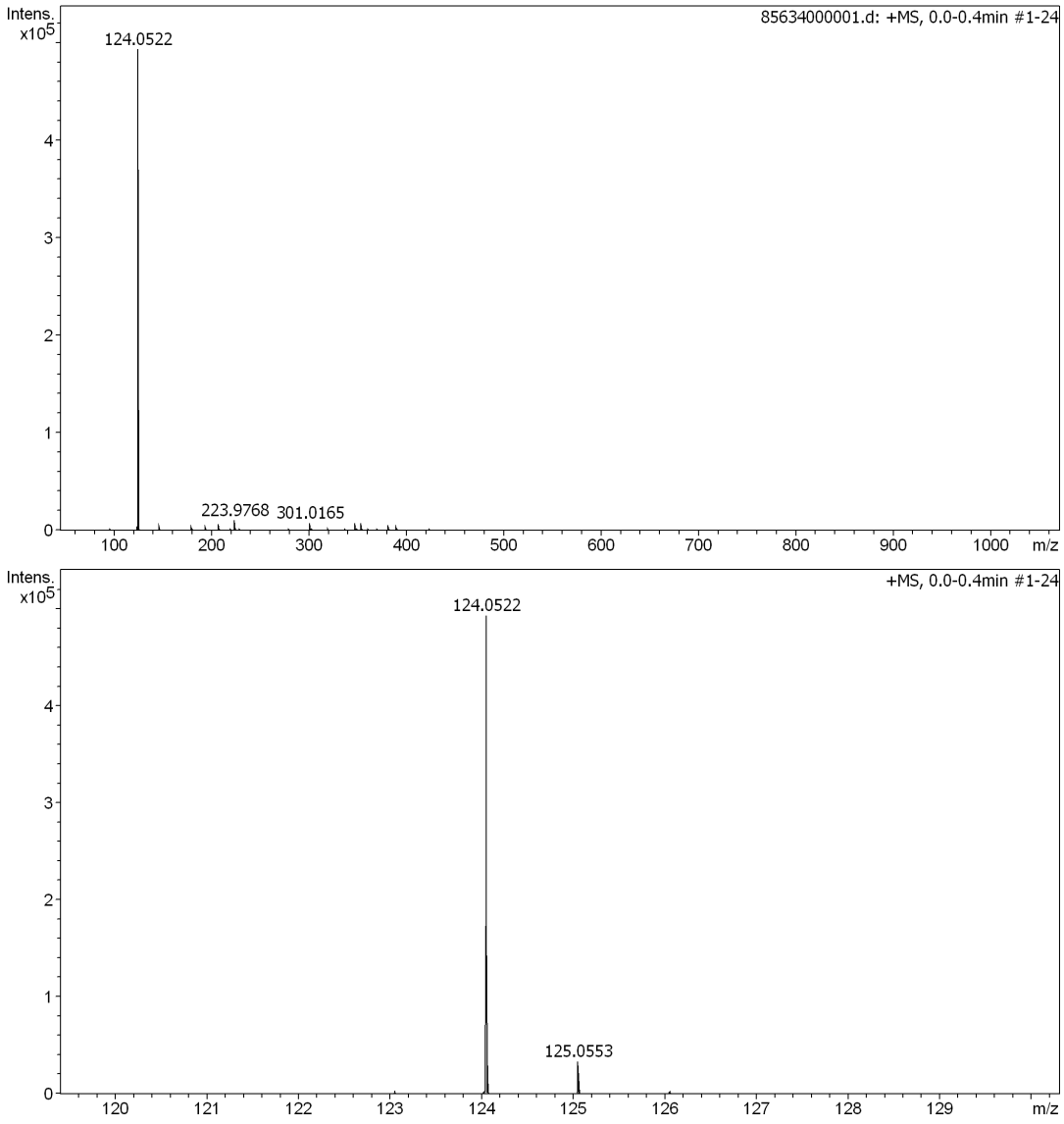

Scheme 75: MS-HRMS of [^{15}N]isonicotinamide

	m/z	Intensity	Assignment	Formula
calculated	124.12	100 %	$(M+H)^+$	$C_5H_6N^{15}N$
		5.4 %		
found	124.12	100 %	$(M+H)^+$	$C_5H_6N^{15}N$
		5.4 %		

Table 40: MS-HRMS of [^{15}N]isonicotinamide

B.1.2 High-resolution MS of [4-^{15}N]aminopyridine 5

Generic Display Report

Analysis Info

Analysis Name	E:\Data\MS_MessService\85958000001.d	Acquisition Date	12/23/2021 12:27:45 PM
Method	tune_low_MS_Service_12_21.m	Operator	msc
Sample Name	AP	Instrument	maXis
Comment	Cikan / OC Ergebnis +/- 5ppm ACN / MeOH + 1% H2O		

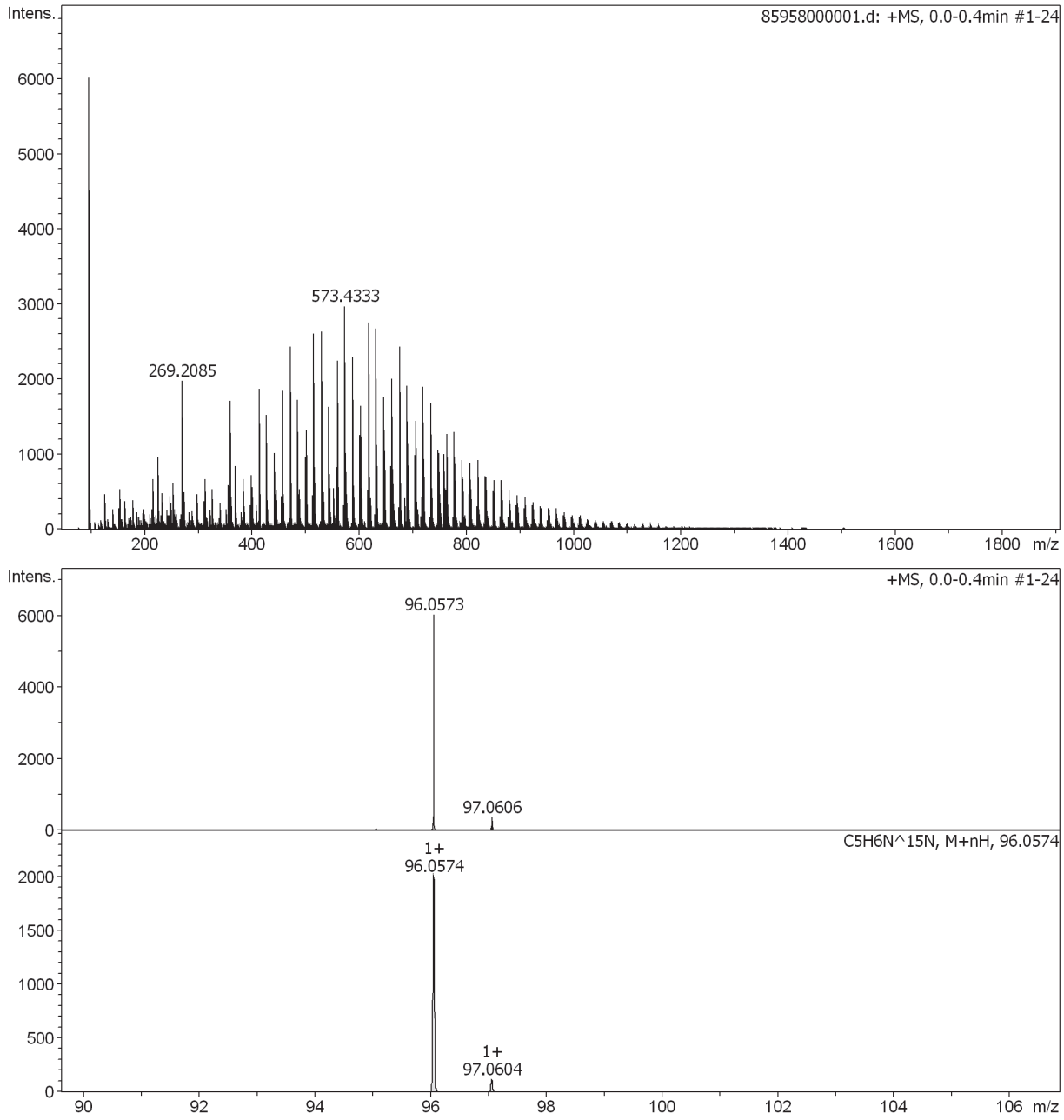

Bruker Compass DataAnalysis 4.1 printed: 12/23/2021 1:47:25 PM by: msc Page 1 of 1

Scheme 76: MS-HRMS of [4-^{15}N]aminopyridine

	m/z	Intensity	Assignment	Formula
calculated	96.0574	100 %	$(M+H)^+$	$C_5H_6N\ ^{15}N$
	97.0604	5.4 %		
found	96.0573	100 %	$(M+H)^+$	$C_5H_6N\ ^{15}N$
	97.0606	5.4 %		

Table 41: MS-HRMS of [4-^{15}N]aminopyridine

B.1.3 MS of brominated [4-^{15}N]aminopyridine 5c

Generic Display Report

Analysis Info

Analysis Name	D:\Data\MS_MessService\83919_HofUml._amazon.d	Acquisition Date	10/7/2021 11:35:11 AM
Method	MSC-Service_direct-injection.m	Operator	MSC
Sample Name	83919_Hof.Uml._amazon	Instrument	amaZon speed ETD
Comment	Lichtenecker / Org.Chem. ACN / MeOH + 1 % H2O		

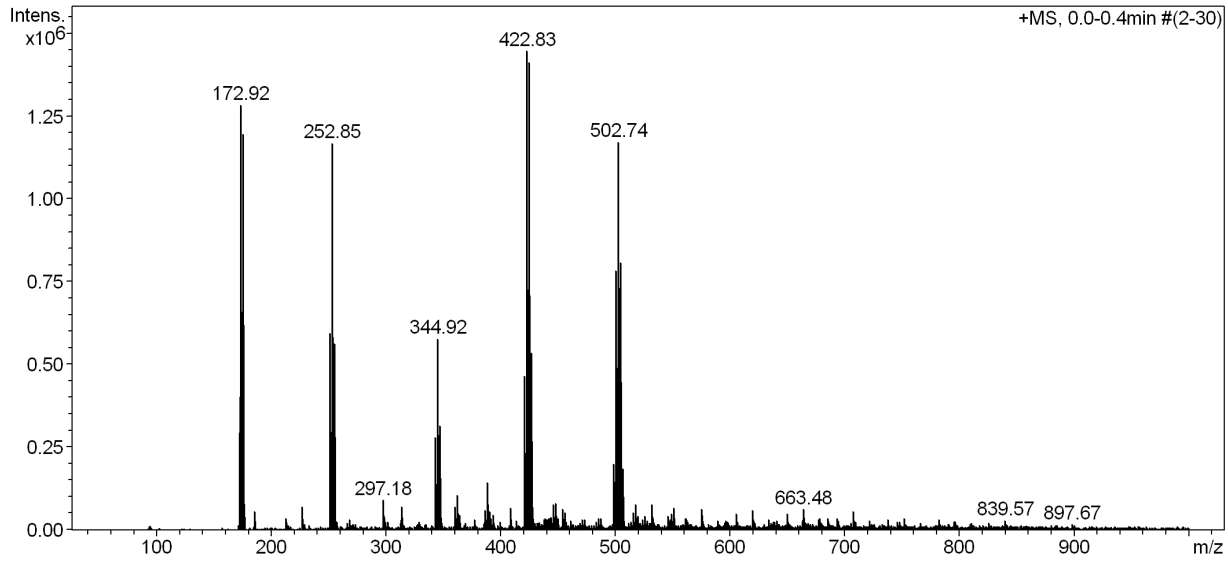

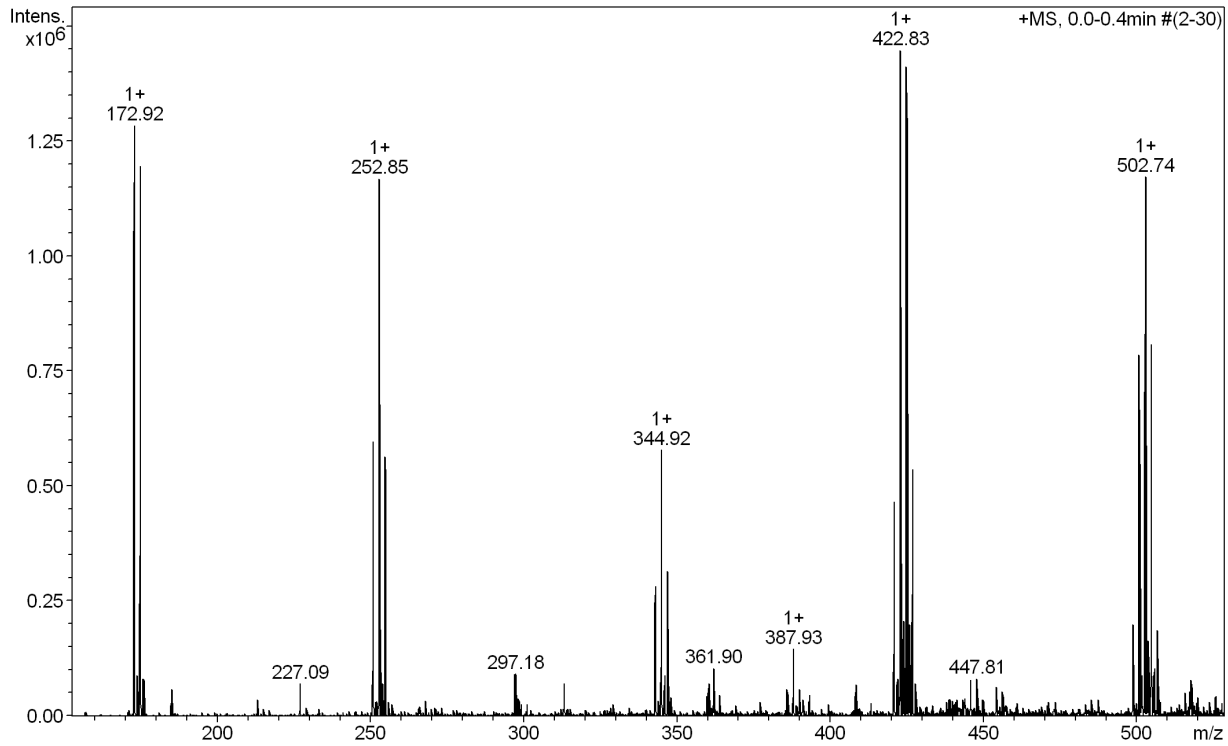

Bruker Compass DataAnalysis 4.0 printed: 10/7/2021 11:43:01 AM Page 1 of 1

Scheme 77: MS-HRMS of brominated [4-^{15}N]aminopyridine

	m/z	Intensity	Assignment	Formula
calculated	251.8721	100 %	$(M+H)^+$	$C_5H_4Br_2N_2$
	249.8741	51.3 %		
	253.8700	48.8 %		
found	252.85	100 %	$(M+H)^+$	$C_5H_4Br_2N_2$
	250.81	51 %		
	254.85	49 %		

Table 42: MS-HRMS of brominated [4-^{15}N]aminopyridine

B.1.4 High-resolution MS of [4-^{15}N]amino – [3-^{15}N]nitropyridine 6

Generic Display Report

Analysis Info

Analysis Name	E:\Data\MS_MessService\85959000001.d	Acquisition Date	12/23/2021 12:36:44 PM
Method	tune_low_MS_Service_12_21.m	Operator	msc
Sample Name	ANP	Instrument	maXis
Comment	Cikan / OC Ergebnis +/- 5ppm ACN / MeOH + 1% H2O		

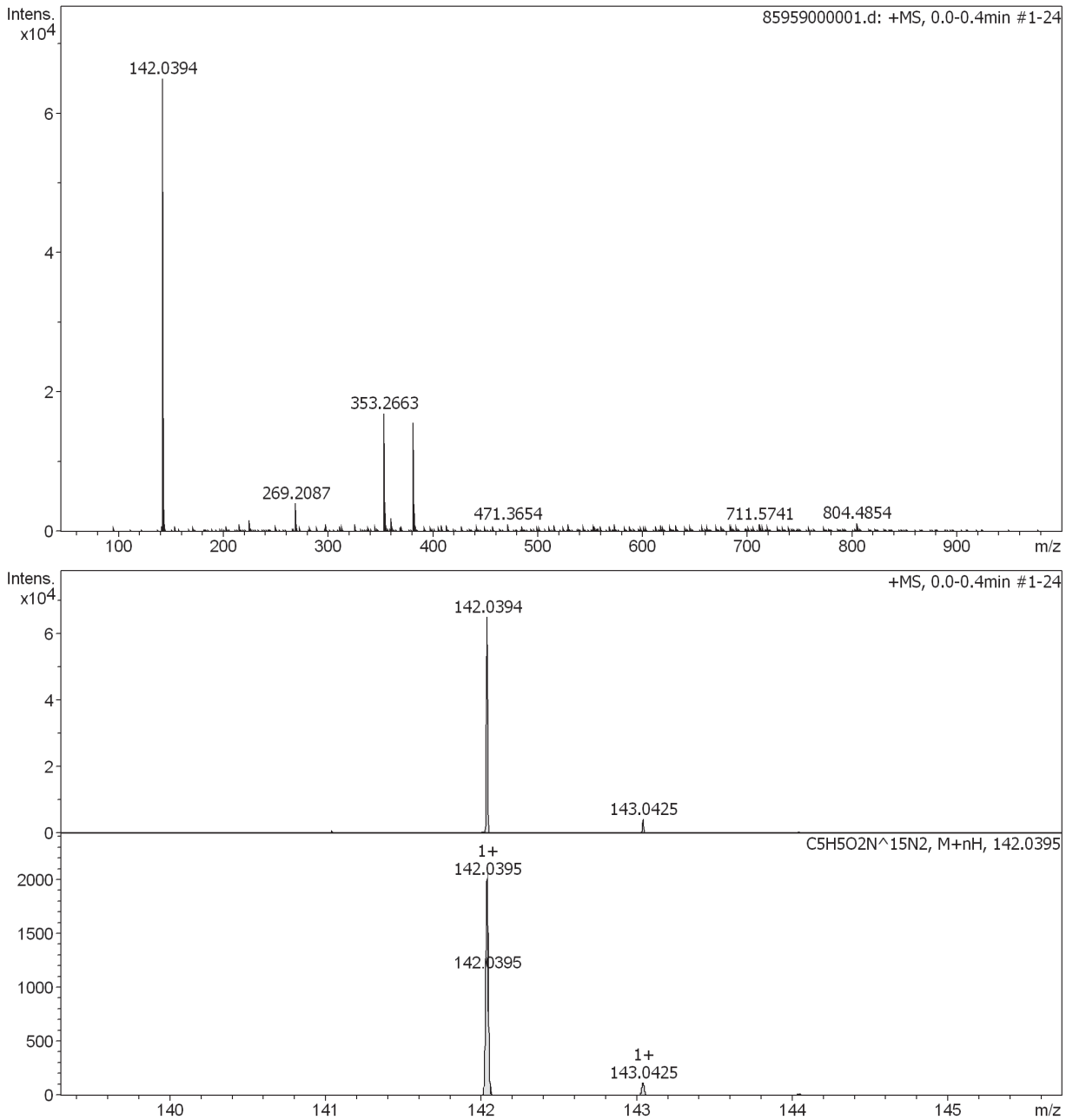

Bruker Compass DataAnalysis 4.1 printed: 12/23/2021 1:50:24 PM by: msc Page 1 of 1

Scheme 78: MS-HRMS of [4-^{15}N]amino – [3-^{15}N]nitropyridine

	m/z	Intensity	Assignment	Formula
calculated	142.0395	100 %	$(M+H)^+$	$C_5H_5O_2N^{15}N_2$
	143.0425	5.4 %		
found	142.0394	100 %	$(M+H)^+$	$C_5H_5O_2N^{15}N_2$
	143.0425	5.4 %		

Table 43: MS-HRMS of [4-^{15}N]amino – [3-^{15}N]nitropyridine